AZADMED.com

www.azadmed.com

azaadtejaratpars

@azadmed2

88 98 80 63 - 6

J Dent Sci 2009;4(3):103–109

ELSEVIER

ORIGINAL ARTICLE

Factors influencing the length of the interproximal dental papilla between maxillary anterior teeth

Min-Chieh Chen,[1,2] Chiu-Po Chan,[2,3] Yu-Kang Tu,[4] Yu-Fang Liao,[2,5] Yen-Chen Ku,[1,2] Leung-Kuen Kwong,[1,2] Whei-Lin Pan,[2,3] Yuh-Ren Ju[2,3]*

[1]Department of Dentistry, Chang Gung University, Chang Gung Memorial Hospital, Taipei, Taiwan
[2]Graduate Institute of Dental and Craniofacial Science, Chang Gung University, Taoyuan, Taiwan
[3]Department of Periodontics, Chang Gung University, Chang Gung Memorial Hospital, Taipei, Taiwan
[4]Department of Periodontology, Leeds Dental Institute and Division of Biostatistics, Centre for Epidemiology and Biostatistics, University of Leeds, Leeds, UK
[5]Department of Craniofacial Orthodontics, Chang Gung University, Chang Gung Memorial Hospital, Taipei, Taiwan

Received: Apr 17, 2009
Accepted: Jul 22, 2009

KEY WORDS:
contact area;
interdental distance;
interproximal dental papilla;
keratinized gingiva;
radiography

Background/purpose: The presence of interproximal dental papillae in maxillary anterior teeth is a key esthetic factor and a great concern for dentists and patients. The aim of this study was to determine the factors associated with the length of the interproximal dental papilla in anterior teeth.
Materials and methods: In total, 102 interproximal sites of maxillary anterior teeth in 30 patients were examined.
Results: TempBond mixed with barium sulfate was applied to the tip of the interproximal dental papillae and mucogingival junction using a periodontal probe. Periapical films using a parallel technique were then taken. The presence of the interproximal dental papilla was determined on the radiographs. If the tip of the interproximal dental papilla was at the base of the contact point, the papilla was recorded as being present. If not, the papilla was considered to be recessed. The radiographs were transferred to a computer and analyzed using ImageJ software. Age, sex, and the following parameters were measured: the length of the interproximal dental papilla, the distance between the base of the contact point and bone crest, the width of keratinized gingiva, and the interdental distance. Results showed that the length of the interproximal dental papilla was significantly and individually related to the distance from the contact point to the bone crest, the width of the keratinized gingiva, and the interdental distance.
Conclusion: The width of the keratinized mucosa was the predominant factor affecting the length of the interproximal dental papilla.

*Corresponding author. Department of Periodontics, Chang Gung University, Chang Gung Memorial Hospital, 6F, 199, Dunhua North Road, Songshan District, Taipei 105, Taiwan.
E-mail: emily_dot@hotmail.com

Introduction

In addition to maintaining dental and periodontal health, dental esthetics has become a great concern for both dental practitioners and patients. Increasing numbers of doctors and patients demand the eradication of dental and periodontal diseases and also the restoration of dental esthetics, for which the gingival plane, gingival outline, and gingival and interproximal dental papilla recession in the anterior teeth are particularly important.[1] The presence of interproximal papillae between the maxillary anterior teeth is a key esthetic component,[2] and the contour of the interdental tissues, and the color and texture of keratinized tissues are essential for esthetic anterior prostheses.[3] The various problems associated with the recession of interproximal dental papillae such as food impaction, esthetics, and phonetics,[4] known as the "black hole" problem, pose a great challenge for dental treatment.

The form and volume of interdental tissues are determined by the morphology of the adjacent teeth. Cohen[5] first described the col as non-keratinized or parakeratinized tissue in the interproximal area with buccal and lingual peaks of keratinized tissue. The interdental papillae between the incisors are usually pyramidal-shaped or a slight gingival col, depending upon the location of the contact area and the height of the gingiva.[5–7] Matherson and Zander[8] reported that the col took the shape of the contact area of the adjacent teeth but not the underlying alveolar bone. The shape of the interproximal dental papilla is also determined by the proximal crown forms and the course of the cementoenamel junction (CEJ).[9] The contour and shape of the interproximal dental papilla is also affected by the periodontal biotype.[10–13] There are two periodontal biotypes: thin scalloped and thick flat types. Thin scalloped periodontium is characterized by thin gingival tissue and long interproximal dental papilla, while the thick flat type is characterized by thick gingival tissue and a short, wide papilla.[10–13]

Tarnow et al.[4] reported that when the distance from the contact point to the bone crest is ≤ 5 mm, the papilla is present almost 100% of the time. Other studies[14–19] showed similar results. The principle is widely used in clinical prevention and management of loss of the interproximal dental papilla, including surgical rebuilding of the interdental papilla. However, the relationship between the presence of the interproximal dental papilla and its length remains unclear, and there is no study in the literature investigating factors related to the length of the interproximal dental papilla.

The purpose of this study was to evaluate, by a noninvasive method, the factors that are related to the length of the interproximal dental papilla. The factors investigated included: (1) the distance (D1) between the contact point and the bone crest, (2) the width (D2) of the keratinized gingiva, and (3) the interdental distance (D3) at the level of the bone crest.

Materials and methods

The study protocol was approved by the local institutional review board. Patients who visited the periodontal department at Chang Gung Memorial Hospital and received supportive periodontal therapy from September 2007 to February 2008 were enrolled in this study. All patients were older than 20 years, with no systemic compromising problems including pregnancy. They had no history of taking medications known to increase the risk of gingival enlargement. All had healthy gingiva with periodontal probing depths of <5 mm and plaque and gingival index (Loe and Silness[20]) grades of 0–1. The sites selected for the measurements were the interproximal dental papillae from the maxillary right to left canines. The interproximal dental papillae between teeth with dental implants, artificial crowns, proximal/cervical restorations or abrasions were excluded.

The authors established the experimental procedures and made the measurements. A technician took all periapical radiographs. Radiopaque material consisting of a 2:1 (v/v) mixture of TempBond (Kerr Corp., Orange, CA, USA) and barium sulfate was placed on the tip of the papilla with its coronal margin at the mucogingival junction (MGJ) using a periodontal probe (Fig. 1). Only a minimal amount of radiopaque material was needed, because the radiopacity was greatly enhanced by the contrast media. Working time of TempBond was less than 90 seconds.

Three periapical radiographs of the test sites in each patient were taken using a parallel technique with a film holder (XCP; Rinn, Elgin, IL, USA). The available radiographs were of good quality and had no overlap. All radiographs included a ruler and were digitized using a digital camera (Nikon Coolpix 4500; Nikon Inc., Melville, NY, USA) with 2272×1704 input pixels at the same time; the image format was JPEG. After digitization, all images were transferred to a personal computer and examined using the same monitor. In a dark room,[14,21,22] measurements of the digital images were undertaken using ImageJ freeware from the National Institutes of Health (http://rsb.info.nih.gov/ij).

The variables measured on the periapical radiographs included: (1) the length (L) of the interproximal dental papilla, i.e., the distance from the

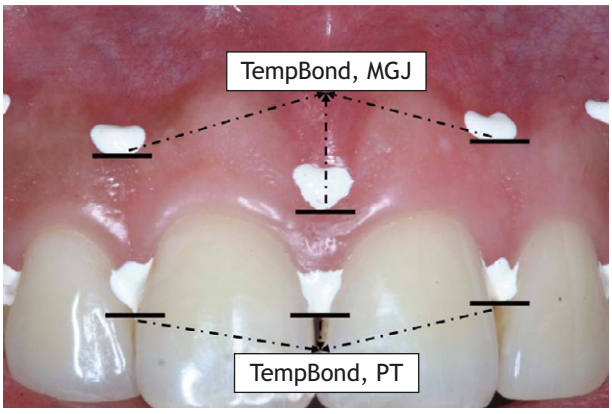

Fig. 1 TempBond and barium sulfate placed with a probe on the tip of the papilla (PT) and mucogingival junction (MGJ).

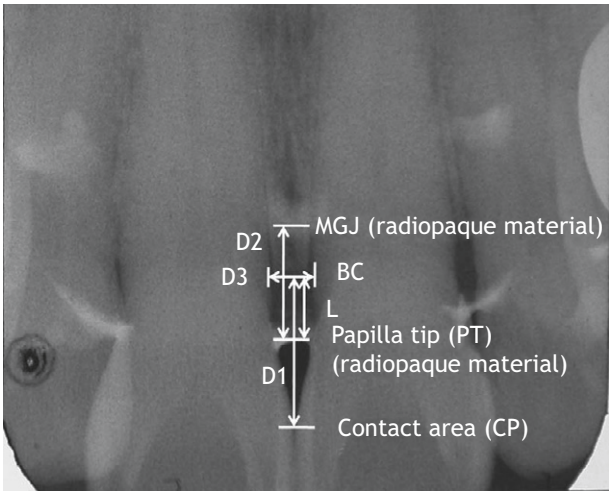

Fig. 2 Measurements taken on the radiographs. L=the length of the interproximal dental papilla, the distance from the papilla tip (PT; radiopaque material) to the bone crest (BC); D1=the distance between the contact point (CP) and BC; D2=the distance from the PT to the mucogingival junction (MGJ; radiopaque material); D3=the interdental distance at the bone crest level.

tip of the papilla to the bone crest; (2) the distance (D1) from the base of the contact area to the bone crest; (3) the width (D2) of keratinized gingiva, i.e., the distance from the tip of the papilla to the MGJ; and (4) the interdental distance (D3) between two natural teeth at the bone crest level paralleling the CEJ (Fig. 2). Every measurement was repeated 10 times, and the average was recorded. All measurements were rounded to the nearest 0.01 mm.

Statistical analysis

Owing to the clustered data structure in this study, generalized estimating equations (GEEs)[23,24] were employed to account for clustering of multiple teeth within individual patients. The dependent variable was the length of the interproximal dental papilla measured in millimeters. Associations between the dependent variable and the explanatory variables of age, sex, D1, D2, and D3 were first tested separately. When two or more explanatory variables significantly influenced the length of the interproximal dental papillae, those factors were combined in the GEE analysis. Those with significant results were the predominant factors associated with the length of the interproximal dental papilla.

Table 1. Demographic characteristics and interdental area data of the study population

Age, mean±SD (range), yr	53.8±11.5 (28–78)
Measurements, mean±SD (range), mm	
L	3.80±0.72 (2.3–5.7)
D1	5.26±1.59 (2.3–9.4)
D2	4.41±1.29 (1.6–7.5)
D3	1.65±0.66 (0.4–3.9)
Sex, *n* (%)	
Male	13/30 (43.33)
Female	17/30 (56.67)
Papillary presence*, *n* (%)	
Yes	45/102 (44.12)
No	57/102 (55.88)

*If the tip of the papilla was at the base of the contact point, the papilla was defined as being present; if not, the papilla was defined as being not present. SD=standard deviation; L=length of the interproximal dental papilla; D1=distance between the contact point and bone crest; D2=distance from the papilla tip to the mucogingival junction; D3=interdental distance at the bone crest level.

Results

In total, 30 patients (13 males and 17 females) who met the selection criteria were included in the study. Patients had a mean age of 53.8±11.5 years (range, 28–78 years). Of the 150 interproximal sites of the maxillary anterior teeth from the left to the right canine, 48 sites were excluded; only 102 sites were investigated in this study. The mean value of the length of the interproximal dental papilla was 3.80±0.72 mm, that of the distance from the contact point to the bone crest was 5.26±1.59 mm, that of the width of the keratinized gingiva was 4.41±1.29 mm, and that of the interdental distance was 1.65±0.66 mm (Table 1).

Results in Table 2 show that the lengths of the interproximal dental papillae varied from 3 to 6 mm, with the majority at 4–5 mm. The percentage of the presence of interproximal dental papillae was

Table 2. Presence of papilla versus the length (D2) of the interproximal dental papilla*

	Distance from the papilla tip to the crestal bone (mm)				Total
	3	4	5	6	
Papilla, *n*	15	51	32	4	102
Present†, *n* (%)	9 (60.00)	20 (39.22)	14 (43.75)	2 (50.00)	45 (44.12)
Recessed‡, *n* (%)	6 (40.00)	31 (60.78)	18 (56.25)	2 (50.00)	57 (55.88)

*When the data were categorized, all measurements were rounded to the nearest millimeter; †recorded as present if the tip of the interproximal dental papilla (radiopaque material) was at the base of the contact area; ‡recorded as recessed if a space was visible apical to the contact area.

Table 3. Generalized estimating equation multivariable linear regression for papillary length for the 102 papillae

	Regression coefficient*	P
D1	0.11	0.02
D2	0.14	0.0003

*Indication of change in the mean papillary length (in millimeters) per unit increase in the potential variables; a positive sign indicates a longer papilla for a unit increase in the potential variable. D1=distance between the contact point and bone crest; D2=distance from the papilla tip to the mucogingival junction.

similar in each group of lengths of the interproximal dental papillae. Relationship between the presence of the interproximal dental papilla and its length was not significant ($P=0.58$) according to the GEE analysis.

Results from the GEE models are presented in Table 3. In the univariate analysis, the length of the interproximal dental papilla was significantly related to two factors: the distance from the contact point to the bone crest, and the width of the keratinized gingiva ($P<0.05$). In the multivariate analysis, both were put in a GEE to test their independent associations after adjusting for other variables in the model. Both the distance from the contact point to the bone crest and the width of the keratinized gingiva were significantly influencing the length of the interproximal dental papilla ($P<0.05$). However, the width of the keratinized gingiva was the strongest determinant factor.

Discussion

Previous studies by Tarnow et al.[4] and Cho et al.[15] showed that when the distance from the contact point to the bone crest is ≤ 5 mm, the interproximal dental papilla is always present. However, they used a sounding technique under anesthesia on the facial aspect of the contact point, and verified these measurements by reflecting the gingiva. Some points should be considered. First, sounding with a probe might cause a certain degree of compression of the interproximal dental papilla. Second, the measured points on the facial aspect of the contact point might fail to reveal the apical tip of the contact area and crestal bone resorption. In addition, surgery always leads to discomfort and fear in patients and may even cause unfavorable recession of the interproximal dental papilla or trauma of supporting tissues.[4,25]

A simple, convenient and repeatable method to study the interproximal dental papilla is, therefore, desirable. The thickness of the masticatory mucosa and gingiva can be determined ultrasonically, but this does not apply to interproximal dental papillae.[26,27] Olsson et al.[28] introduced a method of measuring the length of the interproximal dental papilla with the aid of clinical photographs. Others have developed an index for assessing the contour of the interproximal dental papilla.[29,30] Use of radiographs as a noninvasive method[14,16–19,31–33] was also developed. Lee et al.[14] tested the accuracy of periapical films for measuring the length of soft tissue from the top of the interproximal dental papilla to the crestal bone. They compared periapical films using a parallel technique and bone probing method under local anesthesia. Results suggested that the noninvasive method using a radiopaque material and periapical radiographs could be utilized to measure the length of interproximal dental papillae with high accuracy.

Several radiopaque materials are used to increase the contrast. Lee et al.[14,31,33] used an endodontic sealer plus barium sulfate as an indicator of the MGJ. However, endodontic sealer (Tubli-Seal; Kerr Corp.) flows and does not set. It is not easy to apply to test sites, especially when saliva is not isolated, and it is too sticky to be easily removed from the mucosa. Chang[17–19] used Caviton (GC Corp., Tokyo, Japan) to block the interdental space due to recession of interproximal dental papillae.

This radiopaque material helps reveal the tip of the interproximal dental papilla on periapical film. Caviton might also cause compression of the interproximal dental papilla, especially when the distance from the contact point to the tip of the interproximal dental papilla is <1 mm. In addition, it is very difficult to apply Caviton to the MGJ.

In this study, a noninvasive method with periapical X-rays and TempBond as the radiopaque material was used. As TempBond flows, it is much easier to apply to test sites. Its working time is 90 seconds, which is decreased by the addition of barium sulfate. When it sets, it attaches to soft tissues and does not detach even in the presence of saliva. It is also easy to remove from the mucosa after the radiographs have been taken.

In this study, the lengths of the interproximal dental papillae varied from 3 to 6 mm, with 80% of them at 4–5 mm. The biologic width, first described by Garguilo et al.[34], consists of 1.07 mm of connective tissue attachment and 0.97 mm of junctional epithelium. Kois[35] described this as the dentogingival complex. It was shown that the average dimension of the dentogingival complex in natural teeth is 3 mm at the facial aspect and 4.5 mm at the interproximal aspect.[34–37] In this study, the length of the interproximal dental papilla was measured from the tip of the papilla to the bone crest. This comprises the biologic width (connective tissue attachment plus junctional epithelium) and free (marginal) gingiva. The free gingiva forms the soft tissue wall of the gingival sulcus. The histologic sulcular depth was reported to be 1.8 mm, varying 0–6 mm,[38] while other studies reported 1.5 mm[39] and 0.69 mm.[34] Therefore, the width of the dentogingival complex (3–4.5 mm) plus the length of the free gingiva (0.69–1.8 mm) is approximately 3.69–6.3 mm. It was similar in this study; the length of the interproximal dental papilla was 3–6 mm (Table 2).

The results of this study revealed that the length of the interproximal dental papilla was significantly and individually related to two factors: the distance between the contact point and the bone crest, and the width of the keratinized gingiva. This means that when the distance from the contact point to the bone crest increases, the length of the interproximal dental papilla also increases. However, when the distance from the contact point to the bone crest is ≤5 mm, the length of the interproximal dental papilla is limited. Tarnow et al.[40] also studied the vertical distance from the crest of the bone to the height of the interproximal dental papilla between adjacent implants. They showed that 2–4 mm (average, 3.4 mm) of soft tissue height can be expected to cover the interimplant crest of bone; however, no interimplant distance was actually defined.

The results also illustrated that the length of the interproximal dental papilla increased when the interdental distance increased. In an implant study, Lee et al.[33] compared two different implant systems, and both showed similar dimensions of interproximal soft tissue (3.3–3.4 mm) between adjacent implants, irrespective of the horizontal distance of the fixtures.

This study showed that a wider zone of keratinized gingiva had a longer interproximal dental papilla. The GEE analysis also indicated that the width of the keratinized gingiva was the predominant factor associated with the length of the interproximal dental papilla. This was similar to the study by Lee et al.[31] on dental implants, which revealed that the dimension of keratinized gingiva between two adjacent implants might be related to the dimension of the interproximal dental papilla. However, the relationship between the width of keratinized gingiva in the interproximal region and the dimension of the interproximal papilla between two natural teeth was not investigated until now.

Keratinized gingiva is composed of attached gingiva and free gingiva. The width of the attached gingiva on the facial aspect differs in different areas of the mouth.[41] The attached gingiva functions as a barrier to penetration into the deeper tissue by microbes and noxious agents.[42] It is generally greatest in the incisor region (3.5–4.5 mm in the maxilla and 3.3–3.9 mm in the mandible). Usually about 1 mm wide, the marginal gingiva forms the soft tissue wall of the gingival sulcus. After complete tooth eruption, the free gingival margin is located on the enamel surface approximately 1.5–2 mm coronal to the CEJ.[41]

Wennström et al.[43,44] studied the dimensions of the gingiva in beagles. They found that gingival units with a wide zone of keratinized gingiva were more voluminous than units with a narrow zone. Olsson et al.[28] also found a strong relationship ($P=0.001$) between the width of keratinized gingiva and the thickness of the gingiva. In orthodontic treatment, an increased buccolingual thickness of tissue at the facial aspect of the teeth results in coronal migration of the soft tissue margin.[45]

Chang[18,19] showed a positive relationship between age and interdental distance and a negative relationship between age and papilla height. Those results differed from this study, which revealed that age did not significantly influence the presence or length of the interproximal dental papilla. Wara-aswapati et al.[46] found that the palatal masticatory mucosa became thicker with an increase in age. Other studies found no age-related differences in the gingival epithelium of humans or dogs.[47,48] However, Vandana and Savitha[49] found

that the gingiva was thicker in younger than older individuals.

Wara-aswapati et al.[46] and Vandana and Savitha[49] revealed that the gingiva and palatal mucosae of males were thicker than those of females. However, in this study, the univariate analysis revealed that sex did not significantly influence the presence of the interproximal dental papilla or its length, which was similar to studies by Chang.[18,19]

Nowadays, patients have increasing esthetic demands for dental treatments; the principle of the distance of contact point to the bone crest being $\leq$5 mm indicates that the interproximal dental papilla is almost always present. Alterations in the position of the contact point with the ceramic veneer or crown can induce creeping loss of papillae. In addition, orthodontic treatment in conjunction with tooth stripping to relocate the contact point more apically can be performed to reduce the "black triangle".[50]

However, in severe alveolar bone resorption cases, usually in periodontal patients, the prosthetic method fails to recover the papilla recession. Recent advances in periodontal plastic surgery have enhanced the periodontist's ability to address these concerns. Nemcovsky[51] used an advanced papillary flap combined with a gingival graft to augment the soft tissue in the interdental area. Han and Takei[52] proposed an approach based on using a semilunar incision and a subepithelial free gingival connective tissue graft which is placed beneath the coronally positioned interdental tissue, to attain the goal of papilla reconstruction. Azzi et al.[53,54] reconstructed the interdental papilla using a buccal and palatal split-thickness flap and a connective tissue graft in cases including Miller Class IV recession. However, the blood supply is the key element for success. As previously stated, the keratinized gingival width is the strongest determinant of papillary length, so surgical procedures to increase the dimension of the keratinized gingiva might be helpful in reconstructing the papilla. Although the length of the interproximal dental papilla is not significantly associated with the presence of the interproximal dental papilla, and even if the interdental papilla cannot be completely rebuilt, the black triangle problem can be minimized to achieve patients' demands. Future research focused on the effectiveness would be clinically significant.

The main limitation of this study is that the periodontal biotype was suggested to affect gingival recession.[10–13] However, it is impossible to define the biotype in a radiographic way.

In summary, a newly designed noninvasive method was shown to facilitate the study of the interproximal dental papilla and provides accurate and repeatable measurements. The width of the keratinized mucosa was the predominant factor associated with the length of the interproximal dental papilla. Determining interrelationships of each factor that influences the length of the interproximal dental papilla requires further studies. Additional studies on the interproximal papilla between implants are also necessary.

References

1. Sclar AG. Systematic evaluation of the esthetic implant patient. In: Sclar AG, ed. *Soft Tissue and Esthetic Considerations in Implant Therapy*. Chicago: Quintessence Publishing, 2003:13–41.
2. Kokich VG. Adjunctive role of orthodontic therapy. In: Newman MG, Takei HH, Klokkevold PR, Carranza FA, eds. *Carranza's Clinical Periodontology*, 10th ed. St Louis, MO: Elsevier, 2006:856–70.
3. Tarnow DP, Eskow RN. Considerations for single-unit esthetic implant restorations. *Compend Contin Educ Dent* 1995;16:778, 780, 782–4.
4. Tarnow DP, Magner AW, Fletcher P. The effect of the distance from the contact point to the crest of bone on the presence or absence of the interproximal dental papilla. *J Periodontol* 1992;63:995–6.
5. Cohen B. Morphological factors in the pathogenesis of periodontal disease. *Br Dent J* 1959;107:31–9.
6. Cohen B. A study of the periodontal epithelium. *Br Dent J* 1962;112:55–64.
7. Fiorellini JP, Kim DM, Ishikawa SO. The gingiva. In: Newman MG, Takei HH, Klokkevold PR, Carranza FA, eds. *Carranza's Clinical Periodontology*, 10th ed. St Louis, MO: Elsevier, 2006:46–67.
8. Matherson DG, Zander HA. Evaluation of osseous surgery in monkeys. *J Dent Res* 1963;42:116. [Abstract 326]
9. Lindhe J, Karring T. Anatomy of the periodontium. In: Lindhe J, Karring T, Lang NP, eds. *Clinical Periodontology and Implant Dentistry*, 3rd ed. Copenhagen: Munksgaard, 1998:19–68.
10. Ochsenbein C, Ross S. A reevaluation of osseous surgery. *Dent Clin North Am* 1969;13:87–102.
11. Becker W, Ochsenbein C, Tibbetts L, Becker BE. Alveolar bone anatomic profiles as measured from dry skulls: clinical ramifications. *J Clin Periodontol* 1997;24:727–31.
12. Weisgold AS. Contours of the full crown restoration. *Alpha Omegan* 1997;70:7–89.
13. Olsson M, Lindhe J. Periodontal characteristics in individuals with varying form of the upper central incisors. *J Clin Periodontol* 1991;18:78–82.
14. Lee DW, Kim CK, Park KH, Cho KS, Moon IS. Non-invasive method to measure the length of soft tissue from the top of the papilla to the crestal bone. *J Periodontol* 2005;76:1311–4.
15. Cho HS, Jang HS, Kim DK, et al. The effects of interproximal distance between roots on the existence of interdental papillae according to the distance from the contact point to the alveolar crest. *J Periodontol* 2006;77:1651–7.
16. Wu YJ, Tu YK, Huang SM, Chan CP. The influence of the distance from the contact point to the crest of bone on the presence of the interproximal dental papilla. *Chang Gung Med J* 2003;26:822–8.
17. Chang LC. The presence of a central papilla is associated with age but not gender. *J Dent Sci* 2006;1:161–7.
18. Chang LC. The central papilla height in association with age and gender—assessed with a new method. *Chin J Periodontol* 2006;11:271–9.

19. Chang LC. The association between embrasure morphology and central papilla recession. *J Clin Periodontol* 2007;34: 432–6.
20. Loe H, Silness J. Periodontal disease in pregnancy, I: prevalence and severity. *Acta Odontol Scand* 1963;21: 533–51.
21. Attaelmanan A, Borg E, Grondahl HG. Digitisation and display of intra-oral films. *Dentomaxillofac Radiol* 2000;29: 97–102.
22. Kim TS, Benn DK, Eickholz P. Accuracy of computer-assisted radiographic measurement of interproximal bone loss in vertical bone defects. *Oral Surg Oral Med Oral Pathol Oral Radiol Endod* 2002;94:379–87.
23. Liang KY, Zeger SL. Longitudinal data analysis using generalized linear models. *Biometrika* 1986;73:13–22.
24. Liang KY, Zeger SL. Regression analysis for correlated data. *Annu Rev Public Health* 1993;14:43–68.
25. Grunder U. Stability of the mucosal topography around single-tooth implants and adjacent teeth: 1-year results. *Int J Periodontics Restorative Dent* 2000;20:11–7.
26. Muller HP, Schaller N, Eger T. Ultrasonic determination of thickness of masticatory mucosa: a methodologic study. *Oral Surg Oral Med Oral Pathol Oral Radiol Endod* 1999; 88:248–53.
27. Muller HP, Schaller N, Eger T, Heinecke A. Thickness of masticatory mucosa. *J Clin Periodontol* 2000;27:431–6.
28. Olsson M, Lindhe J, Marinello CP. On the relationship between crown form and clinical features of the gingiva in adolescents. *J Clin Periodontol* 1992;20:570–7.
29. Jemt T. Regeneration of gingival papillae after single implant treatment. *Int J Periodontics Restorative Dent* 1997; 17:327–33.
30. Nemcovsky CE, Moses O, Artzi Z. Interproximal papillae reconstruction in maxillary implants. *J Periodontol* 2000; 71:308–14.
31. Lee DW, Park KH, Moon IS. Dimension of keratinized mucosa and the interproximal papilla between adjacent implants. *J Periodontol* 2005;76:1856–60.
32. Martegani P, Silvestri M, Mascarello F, et al. Morphometric study of the interproximal unit in the esthetic region to correlate anatomic variables affecting the aspect of soft tissue embrasure space. *J Periodontol* 2007;78:2260–5.
33. Lee DW, Park KH, Moon IS. Dimension of interproximal soft tissue between adjacent implants in two distinctive implant systems. *J Periodontol* 2006;77:1080–4.
34. Garguilo AW, Wentz FM, Orban B. Dimensions of the dentogingival junction in humans. *J Periodontol* 1961;32:261–7.
35. Kois JC. Altering gingival levels: the restorative connection, part 1: biologic variables. *J Esthet Dent* 1994;6:3–9.
36. Ingber JS, Rose LF, Coslet JG. The "biological width"—a concept in periodontics and restorative dentistry. *Alpha Omegan* 1977;70:62–5.
37. Vacek JS, Gher ME, Assad DA, Richardson AC, Giambarresi LI. The dimensions of human dentogingival junction. *Int J Periodontics Restorative Dent* 1994;14:154–65.
38. Orban B, Kohler J. Die physiologische Zahn-fleischtasche, Epithelansatz und Epitheltiefenwucherung. *Z Stomatol* 1924; 22:353.
39. Weski O. Die chronische marginales Entzündungen des Alveolar-fortsatzes mit besonderer Berücksichtigung der Alveolrpyorrhoe. *Vierteljahrschr Zahnheilk* 1922;38:1.
40. Tarnow D, Elian N, Fletcher P, et al. Vertical distance from the crest of bone to the height of the interproximal papilla between adjacent implants. *J Periodontol* 2003;74:1785–8.
41. Bowers GM. A study of the width of the attached gingiva. *J Periodontol* 1963;34:210.
42. Ainamo J, Talari A. The increase with age of the width of attached gingiva. *J Periodontal Res* 1976;11:182–8.
43. Wennström JL, Lindhe J, Nyman S. Role of keratinized gingiva for gingival health: clinical and histologic study of normal and regenerated gingival tissue in dogs. *J Clin Periodontol* 1981;8:311–28.
44. Wennström JL, Lindhe J, Nyman S. The role of keratinized gingiva in plaque-associated gingivitis in dogs. *J Clin Periodontol* 1982;9:75–85.
45. Wennström JL. Mucogingival considerations in orthodontic treatment. *Semin Orthod* 1996;2:46–54.
46. Wara-aswapati N, Pitiphat W, Chandrapho N, Rattanayatikul C, Karimbux N. Thickness of palatal masticatory mucosa associated with age. *J Periodontol* 2001;72:1407–12.
47. Karring T, Löe H. A computerized method for quantitative estimation of the epithelium-connective tissue interface applied to the gingiva of various age groups. *Acta Odontol Scand* 1973;31:241–8.
48. Berglundh T, Lindhe J, Sterrett JD. Clinical and structural characteristics of periodontal tissues in young and old dogs. *J Clin Periodontol* 1991;18:616–23.
49. Vandana KL, Savitha B. Thickness of gingiva in association with age, gender and dental arch location. *J Clin Periodontol* 2005;32:828–30.
50. Miller PD Jr, Allen EP. The development of periodontal plastic surgery. *Periodontol 2000* 1996;11:7–17.
51. Nemcovsky CE. Interproximal papilla augmentation procedure: a novel surgical approach and clinical evaluation of 10 consecutive procedures. *Int J Periodontics Restorative Dent* 2001;21:553–9.
52. Han TJ, Takei HH. Progress in gingival papilla reconstruction. *Periodontol 2000* 1996;11:65–8.
53. Azzi R, Etienne D, Carranza F. Surgical reconstruction of the interdental papilla. *Int J Periodontics Restorative Dent* 1998;18:466–73.
54. Azzi R, Etienne D, Sauvan JL, Miller PD. Root coverage and papilla reconstruction in Class IV recession: a case report. *Int J Periodontics Restorative Dent* 1999;19:449–55.

J Dent Sci 2009;4(3):110–117

ORIGINAL ARTICLE

Fracture resistance and failure modes of CEREC endo-crowns and conventional post and core-supported CEREC crowns

*Chia-Yu Chang,[1] Jau-Shing Kuo,[1] Yang-Sung Lin,[2] Yen-Hsiang Chang[1]**

[1]Department of Operative Dentistry, Chang Gung Memorial Hospital, Tao-Yuan, Taiwan
[2]Department of Mechanical Engineering, Chang Gung University, Kweishan, Taoyuan, Taiwan

Received: May 14, 2009
Accepted: Aug 15, 2009

KEY WORDS:
CAD-CAM;
CEREC;
endo-crown;
failure modes;
fracture resistance

Background/purpose: The purpose of this *in vitro* study was to compare the fracture resistance and failure modes of CEREC endo-crowns with the CEREC classic designed crown supported with glass fiber-reinforced composite posts and composite cores. The influences of thermal cycling and fatigue loading on both types of restorations were also investigated.
Materials and methods: Twenty extracted intact maxillary premolars were randomly divided into two groups (C and E). The crown portion of the specimens was removed to 1.5 mm above the cementoenamel junction (CEJ). All specimens were endodontically treated with a nickel-titanium rotary system and obturated with gutta-percha by a vertical compaction technique. In group C (n=10), teeth were restored with glass fiber-reinforced composite posts and composite cores with a 1.0-mm wide circumferential shoulder margin at the CEJ and a 1.5-mm ferrule. In group E (n=10), teeth were prepared for fabrication of CEREC endo-crowns. Both types of ceramic crowns were produced from ProCAD ceramic blocks utilizing a CEREC 3D CAD-CAM unit, and these were bonded to the preparations with an adhesive system and composite resin cement. Teeth were thermally cycled (2000 cycles of 5°C/55°C with a dwell time of 30 seconds,) and fatigue loaded (20,000 cycles at 5 kg and 3 Hz) in a custom-made fatigue simulator. All specimens were loaded in a universal testing machine with a cross-head speed of 0.5 mm/s until fracture occurred. Fracture resistance and failure modes were statistically evaluated with a t test and χ^2 test.
Results: The mean fracture resistance±standard deviation was recorded as follows: 1163.30±163.15 N for group C and 1446.68±200.34 N for group E. A significant difference was found between groups with respect to fracture resistance ($P<0.05$). Regarding failure modes, most specimens of both groups exhibited unfavorable fractures, and no significant difference was found between the two groups.
Conclusion: The bonded ceramic endo-crowns showed a significantly higher fracture resistance than the classic reinforced and designed group and, therefore, offer a feasible alternative for severely damaged teeth.

*Corresponding author. Department of Operative Dentistry, Chang Gung Memorial Hospital, 123, Ding-Hu Road, Kueishan, Taoyuan 33345, Taiwan.
E-mail: cyh4714@hotmail.com

Introduction

The rehabilitation of severely damaged coronal hard tissue and endodontically treated teeth is always a challenge in reconstructive dentistry. Clinical concepts regarding the restoration of non-vital teeth are controversial and are based on profuse and inconclusive empirical literature. The primary reason for reduction in stiffness and fracture resistance of endodontically treated teeth is the loss of structural integrity associated with caries, trauma, and extensive cavity preparation, rather than dehydration or physical changes in the dentin.[1–4] Reduction of the tooth architecture results in increased cuspal deflection during loading (either continuous or cyclic) and delayed cuspal recovery following removal of the load.[5–7] Therefore, the loss of structural integrity increases the occurrence of crown fractures and microleakage at the margins of restorations in endodontically treated teeth compared with "vital" teeth.[4,8] Additionally, the lack of vitality greatly restrains the sensory feedback during peak loads and results in non-vital teeth being more prone to fracture.

The classical approach for restoring endodontically treated teeth is to build up the tooth with a post and core, which have physical properties close to those of natural dentin, utilizing adhesive procedures and placement of full-coverage crowns with a sufficient ferrule.[9–11] A ferrule with 1 mm of vertical height was shown to double the resistance to fracture versus teeth restored without a ferrule.[12] Another study showed that a ferrule with 1.5–2 mm of vertical tooth structure has maximum beneficial effects and more favorable fracture patterns.[13] With this understanding, additional treatments such as surgical crown lengthening or orthodontic tooth extrusion are recommended if the minimal ferrule effect cannot be obtained.[1,14] Additionally, a significantly lower static failure load occurs after crown lengthening is accomplished.[15] Preparation of a post space also increases the risk of accidental root perforation.

With recent developments of adhesive techniques and ceramic materials, the advantage of adhesive restorations is that a macroretentive design is no longer a prerequisite if there are sufficient tooth surfaces for bonding. With the adhesive technique, creating a ferrule is a drawback because of loss of the natural tooth structure and enamel. Minimally invasive preparations to preserve a maximum amount of tooth structure are considered the gold standard for restoring teeth. Endo-crowns strictly follow this rationale owing to a decay-orientated design concept. This type of preparation consists of a circumferential 1.0–1.2-mm butt margin and a central retention cavity inside the pulp chamber, and constructs both the crown and core as a single-unit, i.e., a "monobloc".[16,17] The monobloc foundation of this technique utilizes the available surface in the pulp chamber to obtain stability and retention of the restoration through adhesive bonding. Moreover, dental computer-aided design/computer-aided manufacturing (CAD-CAM) systems realize the possibility of chair-side design and automatic production of these single-unit ceramic restorations.

In vitro studies reported that bonded endo-crowns showed comparable fracture load values compared with conventional crowns.[18,19] Several clinical case reports showed the potential of this restorative approach to provide adequate function and esthetics, even with compromised tooth integrity of non-vital molars.[17,20–24] Two techniques were demonstrated for the production of all-ceramic endo-crowns: the single-visit CEREC 3D (Sirona Dental Systems, Bensheim, Germany) CAD-CAM technique and the Empress II (Ivoclar Vivadent, Schaan, Liechtenstein) pressed ceramic technique. Bindl and Mörmann[16] reported that 19 adhesively bonded CEREC endo-crowns (4 premolars and 15 molars) in 13 patients functioned satisfactorily for over 28 months, and the only molar endo-crown which failed was because of recurrent caries. The overall clinical quality of CEREC endo-crowns was good, and the clinical concepts appeared feasible. However, the samples used in most of those clinical cases were molars or incisors.

Salis et al.[25] described a higher prevalence of fractured maxillary premolars compared with mandibular premolars. In the maxilla, 49% of fractures occurred in premolars, of which half involved the functional cusp. Maxillary premolars are usually bulkier than the anterior teeth, but are often single-rooted teeth. The height of the cusps is more highly related to the area of the base. Consequently, they are more likely to be subjected to lateral forces during mastication than molars because of the steep cuspal incline. Therefore, all of these factors make maxillary premolars prone to fracture after restoration.

Clinically, the accumulation of microstructural damage during mastication, which is enhanced in an aqueous environment,[26] may induce catastrophic failure, while prior cyclic loading significantly decreases the fracture strength of all-ceramic crowns.[27] Since fatigue loading and thermal cycling are important factors in regard to the clinical performance of restorations, their influences on both types of restorations were also investigated in the present study.

This *in vitro* study examined the fracture resistance and fracture modes after thermal cycling and fatigue loading of CEREC endo-crowns and classically constructed CEREC ceramic crowns with glass fiber-reinforced composite posts in extensively

damaged and endodontically treated maxillary premolars. The hypotheses of this study were as follows:

1. There is no difference between the mean fracture resistance of teeth restored with CEREC endo-crowns and that of teeth restored with classic CEREC ceramic crowns with a glass fiber-reinforced composite resin post and composite resin core.
2. Endo-crowns have more favorable fracture properties than conventional post and core-supported CEREC crowns.

Materials and methods

Twenty intact, non-carious, human maxillary premolars without cracks, extracted for orthodontic reasons, were cleaned and stored at 18ºC in normal saline and randomly assigned to two groups of 10 teeth each. Teeth of similar size and shape were selected by root length and crown dimensions after measuring the buccolingual and mesiodistal widths at the cementoenamel junction (CEJ) in millimeters, and allowing a maximum deviation of 10% from the mean.[8] The crown portion of all premolars was removed to within 1.5 mm above the CEJ and endodontically treated with ProTaper nickel-titanium (Ni-Ti) rotary files, a 16:1 contra angle handpiece, and ATR Tecnika Vision Motor (Dentsply Maillefer, Ballaigues, Switzerland) according to the manufacturer's instructions, and was obturated with gutta-percha by a vertical compaction technique. Specimens were restored with classic CEREC all-ceramic crowns in group C, while teeth were restored with CEREC endo-crowns in group E (Fig. 1).

In group E, the "endo" preparation consisted of a circular butt margin with a depth of the central retention cavity of 5 mm from the cavosurface margin with rounded internal line angles.[17] In group C, all specimens were prepared with a 1.0-mm-wide circumferential butt margin at the CEJ and a 1.5-mm ferrule. The standardized depth was verified using a scaled periodontal probe (instrument number 23/UNC 15; Hu-Friedy, Chicago, IL, USA). All preparations were made by means of a number 56 high-speed bur (60018; Midwest, Des Plaines, IL, USA) with water coolant; the bur was replaced every five preparations. In group C, tapered glass fiber-reinforced composite posts (Premier Anatomic IP-110-VR; Innotech, Robbio, Pavia, Italy) were identically adhesively cemented to teeth with All-Bond 1 and C & B Cement (Bisco, Schaumburg, IL, USA) according to the manufacturer's instructions, leaving a 5-mm apical gutta-percha seal, and a built up composite resin core (A2, Filtek Z250; 3M ESPE, Seefeld, Germany).

Both the ceramic endo-crowns (group E) and conventional ceramic crowns (group C) were designed using the CEREC 3D CAD-CAM unit (Sirona Dental Systems) and machined from ProCAD leucite-reinforced ceramic blocks (200, I14; Ivoclar Vivadent). CEREC software version 3.01 (Sirona Dental Systems) and the "crown/correlation" mode were used for the construction of the experimental crowns. The all-ceramic crowns were fitted and polished using CeramiPro Dialite polishing discs (L260DBC, L260 DRM and L260GXF; Brasseler, Savannah, GA, USA).

Before insertion, the intaglio surfaces of the ceramic crowns were etched with hydrofluoric acid (Ultradent Porcelain Etch, 9%; Ultradent Products, South Jordan, UT, USA) for 60 seconds, then rinsed for 60 seconds with running water and dried for 30 seconds with oil-free air. A silane-coupling agent (Monobond S; Ivoclar Vivadent) was applied and allowed to dry for 1 minute. The abutments were etched with 37% phosphoric acid-etching gel (Ultra Etch; Ultradent Products) for 40 seconds, rinsed for 30 seconds, and dried with oil-free air for another 20 seconds. The adhesive system (Syntac Classic; Ivoclar Vivadent) was applied to the preparations according to the manufacturer's instructions.

All crowns were adhesively luted with Variolink II luting composite resin cement (low viscosity; Ivoclar Vivadent). The Variolink II base and catalyst were mixed at a 1:1 ratio and coated onto the inner surface of the crowns. Crowns were seated with light finger pressure, and excess luting material was removed. The light-polymerizing unit (Bluephase; Ivoclar Vivadent) was held on the buccal, mesial, lingual, distal and occlusal surfaces for 1 minute. The curing power was 1200 mW/cm^2. The curing mode was initiated with a soft start for 30 seconds, followed by high-power mode for 30 seconds.

Before testing, each tooth was vertically mounted in self-cured acrylic resin (Truetime Industrial, Tainan, Taiwan) in customized stainless steel mounting rings for the thermal cycling, fatigue loading, and load-to-failure test. The crowns of the teeth remained free of the acrylic, and the root was covered to a height 2 mm below the CEJ (which is approximately the level of alveolar bone in a healthy tooth). The rings were removed following the mounting procedure. All specimens were stored in saline at room temperature for 24 hours before testing.

Specimens were subjected to thermocycling at 5ºC for 30 seconds and at 55ºC for 30 seconds for 2000 cycles in a thermal cycling machine (custom made; Chang Gung University, Taoyuan, Taiwan).

According to a study by Chen et al.[27], the rapid rate of decline in strength of a ceramic restoration leveled off after 10,000 cycles of dynamic loading. Hence, all specimens were prior fatigue-loaded

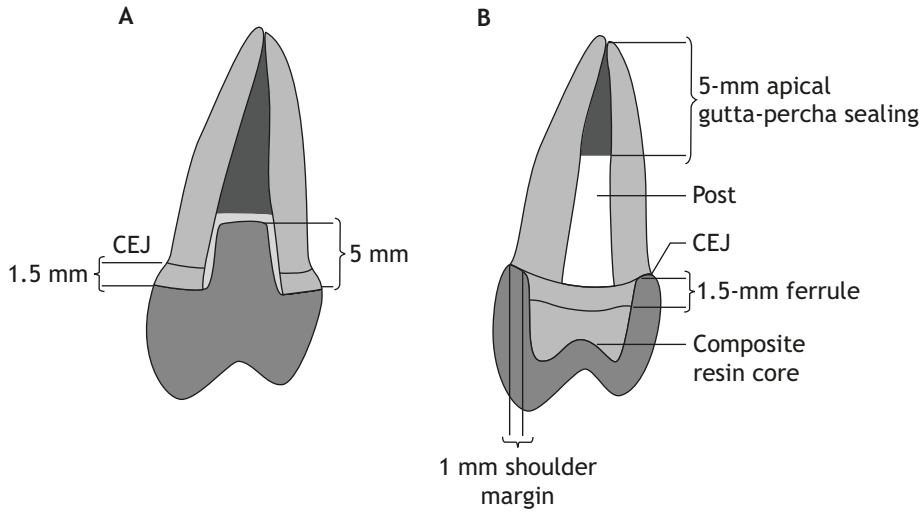

Fig. 1 Scheme of tooth preparation of the experimental teeth. (A) Group E: "endo" preparation. (B) Group C: classic preparation. CEJ=cementoenamel junction.

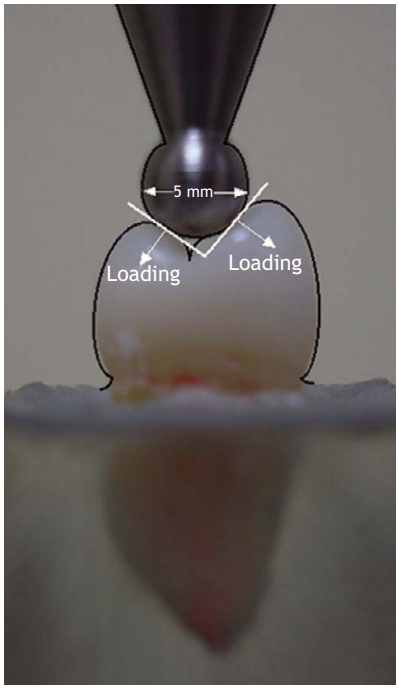

Fig. 2 Position of the specimen in the setup for cycling and static loading.

with 5 kg/cm^2 at 3 Hz for 20,000 cycles in the fatigue simulator (custom made; Chang Gung University). Steel spheres (5.00-mm radius of curvature), the same as those used in the load-to-failure test, were used as antagonists against the test crowns and were loaded cyclically at the same area of the crowns as in the universal testing machine. Each specimen was identically positioned in a metal holder so that the steel sphere simultaneously contacted the two cuspal inclines and was loaded along the long axis of the specimen (Fig. 2). For the load-to-failure test, 20 crowns from both groups were loaded in the universal testing machine with a cross-head speed of 0.5 mm/s until facture occurred.

The fracture resistance was recorded in newtons, and the failure modes of all samples were assessed from periapical radiographs after fracture by two observers. "Favorable failures" were defined as repairable failures above the level of bone simulation and included adhesive failures. On the contrary, "unfavorable failures" were defined as non-repairable, catastrophic failures below the level of bone simulation, including vertical root fractures.[28] The fracture resistance was evaluated by *t* test statistics, and a χ^2 test was used to compare the failure modes of specimens. The level of significance was set at $P<0.05$.

Results

The mean, median, standard deviation, and minimum and maximum fracture resistances are shown in Table 1. Group E revealed a higher mean fracture resistance (1446.68±200.34 N) than that of group C (1163.30±163.15 N), and the independent *t* test revealed a statistically significant difference between the mean fracture resistance of the two groups ($P=0.0039$). All tooth specimens of both groups fractured in a direction continuous with the fracture line of the crown. The failure modes are shown in Table 2. Most of the failure modes in both groups were unfavorable (65%). The majority of the failure modes (55%) consisted of an oblique shearing of the buccal cusp from the occlusal fissure to the buccal coronal third of the root area. One classic ceramic crown lost adhesion of the resin to the dentin and completely broke. A crack line in a

Table 1. Fracture strength (in newtons) of the two groups

Fracture strength (N)	Group E ($n=10$)	Group C ($n=10$)
Mean	1446.68*	1163.30*
Median	1472.18	1110.61
Standard deviation	200.34	163.15
Maximum	1745.42	1408.20
Minimum	1120.00	1000.50

*Fracture loads significant differed, P=0.0039 (*t* test). Standard deviation Group E=group with endo-crowns; Group C = group with classic all-ceramic crowns.

Table 2. Frequencies of different fracture modes in the two groups

	Group E* ($n=10$)	Group C* ($n=10$)
Unfavorable fracture		
Buccal cusp	5	4
Palatal cusp	1	2
Both cusps	1	
Favorable fracture		
Buccal cusp	1	1
Palatal cusp	2	2
Both cusps		1

*Fracture modes did not significant differ, P = 0.6392 (χ^2 test). Group E = group with endo-crowns; Group C = group with classic all-ceramic crowns.

mesiodistal direction was observed on another abutment. The χ^2 test demonstrated no significant difference in the frequencies of favorable and unfavorable failure modes between the two groups (P=0.639).

Discussion

This *in vitro* study simulated the "compromised biomechanical condition" of severely damaged and endodontically treated maxillary premolars. The classical treatment option is a custom-made casting post-and-core covered by metal or porcelain fused to a metal crown with a sufficient ferrule. However, Gegauff[15] reported that surgical crown lengthening to create a ferrule demonstrated a significantly lower static failure load because of the decrease in the cross section of the preparation combined with an altered crown-to-root ratio. Creating a sufficient ferrule might cause the loss of sound tooth structure and result in compromised bonding strength, because enamel is preferred to dentin for bonding.[29,30] In the present study, creating a sufficient ferrule might have been one of the reasons that the classic crown had a lower fracture resistance than the endo-crowns.

The thickness of the ceramic occlusal portion of endo-crowns is usually 3–7 mm. An *in vitro* study showed that the fracture resistance of ceramic crowns increases with increasing occlusal thickness.[31] Mörmann et al.[18] also reported that the fracture resistance of endo-crowns with an occlusal thickness of 5.5 mm was two times higher than that of ceramic crowns with a classic preparation and an occlusal thickness of 1.5 mm. In this study, the higher fracture resistance of adhesively bonded ceramic endo-crowns corresponded with those previous reports.

Clinically, the normal biting force is 222–445 N for the maxillary premolar area,[32] and the occlusal force was observed to be as high as 520–800 N during clenching.[33] It was also reported that intact maxillary premolars fractured at a load of approximately 1121–1124.6 N.[8,34] This study showed that the fracture resistance of endo-crowns was greater than that of intact premolars, and the endo-crown design could restore the structural integrity and the strength of an endodontically treated and severely decayed tooth. However, Bindl et al.[35] reported that the survival rate of CEREC endo-crowns over 55 months was comparable to classically constructed crowns on molars (87.1%), but was inadequate for premolar crowns (68.8%). It is noteworthy that all of the failures of endo-crowns on premolars in that study were caused by loss of adhesion. Loss of adhesion of endo-crowns on premolars may have been because the surface for adhesive bonding was smaller, and the greater ratio of the prepared tooth structure to the overall crown and cusp height resulted in higher leverage on the premolars than molars. Salis et al.[25] also described that premolars with deep occlusal fissures are more flexible than those with shallow or no fissures. Therefore, the morphologic design of the endo-crown on maxillary premolars should have a flatter occlusal table to reduce the height of the crown and the cuspal inclines resulting in shallower fissures to reduce cuspal deflection and the risk of fracture during mastication.

The use of human teeth as abutment material in this study might have increased the variability of the fracture load compared with artificial manufactured abutments. Additional variable factors which must be considered are the tooth anatomy, abutment retention after manual preparation, and the character of the surface structure for bonding. In spite of these variables, the use of human teeth as the abutment material more closely approximates a clinical situation with respect to tooth architecture and morphology. Furthermore, the dentin and enamel surface for bonding, the contour of the pulp

chamber and root canals for post placement, and the ratio between the crown and root are more accurate than on an artificial resin tooth. At the same time, the selection of teeth of similar sizes and shapes was performed before testing to minimize possible variations and errors.

In this study, the lack of a simulated periodontal ligament was permissible, because it was expected that with single crowns, there is practically no difference in the fracture resistance between teeth with and without this shock absorbing layer around roots under a static loading test. Furthermore, our experience with artificial silicone periodontium around the roots of abutment teeth showed that the thickness of the silicone layers is more than that in clinical situations. Moreover, a non-standardized artificial silicone periodontium might cause uncontrolled mobility of abutment teeth and more errors. In despite of the conformity of the strength of the restored teeth, the fracture patterns of static loading and rigidly mounted teeth might be atypical of those found clinically. The slow loading rate of static loading did not simulate the clinical situation in which tooth fractures occur quickly and accidentally.

Most of the failure modes of both groups in the present study were unfavorable (65%), and the majority of failure modes (55%) were an oblique shearing of the buccal cusp from the occlusal fissure to the buccal coronal third of the root. The fracture path for maxillary premolars in the present study was similar to that of intact maxillary premolars receiving repeated rapid impacts as reported by Salis and colleagues.[25] Most of the fractures involving the root imply that a significant amount of force was transmitted to the root. Consequently, when fractures are so severe, extensive surgical crown lengthening is often required. From this aspect, extraction might be a more suitable treatment option.

Stress distribution and initiation of fracture were not specifically examined in this study. According to the failure modes in the present study, the major stress concentration was at the base of the occlusal fissure. This finding is in accord with a report by Salis and coworkers.[25] Zarone et al.[36] reported that the stress concentration in maxillary central incisors restored with an endo-crown is at the interface according to a three-dimensional finite element analysis. The interfaces of materials with different elastic moduli result in a weak point of a restorative system, because the stiffness mismatch of different materials influences the stress distribution. Differences in the elastic moduli among ceramic, luting cement and the dentin might pose a risk of root fracture. Newly developed materials with mechanical properties as similar as possible to those of natural tooth hard tissues may decrease the frequency of unfavorable root fractures.

The loading position and loading angle relative to the post site in group C may have influenced the fracture modes, because tensile stresses at the adhesive interfaces among the glass fiber-reinforced composite post, the composite resin core, and the ceramic crown would weaken the structure. Using an endo-crown restoration presents an advantage of reducing the effect of multiple interfaces in the restorative system and thereby makes the experimental tooth more similar to a monobloc.

In considering the effect of loading cycles, DeLong et al.[37] and Sakaguchi et al.[38] reported that amalgam and composite material wear produced after 240,000 to 250,000 masticatory cycles in a chewing simulator corresponded to the wear measured after 1 year of clinical service. Therefore, in most laboratory studies, 1,200,000 cycles are used to simulate a service time of 5 years.[38] According to another study,[27] the fracture load of Vita Mark II crowns showed a decrease with increasing load cycles, and the rapid rate of decline in fracture strength leveled off after 10,000 cycles of loading. However, these correlations may only be related to the specific materials tested with specific parameters, so they cannot be generalized too widely. In the present study, the fatigue test was only run for 20,000 cycles to reduce operation and evaluation time. None of the ProCAD crowns subjected to this amount of cyclic loading demonstrated any evidence of cracking. Perhaps a higher number of fatigue cycles would have produced different results, with evidence of cracks during dynamic loading and lower fracture load values.

The development of in-office CAD-CAM systems and software offers several advantages in clinical practice. First, with the change in the grinding system from discs to a stepped cylindrical diamond bur and a cylindrical diamond with a tapered tip, the more-flexible CAD-CAM shaping technique allows custom shaping and more precise milling of ceramic crowns. Furthermore, the adaptation of the inner surface of a restoration and the replication of the occlusal morphology are better. Second, endo-crowns can be produced and seated in one appointment. Third, this method saves time and reduces expenses associated with a build-up procedure of the post and core. Despite these advantages, there are clinical problems with the depth of the optical impression to record the crown, pulp chamber, and part of the canal. According to a study by Mörmann and Bindl,[39] the depth scale of the intraoral scanning camera is limited to a single value of 6.4 mm with CEREC 2. Even with the time-consuming effort required for software-supported adjustments, the optical depth of field is 14 mm. The limited optical depth of field might result in a blurred image of the central retention cavity of the endo preparation if

adjacent teeth limit the position of the camera head. With improvements in the intraoral three-dimensional scanning camera of the CEREC 3D unit, the depth scale is extended to about 20 mm through "double triangulation". Extended depth of field through double triangulation, thereby, overcomes this limitation.[39]

According to the results of the present study, the first hypothesis was accepted, and the fracture resistance of CEREC endo-crowns was better than that of classic crowns. The second hypothesis was rejected, since there was no significant difference in the failure modes between the two groups.

In summary, endo-crowns provide an alternative to conventional treatment of severely compromised posterior teeth, especially in situations such as a flared root canal, inadequate clinical crown length, and insufficient interocclusal space. According to the present study, endo-crowns should be considered a feasible, conservative and esthetic restorative approach. These adhesive monobloc restorations preserve the maximum tooth structure, reduce the need for a macroretentive geometry, and provide more efficient and better esthetic results than metal or porcelain fused to metal crowns. Despite the suggestion by Pissis[17] that there must be a 3-mm diameter cylindrical pivot and 5-mm depth for the first maxillary premolars and at least 5-mm diameter and 5-mm depth for molars, the precise dimensions of the central retention cavity of the endo preparation are not clearly determined. Further prospective *in vitro* and *in vivo* studies to evaluate the determinative factors and dimensions of the central retention cavity and clinical studies to test the longevity of endo-crowns as a single prosthesis and abutment of fixed partial dentures are necessary.

Acknowledgments

The authors greatly thank Mr Yu-Wen Chang, technician of the Department of General Dentistry, Chang Gung Memorial Hospital, Tao-Yuan, Taiwan, for his kind assistance in designing and fabricating the CEREC crowns. Assistance with material testing from Dr Chun-Li Lin and Mr Chih-Chao Yang, Department of Mechanical Engineering, Chang Gung University, Taoyuan, Taiwan, is also highly appreciated.

References

1. Schwartz RS, Robbins JW. Post placement and restoration of endodontically treated teeth: a literature review. *J Endod* 2004;30:289–301.
2. Papa J, Cain C, Messer HH. Moisture content of vital vs endodontically treated teeth. *Endod Dent Traumatol* 1994; 10:91–3.
3. Huang TJ, Schilder H, Nathanson D. Effects of moisture content and endodontic treatment on some mechanical properties of human dentin. *J Endod* 1992;18:209–15.
4. Reeh ES, Messer HH, Douglas WH. Reduction in tooth stiffness as a result of endodontic restorative procedures. *J Endod* 1989;15:512–6.
5. Panitvisai P, Messer HH. Cuspal deflection in molars in relation to endodontic and restorative procedures. *J Endod* 1995;21:57–61.
6. Jantarat J, Palamara JE, Messer HH. An investigation of cuspal deformation and delayed recovery after occlusal loading. *J Dent* 2001;29:363–70.
7. Gutmann JL. The dentin-root complex: anatomic and biologic considerations in restoring endodontically treated teeth. *J Prosthet Dent* 1992;67:458–67.
8. Soares PV, Santos-Filho PC, Martins LR, Soares CJ. Influence of restorative technique on the biomechanical behavior of endodontically treated maxillary premolars, part I: fracture resistance and fracture mode. *J Prosthet Dent* 2008; 99:30–7.
9. Bitter K, Kielbassa AM. Post-endodontic restorations with adhesively luted fiber-reinforced composite post systems: a review. *Am J Dent* 2007;20:353–60.
10. Dietschi D, Duc O, Krejci I, Sadan A. Biomechanical considerations for the restoration of endodontically treated teeth: a systematic review of the literature, part I: composition and micro- and macrostructure alterations. *Quintessence Int* 2007;38:733–43.
11. Dietschi D, Duc O, Krejci I, Sadan A. Biomechanical considerations for the restoration of endodontically treated teeth: a systematic review of the literature, part II: evaluation of fatigue behavior, interfaces, and in vivo studies. *Quintessence Int* 2008;39:117–29.
12. Sorensen JA, Engelman MJ. Ferrule design and fracture resistance of endodontically treated teeth. *J Prosthet Dent* 1990;63:529–36.
13. Zhi-Yue L, Yu-Xing Z. Effects of post-core design and ferrule on fracture resistance of endodontically treated maxillary central incisors. *J Prosthet Dent* 2003;89:368–73.
14. Sivers JE, Johnson WT. Restoration of endodontically treated teeth. *Dent Clin North Am* 1992;36:631–50.
15. Gegauff AG. Effect of crown lengthening and ferrule placement on static load failure of cemented cast post-cores and crowns. *J Prosthet Dent* 2000;84:169–79.
16. Bindl A, Mörmann WH. Clinical evaluation of adhesively placed Cerec endo-crowns after 2 years—preliminary results. *J Adhes Dent* 1999;1:255–65.
17. Pissis P. Fabrication of a metal-free ceramic restoration utilizing the monobloc technique. *Pract Periodontics Aesthet Dent* 1995;7:83–94.
18. Mörmann WH, Bindl A, Lüthy H, Rathke A. Effect of preparation and luting system on all-ceramic computer-generated crowns. *Int J Prosthodont* 1998;11:333–9.
19. Deesri W, Kunzelmann KH, Ilie N, Hickel R. Fracture strength and Weibull evaluation of the Cerec endocrowns and post-and-core-supported conventional Cerec crowns (abstract 0872). Proceedings of the 81st General Session of the International Association for Dental Research, June 25–28, 2003, Goteborg, Sweden.
20. Lander E, Dietschi D. Endocrowns: a clinical report. *Quintessence Int* 2008;39:99–106.
21. Valentina V, Aleksandar T, Dejan L, Vojkan L. Restoring endodontically treated teeth with all-ceramic endo-crowns—case report. *Stom Glas S* 2008;55:54–64.
22. Otto T. Computer-aided direct all-ceramic crowns: preliminary 1-year results of a prospective clinical study. *Int J Periodontics Restorative Dent* 2004;24:446–55.
23. Göhring TN, Peters OA. Restoration endodontically treated teeth without posts. *Am J Dent* 2003;16:313–8.

24. Adams T. Restoration of an endodontically treated tooth utilizing a single-unit crown and core system. *Pract Periodontics Aesthet Dent* 2000;12:105–8.
25. Salis SG, Hodd JA, Stokes AN, Kirk EE. Pattern of indirect fracture in intact and restored human premolar teeth. *Endod Dent Traumatol* 1987;3:10–4.
26. Wiederhorn SM. Moisture assisted crack growth in ceramics. *Int J Fract Mech* 1968;4:171–7.
27. Chen HY, Hickel R, Setcos JC, Kunzelmann KH. Effects of surface finish and fatigue testing on the fracture strength of CAD-CAM and pressed-ceramic crowns. *J Prosthet Dent* 1999;82:468–75.
28. Fokkinga WA, Le Bell AM, Kreulen CM, Lassila LV, Vallittu PK, Creugers NH. Ex vivo fracture resistance of direct resin composite complete crowns with and without posts on maxillary premolars. *Int Endod J* 2005;38:230–7.
29. Van Meerbeek B, De Munck J, Yoshida Y, et al. Buonocore memorial lecture. Adhesion to enamel and dentin: current status and future challenges. *Oper Dent* 2003;28: 215–35.
30. Tezvergil A, Lassila LV, Vallittu PK. Strength of adhesive-bonded fiber-reinforced composites to enamel and dentin substrates. *J Adhes Dent* 2003;5:301–11.
31. Tsai YL, Petsche PE, Anusavice KJ, Yang MC. Influence of glass-ceramic thickness on Hertzian and bulk fracture mechanisms. *Int J Prosthodont* 1998;11:27–32.
32. Widmalm SE, Ericsson SG. Maximal bite force with centric and eccentric load. *J Oral Rehabil* 1982;9:445–50.
33. Hidaka O, Iwasaki M, Saito M, Morimoto T. Influence of clenching intensity on bite force balance, occlusal contact area, and average bite pressure. *J Dent Res* 1999;78:1336–44.
34. Hannig C, Westphal C, Becker K, Attin T. Fracture resistance of endodontically treated maxillary premolars restored with CAD/CAM ceramic inlays. *J Prosthet Dent* 2005;94:342–9.
35. Bindl A, Richter B, Mörmann WH. Survival of ceramic computer-aided design/manufacturing crowns bonded to preparations with reduced macroretention geometry. *Int J Prosthodont* 2005;18:219–24.
36. Zarone F, Sorrentino R, Apicella D, et al. Evaluation of the biomechanical behavior of maxillary central incisors restored by means of endocrowns compared to a natural tooth: a 3D static linear finite elements analysis. *Dent Mater* 2006;22:1035–44.
37. DeLong R, Sakaguchi RL, Douglas WH, Pintado MR. The wear of dental amalgam in an artificial mouth: a clinical correlation. *Dent Mater* 1985;1:238–42.
38. Sakaguchi RL, Douglas WH, DeLong R, Pintado MR. The wear of a posterior dental composite in an artificial mouth: a clinical correlation. *Dent Mater* 1986;2:235–40.
39. Mörmann WH, Bindl A. All-ceramic, chair-side computer-aided design/computer-aided machining restorations. *Dent Clin North Am* 2002;46:405–26.

J Dent Sci 2009;4(3):118–129

ELSEVIER

ORIGINAL ARTICLE

Improving the video imaging prediction of postsurgical facial profiles with an artificial neural network

Chien-Hsun Lu,[1,2] *Ellen Wen-Ching Ko,*[3,4] *Li Liu*[5]*

[1]Department of Dentistry, Taipei Medical University–Shuang Ho Hospital, Taipei, Taiwan
[2]Department of Dentistry, Mackay Memorial Hospital, HsinChu, Taiwan
[3]Graduate Institute of Craniofacial and Oral Science, Chang Gung University, Taipei, Taiwan
[4]Department of Craniofacial Orthodontics, Chang Gung Memorial Hospital, Taipei, Taiwan
[5]Graduate Institute of Medical Informatics, Taipei Medical University and Taipei Medical University Hospital, Taipei, Taiwan

Received: May 10, 2009
Accepted: Aug 13, 2009

KEY WORDS:
artificial neural network;
improvement;
orthognathic surgery;
prediction;
video image

Background/purpose: With advancements in computer technology, postsurgical video image simulations are becoming more frequently used in orthognathic surgery. Simulations can greatly affect decision making by patients and also provide information to surgeons and orthodontists. However, most of the current commercial video image prediction software is only suitable for patient education but is not precise enough for clinical communication and treatment planning. The purpose of this study was to evaluate and improve post-orthognathic surgery image predictions.
Materials and methods: In this retrospective study, 30 bimaxillary protrusion patients who underwent two jaw surgeries were recruited. Simulations were compared with the actual postsurgical facial profile. An artificial neural network (ANN) was used to improve the predictions.
Results: The lower lip was the least accurate point, and the prediction error on the sagittal plane was +4.0 mm. After applying the ANN to the input data, the prediction error was reduced to +0.3 mm with a >80% improvement rate. The overall probability of the prediction errors being <2 mm was 52% before improvement and 84.5% after improvement. Improvement rates of the average prediction errors on the sagittal and vertical planes were 43.9% and −6.6%, respectively.
Conclusion: With the help of an ANN, the accuracy and reliability of the postsurgical profile video image predictions were greatly improved to a clinically applicable and treatment planning level.

Introduction

Facial esthetic improvement is the main reason patients seek surgical correction of dentofacial deformities.[1] However, the definition of an ideal result for facial improvement after surgical orthodontic treatment is very subjective. Therefore, prevision of the improvement has become an important issue

*Corresponding author. Graduate Institute of Medical Informatics, Taipei Medical University and Taipei Medical University Hospital, c/o College of Public Health, National Taiwan University, Room 438, 4 F, 17, Xu-Zhou Road, Taipei 100, Taiwan.
E-mail: davidliliu@gmail.com

Table 1. Literature review of the least accurate area in software prediction of facial soft tissue changes after orthognathic surgery

Author	Least accurate	Predicted error (mm)	Sample size	Type of surgery	Software
Lu et al.[16]	Lower lip Upper lip	+4.0±2.3 (H) +1.7±2.4 (V)	30	Wassmund maxillary setback Köle mandibular setback	DI
Kazandjian et al.[18]	Upper lip Lower lip	+2.25±3.63 (H) −2.23±2.85 (V)	30	Mandibular setback	QC, PoP
Sameshima et al.[19]	Lower lip	+1.71±1.37 (H) +2.88±2.62 (V)	32	Maxillary impaction	OTP, PrP
Syliangco et al.[20]	Lower lip	+1.61±1.24 (H) +1.77±1.26 (V)	39	Mandibular advancement	OTP, PrP
Konstiantos et al.[21]	Lower lip Pronasal	+1.57±2.0 (H) −1.64±1.4 (V)	21	LeFort I osteotomy	DP
Hing[22]	Lower lip Chin	+1.9±0.38 (H) −0.5±0.78 (V)	16	Mandibular advancement	QC

+ = indicates that the predicted landmark was anterior (horizontal) or inferior (vertical) to the actual one; H = horizontal plane; V = vertical plane; DI = Dolphin Imaging; − = indicates that the predicted landmark was posterior (horizontal) or superior (vertical) to the actual one; QC = Quick Ceph (Orthodontic Processing, CA, USA); PoP = Portrait Planner (Rx Data Inc., TN, USA); OTP = Orthognathic Treatment Planner (Pacific Coast Software, CA, USA); PrP = Prescription Portrait (Rx Data Inc.); DP = Dentofacial Planner (Dentofacial Software, Toronto, Ontario, Canada).

among patients, surgeons, and orthodontists.[2,3] Several measures were proposed to predict the post-surgical facial profile.[4–7] With advancements in digital imaging technology, profile predictions are generated by computer.[8–15] However, the accuracy and reliability of these simulations and the results are often not very satisfactory (Table 1).[16–23] Most authors suggest that current simulation programs are good for patient education but not accurate enough for treatment planning. Therefore, it is important to improve the accuracy and reliability of video image simulations. However, during a literature review, no articles related to improving post-surgical profile video imaging predictions were found. A new methodology should be developed to improve video simulations.

Artificial intelligence is a branch of computer science capable of analyzing complex medical data. Its potential to exploit meaningful relationships within a dataset can be used for diagnosis, treatment, and predicting outcomes in many clinical scenarios.[24] Artificial neural networks (ANNs) are biologically inspired computer programs designed to simulate the way in which the human brain processes information.[25] They are systems that can learn; in most situations, an operator trains the system with a set of input and output data belonging to a particular category. If new data of the same category but beyond the training set are presented to the system, the network can use the learned data to predict outcomes with no specific programming related to the category of events involved.[26]

We propose that ANNs possess the ability to improve post-orthognathic surgery image predictions. The purpose of this study was to evaluate video image predictions after orthognathic surgery and improve them with an ANN.

Materials and methods

This research was based on a previous study published by Lu et al.[16] in 2003. The samples consisted of 30 adult patients who met the following criteria: (1) having no congenital craniofacial deformities; (2) having no head or neck trauma or surgical history; and (3) having undergone the Wassmund procedure to set back the anterior maxilla and the Köle procedure to set back the anterior mandible with or without genioplasty.

Lateral cephalometric radiographs and profile photographs were taken within 6 months before surgery and at least 6 months after surgery. The head films and photographs were acquired in the natural head position with the teeth in centric occlusion and the lips in a relaxed posture. There were no fixed orthodontic appliances shown on either the head films or photographs.

Evaluating the prediction

An (x, y) coordinate system was set up in order to evaluate the accuracy of the prediction (Fig. 1). The SN plane was defined as the horizontal reference

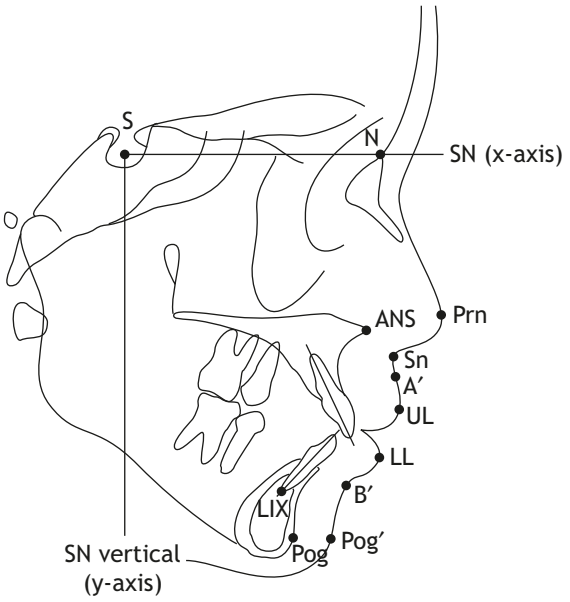

Fig. 1 Cephalometric landmarks used in this study. A′= soft-tissue A point; B′=soft-tissue B point; LIX=lower incisal apex; LL=lower lip; N=nasion; Pog=pogonion; Pog′=soft-tissue pogonion; Prn=tip of the nose; S=sella; Sn=subnasale; UL=upper lip.

plane (x-axis), and a line perpendicular to this plane through the sella was defined as the vertical reference plane (y-axis). Hard-tissue landmarks recorded included the anterior nasal spine (ANS), lower incisor root apex (LIX), and pogonion (pog). The angle of the upper incisor to the SN plane and the lower incisor mandibular plane angle were also recorded. Soft-tissue landmarks recorded included the tip of the nose (Prn), subnasale (Sn), soft-tissue A point (A′), upper lip (UL), lower lip (LL), soft-tissue B point (B′), and soft-tissue pogonion (Pog′). Tracings of the presurgical and postsurgical cephalograms were superimposed at the cranial base to ensure that the (x, y) planes were accurately transferred. The tracings and photographs were then input into the computer, digitized, and superimposed following the instructions of the prediction software (Dolphin Imaging version 6; Dolphin Imaging & Management Solutions, Chatsworth, CA, USA). The perpendicular distances of each landmark to both reference planes (x- and y-axes) were recorded before and after surgery. Treatment changes of hard tissues in each case were obtained from the differences between the pre- and postsurgical linear measurements. The hard-tissue image was moved according to the prescribed distances (the treatment change) using these calculations and the visual treatment objective function in the software. A predicted postsurgical video image was thus generated. The predicted soft-tissue outline and the corresponding coordinates of the soft tissue were also automatically generated. Differences in the soft-tissue outline between the predicted tracing and the actual profile were compared (error of prediction) to test the accuracy of this software.

Improving the prediction with an ANN

Following the instructions of the prediction software we used in this study, eight specific hard-tissue movements were input into the software to generate the prediction. In addition, we wanted to simplify the improvement procedure and avoid modifying the parameters or even reprogramming the software. So improving the prediction focused on altering the input values to the software.

Twenty of the 30 patients were randomly selected to establish the ANN (Group A) and the other 10 patients were used to verify the improvement (Group B). Manual hard-tissue adjustments were performed by one orthodontist and met the adjustment requirements (Fig. 2). The requirements were the designated soft-tissue point prediction errors of <2 mm in the order of Pog′, LL, B′, UL, A′, Sn, and Prn. When the error of the predicted soft-tissue point was adjusted to the required level, the previous soft-tissue points were rechecked to ensure that the prediction errors were still in an acceptable range (<2 mm). If the requirements were not met after 10 trials, the hard-tissue movements were adjusted to achieve the prediction error of the previous soft-tissue point of <2 mm and the prediction error of the present soft-tissue point was as close to 2 mm as possible. After the adjustment, the adjusted hard-tissue movement was recorded and used as a target set of the ANN. In order to provide a larger training sample size for the ANN, the adjustment procedures were performed three times spaced by at least a 1-week interval. Sixty datasets were provided to train the ANN.

The ANN was created with the software NeuroSolutions version 4.2 (NeuroDimension Inc., Gainesville, FL, USA). The adopted neural network was set up with two hidden layers. Each hidden layer possessed the function of a feed-forward back-propagation learning algorithm and was composed of eight processing elements with the tanh axon (Fig. 3). There were eight input neurons for the original treatment changes in hard tissues (original hard-tissue movement) and eight output neurons for adjusted treatment changes of hard tissues (adjusted hard-tissue movement). The input data included the movements of the ANS on the x- and y-axes, Pog on the x- and y-axes, the angle of upper incisor to SN plane, the lower incisor root apex on the *x*- and y-axes, and the lower incisor mandibular plane angle. The original hard-tissue movements of Group A were used as the learning set. The manually

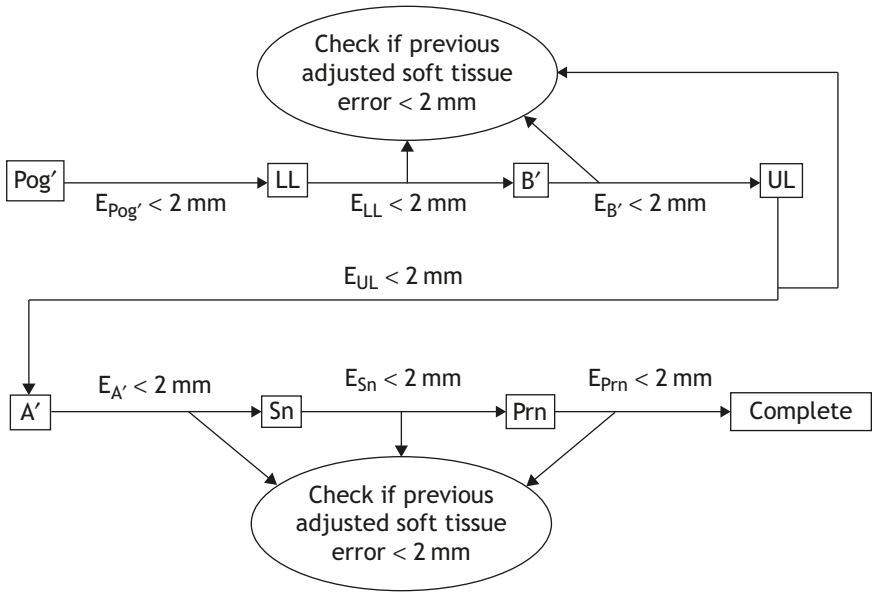

Fig. 2 Adjustment requirement flow chart. A′=soft-tissue A point; B′=soft-tissue B point; E=prediction error; LL=lower lip; Pog′=soft-tissue pogonion; Prn=tip of the nose; Sn=subnasale; UL=upper lip.

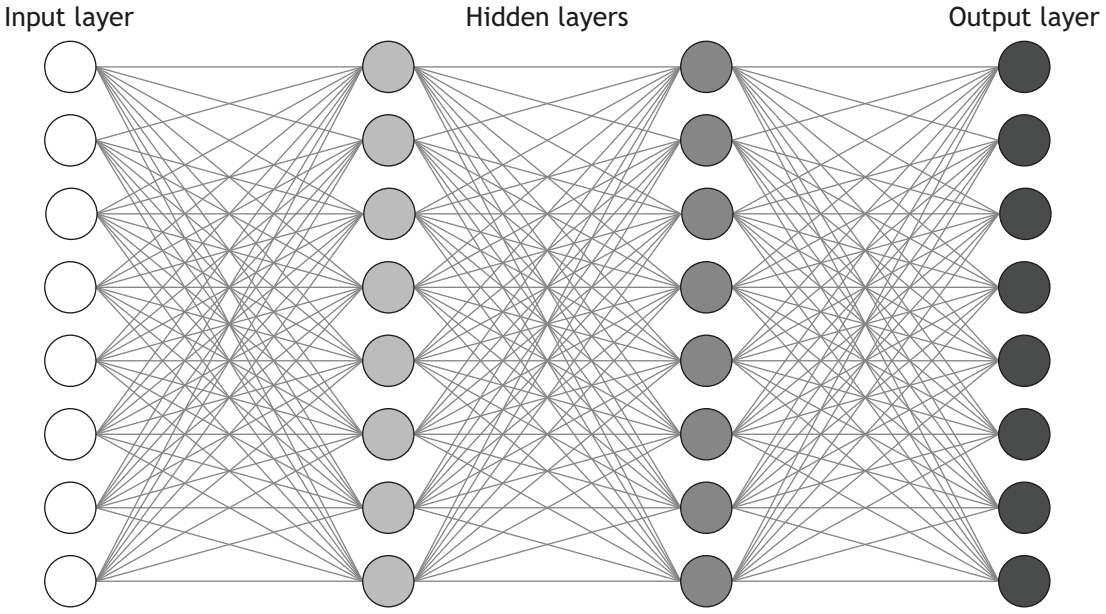

Fig. 3 Architectural graph of the adopted neural network. This network consisted of one input layer, two hidden layers, and one output layer. Each layer possessed eight neurons.

adjusted hard-tissue movements of Group A were used as the target set. The ANN was then trained.

Evaluating the improved prediction

Group B patients were used to test the accuracy of the improvement. The original hard-tissue movements of each patient in Group B were input to the trained ANN, and an adjusted hard-tissue movement was then generated. These new generated values were input to the prediction software, and an improved postsurgical video image prediction was then produced. The prediction errors between the actual final profile and the improved predicted soft-tissue outline were calculated and compared with those without improvement.

Results

Original prediction errors

Data of the original prediction errors were derived from a previous study by Lu et al.[16] When comparing

the landmarks located in the computer-generated prediction with the actual profile change on the sagittal plane (Table 2), mean differences of <1 mm between the two groups were seen in three of seven soft-tissue measurements, including the tip of the nose, soft-tissue A point, and the upper lip. The most accurate region was located at soft-tissue A point. The largest difference was shown in the region of the lower lip. In general, the predictions tended to underestimate the amount of soft-tissue retraction except for the subnasale and soft-tissue pogonion.

When comparing landmarks of the computer-generated prediction with the actual profile changes on the vertical plane, mean differences of <1 mm between the two groups were seen in six of seven soft-tissue measurements, including the tip of the nose, subnasale, soft-tissue A point, the lower lip, soft-tissue B point, and soft-tissue pogonion. The greatest differences were seen in the region of the upper lip with an average of 1.7 mm. The most accurate prediction was located at soft-tissue B point.

When the data were divided into three categories (errors of <1, 1–2, and >2 mm), the frequency of the prediction errors on the sagittal plane (Table 3) presented a wide range of standard deviations (SDs) with a significant bipolar spread, especially in the region of the lower lip. Eighty percent of the predictions had a difference of >2 mm in the lower lip region. The most reliable region of the prediction was located at the tip of the nose, with

Table 2. Prediction errors*

	Sagittal plane		Vertical plane	
	Original prediction† (mm)	Improved prediction (mm)	Original prediction† (mm)	Improved prediction (mm)
Tip of the nose	+0.5±1.2	+0.7±1.5	−0.5±1.5	+0.1±1.8
Subnasale	−1.7±2.1	−2.4±1.1	−0.8±1.5	−1.0±1.4
Soft-tissue A point	+0.1±2.0	0±1.2	+1.0±2.6	+0.2±1.1
Upper lip	+0.8±2.7	+0.6±1.0	+1.7±2.4	+0.6±0.9
Lower lip	+4.0±2.3	+0.8±1.0	+0.3±3.6	−0.1±1.2
Soft-tissue B point	+3.2±3.0	0±1.6	−0.1±3.4	+0.5±1.8
Soft-tissue pogonion	−1.3±3.2	+0.2±0.9	+0.8±3.7	−0.1±0.7

*Data are presented as X (average of differences between the prediction and actual final result)±SD (standard deviation of differences between prediction and actual final result); †data of the original prediction derived from a previous study.[16] + = indicates that the predicted landmark was anterior (sagittal) or inferior (vertical) to the actual one; − = indicates that the predicted landmark was posterior (sagittal) or superior (vertical) to the actual one.

Table 3. Frequency of the prediction errors*

	Sagittal plane						Vertical plane					
	Original prediction† (%)			Improved prediction (%)			Original prediction† (%)			Improved prediction (%)		
	<1 mm	1–2 mm	>2 mm	<1 mm	1–2 mm	>2 mm	<1 mm	1–2 mm	>2 mm	<1 mm	1–2 mm	>2 mm
Tip of the nose	63	27	10	50	30	20	60	20	20	60	20	20
Subnasale	17	27	57	0	50	50	63	13	23	60	20	20
Soft-tissue A point	33	37	30	50	40	10	27	23	50	60	40	0
Upper lip	33	13	53	50	40	10	30	30	40	70	30	0
Lower lip	7	13	80	70	10	20	17	37	47	60	20	20
Soft-tissue B point	13	20	67	20	50	30	23	30	47	60	20	20
Soft-tissue pogonion	23	20	57	70	30	0	10	23	67	80	20	0
Overall‡	27	22	51	44	36	20	33	25	42	64	24	12

*Prediction errors were divided into three categories: errors of <1, 1~2, and >2 mm; †data of original prediction derived from a previous study;[16] ‡the overall value is the average of all prediction errors.

a difference of <1 mm in 63% and <2 mm in 90%. The overall region presented 49% prediction errors of <2 mm on the sagittal plane.

The frequency of prediction errors on the vertical plane was more concentrated when compared with those on the sagittal plane. The most reliable region of prediction was located at the tip of the nose and subnasale with 60% and 63% errors of <1 mm, respectively. The least reliable region was located at the soft-tissue pogonion with only 10% of the prediction errors of <1 mm. The overall region presented 58% of prediction errors of <2 mm on the vertical plane.

The distribution of prediction errors was plotted as scattergrams (Fig. 4). The individual points of the scattergrams were obtained from subtracting the actual final landmarks from the predicted landmarks. The scattergram of the original predictions showed that the prediction error of distribution of the tip of the nose and subnasale was more accurate and concentrated. The tip of the nose, the lower lip, and soft-tissue B point were estimated to be in a more anterior position. The subnasale was estimated to be in a more posterosuperior position. The upper lip was estimated to be in a more inferior position.

Improved prediction errors

When comparing landmarks of the improved computer-generated prediction with the actual profile change on the sagittal plane (Table 2), mean differences of <1 mm between the two groups were seen in six of seven soft-tissue measurements, including the tip of the nose, soft-tissue A point, the upper lip, the lower lip, soft-tissue B point, and the soft-tissue pogonion. The most accurate regions were located at soft-tissue A and B points. The largest differences were shown in the region of the subnasale. In general, the predictions tended to underestimate the amount of soft-tissue retraction except for at the subnasale.

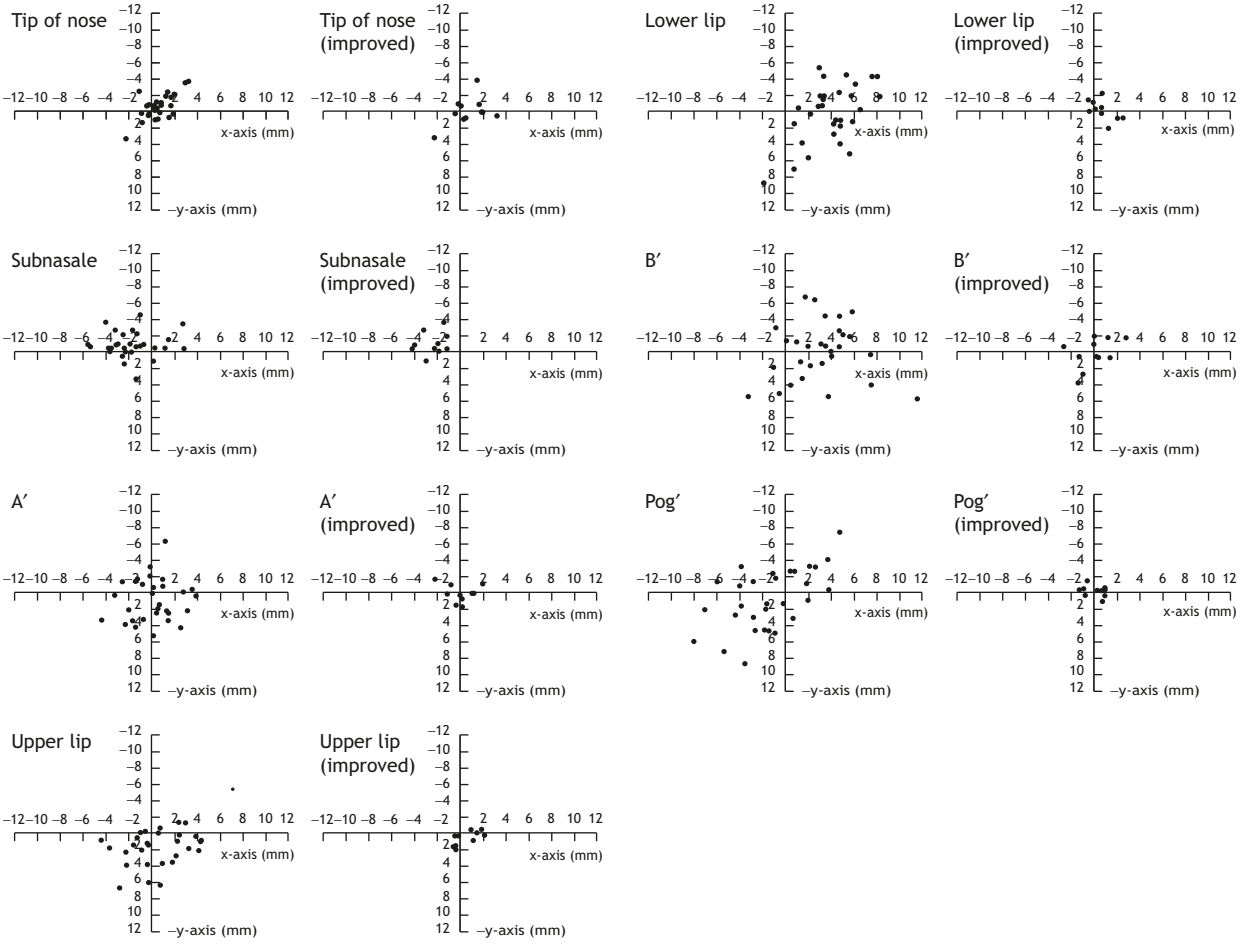

Fig. 4 Scattergrams of the prediction errors. Individual points in the scattergrams were obtained by the coordinates of the predicted landmarks minus those of the actual final landmarks. Positive values indicate that the predicted landmarks were anterior (x-axis) or inferior (y-axis) to the actual ones, while negative values indicate that the predicted landmarks were posterior (x-axis) or superior (y-axis) to the actual ones. Those labeled "improved" were scattergrams with improved predictions. B′ = soft-tissue B point; A′ = soft-tissue A point; Pog′ = soft-tissue pogonion.

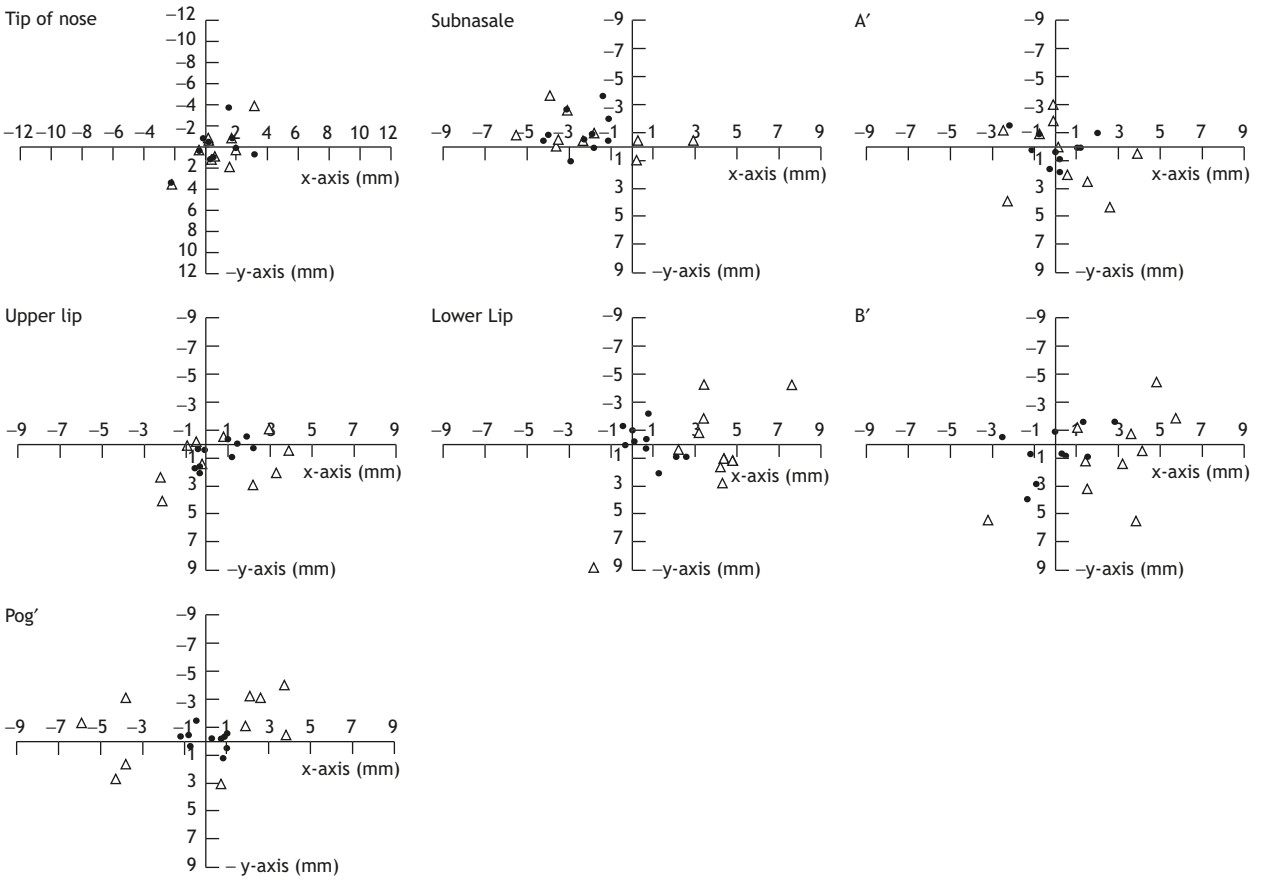

Fig. 5 Scattergrams of the prediction errors of Group B with and without improvement. △=prediction errors without improvement; ●=prediction errors with improvement. A′=soft-tissue A point; B′=soft-tissue B point; Pog′=soft-tissue pogonion.

When comparing landmarks of the improved computer-generated prediction with the actual profile changes on the vertical plane, mean differences of <1 mm between the two groups were seen in six of seven soft tissue measurements, including the tip of the nose, soft-tissue A point, the upper lip, the lower lip, soft-tissue B point, and the soft-tissue pogonion. The greatest differences were seen in the region of the subnasale with an average of 1.0 mm. The most accurate prediction was located at the soft-tissue pogonion.

The frequency of the improved prediction errors (Table 3) of the sagittal plane was located more in the region of <1 mm compared with those without improvement. The most reliable region of the prediction was located at the soft-tissue pogonion, with a difference of <1 mm in 70% and <2 mm in 100%. The second most reliable region was located at the lower lip, with a difference <1 mm in 70% and <2 mm in 80%. The least reliable region of the prediction was located at the subnasale with a difference >2 mm in 50%. The overall region presented 80% of prediction errors of <2 mm on the sagittal plane.

The frequency of prediction errors on the vertical plane was more concentrated when compared with those on the sagittal plane. The most reliable region of prediction was located at the tip of the nose and subnasale with 60% and 63% errors of <1 mm, respectively. The least reliable region was located at the soft-tissue pogonion with only 10% of the prediction errors of <1 mm. The overall region presented 58% of prediction errors of <2 mm on the vertical plane.

After improvement, the scattergrams (Fig. 4) showed that the prediction errors of distribution were more concentrated than those without improvement. The tip of the nose, the upper lip, and the lower lip were estimated to be in a more anterior position. The subnasale was estimated to be in a more posterosuperior position. Soft-tissue B point was scattered around the origin of the coordinates, while the soft-tissue pogonion was distributed near the origin of the coordinates. When comparing the distribution of Group B samples with and without improvement (Fig. 5), we found that the distribution of errors with improvement were more concentrated and also closer to the origin of the coordinates. Because of smaller prediction errors before improvement, the distribution of the scattergram of the tip of the nose with and without

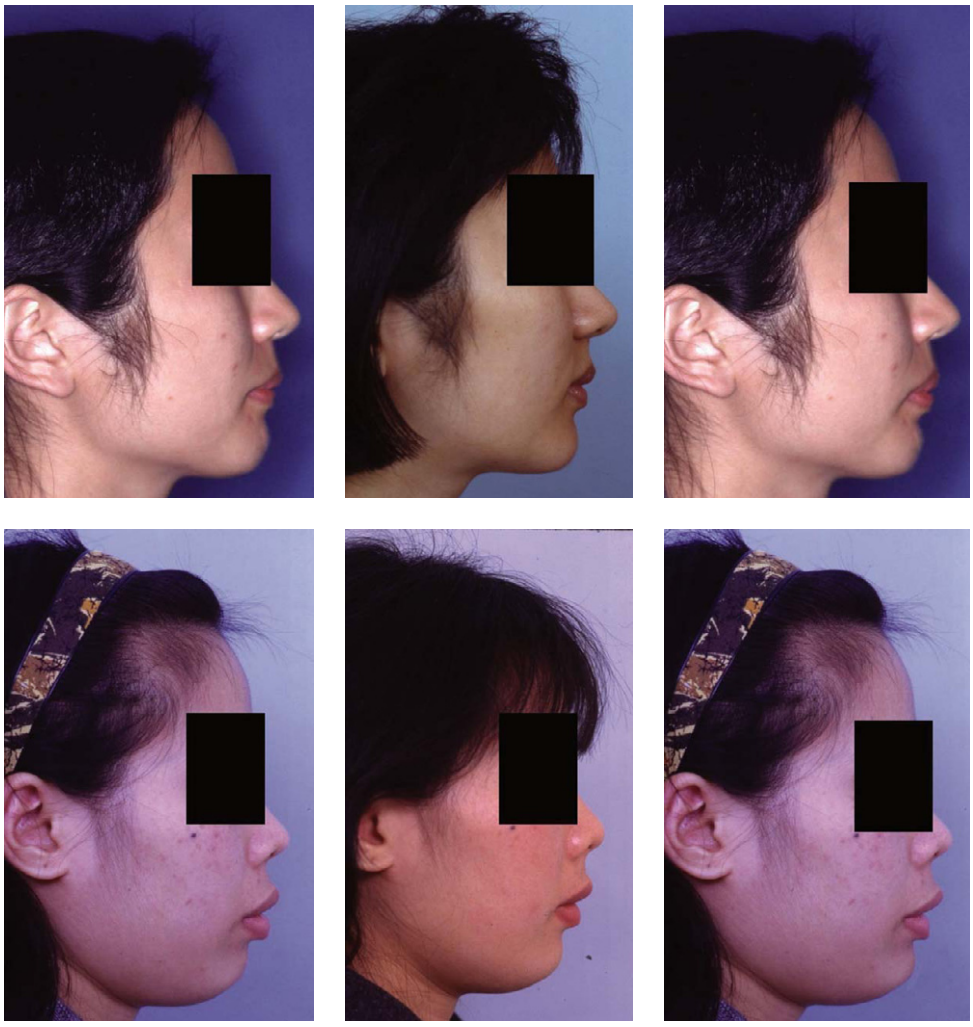

Fig. 6 Two examples of the video prediction and improved video prediction. The computer-generated prediction, actual final image, and improved prediction are represented by the left, middle and right images. Note the differences in the lip region among these images. The improved predictions were more similar to the actual final images.

improvement was similar. The scattergram of the subnasale showed that the prediction errors with improvement were concentrated to the center of those without improvement. The scattergram of the soft-tissue A point, the upper lip, and the soft-tissue pogonion showed that the improved prediction errors were concentrated to the center of those without improvement and were also concentrated to the origin of the coordinates. The scattergram of the lower lip and soft-tissue B point showed that the prediction errors with improvement were concentrated toward the origin of the coordinates.

Examples of predicted profile images, actual postsurgical profiles, and predicted profile images with improvement are presented in Fig. 6.

Performance of the ANN

In order to evaluate the improvement ability of the AAN for each soft-tissue point, the improvement rates were calculated and are listed in Table 4. The improvement rate of the average error was defined as:

$$\frac{|\text{average error of prediction}| - |\text{average error of improved prediction}|}{|\text{average error of prediction}|} \times 100\%$$

The improvement rate of the SD was defined as:

$$\frac{|\text{SD of prediction error}| - |\text{SD of improved prediction error}|}{|\text{SD of prediction error}|} \times 100\%$$

On the sagittal plane, the lower face region showed better improvement when compared with all samples. The improvement rates exceeded 80%. Soft-tissue A and B points were the most greatly improved and showed 100% improvement rates. This means that the prediction errors were eliminated,

Table 4. Improvement rate

	Sagittal plane		Vertical plane	
	Avg (%)	Std (%)	Avg (%)	Std (%)
Compared with all samples				
Tip of the nose	−40.0	−25.0	+80.0	−20.0
Subnasale	−41.2	+47.6	−25.0	+6.7
Soft-tissue A point	+100.0	+40.0	+80.0	+57.7
Upper lip	+25.0	+63.0	+64.7	+62.5
Lower lip	+80.0	+56.5	+66.7	+66.7
Soft-tissue B point	+100.0	+46.7	−400.0	+47.1
Soft-tissue pogonion	+83.3	+71.9	+87.5	+81.1
Compared with Group B				
Tip of the nose	0.0	0.0	+66.7	+5.3
Subnasale	−20.0	+56.0	−25.0	−7.7
Soft-tissue A point	+100.0	+40.0	+66.7	+56.0
Upper lip	+14.3	+56.5	+50.0	+47.1
Lower lip	+77.8	+58.3	+80.0	+68.4
Soft-tissue B point	+100.0	+36.0	+44.4	+41.9
Soft-tissue pogonion	+33.3	+75.7	+88.9	+73.1

Avg = improvement rate of the average error; Std = improvement rate of the standard deviation.

and the average error was 0. The improvement rate of the least accurate point, the lower lip, was 80%. The improvement rates of the tip of the nose and subnasale were negative and showed that the improvement actually made them less accurate. Most SDs of the soft-tissue points improved except for the tip of the nose. The soft-tissue point that possessed the largest SD, the soft-tissue pogonion, had the highest improvement rate of the SD. The improvement rates of the upper and lower lips exceeded 50%. On average, the improvement rate of the average error on the sagittal plane was 43.9%, and that of the SD was 42.9%.

On the vertical plane, the soft-tissue pogonion, the soft-tissue A point, and the tip of the nose possessed the largest improvement rate of average errors when compared with all samples. The improvement rates of these points exceeded 80%. The most greatly improved point was the soft-tissue pogonion which showed 87.5% improvement. The improvement rate of the least accurate point, the upper lip, was 64.7%. The improvement rate of the most accurate point, the soft-tissue B point, was −400%. The improvement rate of the SD of the soft-tissue pogonion was the highest, while that of the tip of the nose was the lowest. The improvement rate of the average error of the tip of the nose was 80%; however, the improvement rate of the SD was −20%. This shows that the range of the error distribution was wider after improvement at this soft-tissue point. On average, the improvement rate of the average error on the vertical plane was −6.6%, and the improvement rate of the SD was 43.1%.

Generally, the overall improvement rate of the average error was 18.7%, and the overall improvement rate of the SD was 43.0%.

Discussion

The basic model of ANNs was proposed by Warren McCulloch (a neurologist) and Walter Pitts (a mathematician) in 1943.[27] They developed a neural network using simple binary threshold functions. According to Mitchell,[28] ANNs provide powerful tools to approach real situations by learning examples. They provide powerful effects in visual recognition, acoustic recognition, and image recognition. They are able to find useful information among original data and establish a model for decision making and results prediction. A feed-forward back-propagation learning ANN[29] was used in this study. Such networks are made up of layers of neurons, typically an input layer, one or more hidden layers, and an output layer. Each layer is fully connected to the other layers. The neurons are connected by links that are associated with numerical weightings. A neural network learns from its experience in a training environment through repeated adjustments of these weightings.

ANNs are widely used in medical research.[30–39] Folland et al.[31] used an ANN to discriminate cardiac sounds. They used multilayer perceptron and radial basis function for their neural network. The results showed that the abilities to discriminate abnormal cardiac sounds were 84% and 88%. Spicker et al.[32]

predicted the sequence of human p53 tumor suppressor gene with an ANN. Ortolani et al.[33] used an ANN to monitor changes in electroencephalographs (EEGs) in order to determine the anesthetic depth of patients. The EEGs of 150 patients were used for the input data, and the anesthetic depth judged by the anesthetist was used as the target set. Another 50 patients were used to test the system, and they found that this ANN was able to detect the anesthetic depth of patients. Baxt et al.[34] used an ANN to quickly diagnose patients with chest pain and discriminate ones with acute cardiac infarction. They trained the ANN with 2204 patients with chest pain and a final diagnosis. The symptoms and signs of another 128 patients with acute cardiac infarction were input into the system, and 121 patients were correctly diagnosed. They concluded that this system was useful for preliminarily diagnosing patients in the emergency room. Lo et al.[37] predicted breast cancer invasion with ANNs. Nine mammographic findings and patient age were used as input data, and the results of a biopsy were used as the output data. They found that the specificity of this system was 100% and the sensitivity was 71%, and thought this knowledge might help in surgical planning and to reduce the costs and morbidity of unnecessary biopsies. In dentistry, ANNs are also used for diagnosis and screening. Devito et al.[38] used an artificial multilayer perceptron neural network to diagnose proximal caries. They trained the network with 160 radiographic images and found that the diagnostic improvement using the neural network was 39.4%. The results were better than the average of the examiners. Radke et al.[39] differentiated normal temporomandibular joints and non-reducing displaced disks with an ANN. All normal subjects were detected as normal patients with 100% specificity, while 86.8% of patients were correctly classified. Speight et al.[30] utilized an ANN for oral cancer screening; they trained the network with 1662 samples and used another 365 samples for the test. They found the sensitivity to be 0.80 and the specificity to be 0.77. For general dentists, the screening sensitivity was 0.74 and the specificity was 0.99. The authors thought that this ANN was applicable considering the costs.

According to research by Romani et al.[40], nearly 50% of orthodontists surveyed could not detect changes of 2 mm in vertical movement of the maxilla. In the present study, 2 mm was chosen as the threshold of tolerance for improved prediction error in order to establish the target set of the ANN. To set up the sequence of the soft-tissue check points when modifying hard-tissue movements, the less accurate points were improved first. In this study, the lower lip and chin region was a less accurate region and the upper lip and nose region was a relatively accurate region. Thus, the sequence of soft-tissue check points began from Pg′ then LL, B′, UL, A′, Sn, and ended at Prn.

Although ANNs are widely used in the fields of both medicine and dentistry, they are mainly used in decision making, diagnosis, and prognosis prediction.[24] No article regarding improving postsurgical facial profile imaging predictions was found during a literature review. Thus, comparisons with similar studies in the literature are difficult to make. However, the present study shows another potential application of ANNs in dentistry.

The results of the present study confirmed that ANNs are able to improve the postsurgical facial profile prediction to a clinically applicable level. After the improvement by the ANN, most of the prediction errors were <1 mm, except for the subnasale. The improvement rate of the subnasale was also the worst among the evaluated soft-tissue landmarks. A similar situation was found at the tip of the nose. This might have been due to the method of gaining the target set in this study. In this study, the movement of hard tissue was adjusted in order to make the prediction more accurate. After one soft-tissue point achieved a prediction error of <2 mm by changing the hard-tissue movement, we went to the next soft-tissue point. It is possible that we adjusted the prediction error of the present soft-tissue point to <2 mm but made the prediction error of the previous soft-tissue points >2 mm. In our protocol, this change would be abandoned, and all prediction errors of the previous soft-tissue points should remain <2 mm. The sequence of the adjustments was the soft-tissue pogonion, the lower lip, soft-tissue B point, the upper lip, soft-tissue A point, the subnasale, and the tip of the nose. The prediction error of the nose region was of least concern, and this might have led to less improvement or even a worse prediction.

From the scattergrams, we found that the improved prediction errors were concentrated in the origin of the coordinate and/or to the center of original prediction errors. It seemed that the improvement in the ANN was to eliminate the most dispersed points and become concentrated at the center of the distribution and the origin of the coordinates.

On the vertical plane, the improvement rate of the most accurate point, soft-tissue B point, was −400%. The improvement rate of this point seemed to be very poor; however, the average prediction error of this point after improvement was rather small (0.5 mm). When compared with Group B samples only, the improvement rate was 44% (Table 4). This might have been due to the average prediction error of the soft-tissue B point of all samples

being smaller than that of Group B, thus the value of the improvement rate was negative.

In this study, the target set of the ANN was obtained by manual adjustment. This means that the intelligence of the operator to make the predicted image more similar to the final actual image was transplanted to the artificial network. The artificial networks process this intelligence with mathematical variables which are optimized during the training process. According to Scott et al.[41], the accuracy of the new predictions of the artificial network depends upon the completeness of the training process and the degree to which the training cases represent the population for which the network will be used. Because of the limited sample size in this study, the manual adjustment was repeated three times in order to provide more training samples for the ANN. The repeated manual adjustment of a specific case might be similar; however, it was regarded as an independent case, because each adjustment provided the independent prediction intelligence and a representative population for the ANN.

Because of limitations of the prediction software, the hard-tissue movement of the ANS, Pog, lower incisor root apex, angle of upper incisor to the SN plane, and lower incisor mandibular plane angle were the only values we were able to modify and improve the predictions. The prediction might be more accurate and reliable if more variables, such as surgical and orthodontic methods, were able to be input to and adjusted by the ANN.

Conclusion

1. The tip of the nose and the upper lip were the most reliable areas when using the video simulation to predict the postsurgical outcomes with bimaxillary protrusion surgery.
2. The prediction of the lower lip was the least accurate area and tended to underestimate the amount of soft-tissue retraction.
3. The frequency of the overall prediction errors of <2 mm without improvement was 52%.
4. With the improvement of the ANN, the average prediction errors and SDs were smaller, and the error distribution became more concentrated.
5. With the improvement of the ANN, the frequency of the overall prediction errors of <2 mm was 84.5%.
6. The improvement rates of the ANN were 18.7% for average errors and 43.0% for the SDs.
7. The ANN possesses the ability to improve the postsurgical video image profile predictions to a clinically applicable and treatment planning level.

References

1. Kiyak HA, Bell R. Psychosocial considerations in surgery and orthodontics. In: Proffit WR, White RP, eds. *Surgical Orthodontic Treatment*. St Louis, MO: Mosby-Year Book, 1991:71–95.
2. Ackerman JL, Proffit WR. Communication in orthodontic treatment planning: bioethical and informed consent issues. *Angle Orthod* 1995;65:253–61.
3. Turpin DL. The need for video imaging. *Angle Orthod* 1995; 65:243.
4. Proffit WR. Treatment planning: the search for wisdom. In: Proffit WR, White RP, eds. *Surgical Orthodontic Treatment*. St Louis, MO: Mosby-Year Book, 1991:142–91.
5. Cohen MI. Mandibular prognathism. *Am J Orthod* 1965;51: 368–79.
6. McNeil RW, Proffit WR, White RP. Cephalometric prediction for orthodontic surgery. *Angle Orthod* 1972;42:154–64.
7. Henderson D. The assessment and management of bony deformities of the middle and lower face. *Br J Plast Surg* 1974;27:287–96.
8. Sarver DM, Johnston MW, Matukas VJ. Video imaging for planning and counseling in orthognathic surgery. *J Oral Maxillofac Surg* 1988;46:939–45.
9. Sarver DM, Johnston MW. Video imaging: techniques for superimposition of cephalometric radiography and profile images. *Int J Adult Orthodon Orthognath Surg* 1990;5:241–8.
10. Sarver DM, Matukas VJ, Weissman SM. Incorporation of facial plastic surgery in the planning and treatment of orthognathic surgical cases. *Int J Adult Orthodon Orthognath Surg* 1991;6:227–39.
11. Lew KK. The reliability of computerized cephalometric soft tissue prediction following bimaxillary anterior subapical osteotomy. *Int J Adult Orthodon Orthognath Surg* 1992;7: 97–101.
12. Takahashi I, Takahashi T, Hamada M, et al. Application of video surgery to orthodontic diagnosis. *Int J Adult Orthodon Orthognath Surg* 1989;4:219–22.
13. Turpin DL. Computers coming on-line for diagnosis and treatment planning. *Angle Orthod* 1990;60:163.
14. Laney TJ, Kuhn BS. Computer imaging in orthognathic and facial cosmetic surgery. *Oral Maxillofac Clin North Am* 1990; 2:659–68.
15. Phillips C, Hill BJ, Cannac C. The influence of video imaging on patients' perceptions and expectations. *Angle Orthod* 1995;65:263–70.
16. Lu CH, Ko EW, Huang CS. The accuracy of video imaging prediction in soft tissue outcome after bimaxillary orthognathic surgery. *J Oral Maxillofac Surg* 2003;61:333–42.
17. Sinclair PM, Kilpelainen P, Phillips C, White RP Jr, Rogers L, Sarver DM. The accuracy of video imaging in orthognathic surgery. *Am J Orthod Dentofacial Orthop* 1995;107:177–85.
18. Kazandjian S, Sameshima GT, Champlin T, Sinclair PM. Accuracy of video imaging for predicting the soft tissue profile after mandibular set-back surgery. *Am J Orthod Dentofacial Orthop* 1999;115:382–9.
19. Sameshima GT, Kawakami RK, Kaminishi RM, Sinclair PM. Predicting soft tissue changes in maxillary impaction surgery: a comparison of two video imaging systems. *Angle Orthod* 1997;67:347–54.
20. Syliangco ST, Sameshima GT, Kaminishi RM, Sinclair PM. Predicting soft tissue changes in mandibular advancement surgery: a comparison of two video imaging systems. *Angle Orthod* 1997;67:337–46.
21. Konstiantos KA, O'Reilly MT, Close J. The validity of the prediction of soft tissue profile changes after LeFort I osteotomy using the Dentofacial Planner (computer software). *Am J Orthod Dentofacial Orthop* 1994;105:241–49.

22. Hing NR. The accuracy of computer generated prediction tracings. *Int J Oral Maxillofac Surg* 1989;18:148–51.
23. Upton PM, Sadowsky PL, Sarver DM, Heaven TJ. Evaluation of video imaging prediction in combined maxillary and mandibular orthognathic surgery. *Am J Orthod Dentofacial Orthop* 1997;112:656–65.
24. Ramesh AN, Kambhampati C, Monson JR, Drew PJ. Artificial intelligence in medicine. *Ann R Coll Surg Engl* 2004;86:334–8.
25. Agatonovic-Kustrin S, Beresford R. Basic concepts of artificial neural network (ANN) modeling and its application in pharmaceutical research. *J Pharm Biomed Anal* 2000;22: 717–27.
26. Alvager T, Smith TJ, Vijai F. The use of artificial neural networks in biomedical technologies: an introduction. *Biomed Instrum Technol* 1994;28:315–22.
27. Anderson D, McNeill G. *Artificial Neural Networks Technology*. A DACS State-of-the Art Report, August 20, 1992. Available at: https://www.thedacs.com/techs/abstracts/abstract.php?dan=347002
28. Mitchell TM. Chapter 4: Artificial neural networks. In: Mitchell TM, ed. Machine Learning. New York: McGraw-Hill, 1997:81–127.
29. Werbos P. *Beyond Regression: New Tools for Prediction and Analysis in the Behavioral Sciences* [PhD thesis]. Cambridge, MA: Harvard University, 1974.
30. Speight PM, Elliott AE, Jullien JA, Downer MC, Zakzrewska JM. The use of artificial intelligence to identify people at risk of oral cancer and precancer. *Br Dent J* 1995;25;179:382–7.
31. Folland R, Hines EL, Boilot P, Morgan D. Classifying coronary dysfunction using neural networks through cardiovascular auscultation. *Med Biol Eng Comput* 2002;40:339–43.
32. Spicker JS, Wikman F, Lu ML, et al. Neural network predicts sequence of *TP53* gene based on DNA chip. *Bioinformatics* 2002;18:1133–4.
33. Ortolani O, Conti A, Di Filippo A, et al. EEG signal processing in anaesthesia: use of a neural network technique for monitoring depth of anaesthesia. *Br J Anaesth* 2002;88: 644–8.
34. Baxt WG, Shofer FS, Sites FD, Hollander JE. A neural computational aid to the diagnosis of acute myocardial infarction. *Ann Emerg Med* 2002;39:366–73.
35. Chen Y, Thosar SS, Forbess RA, Kemper MS, Rubinovitz RL, Shukla AJ. Prediction of drug content and hardness of intact tablets using artificial neural network and near-infrared spectroscopy. *Drug Dev Ind Pharm* 2001;27:623–31.
36. MacDowell M, Somoza E, Rothe K, Fry R, Brady K, Bocklet A. Understanding birthing mode decision making using artificial neural networks. *Med Decis Making* 2001;21: 433–43.
37. Lo JY, Baker JA, Kornguth PJ, Iglehart JD, Floyd CE Jr. Predicting breast cancer invasion with artificial neural networks on the basis of mammographic features. *Radiology* 1997;203:159–63.
38. Devito KL, de Souza Barbosa F, Felippe Filho WN. An artificial multilayer perceptron neural network for diagnosis of proximal dental caries. *Oral Surg Oral Med Oral Pathol Oral Radiol Endod* 2008;106:879–84.
39. Radke JC, Ketcham R, Glassman B, Kull R. Artificial neural network learns to differentiate normal TMJs and nonreducing displaced disks after training on incisor-point chewing movements. *Cranio* 2003;21:259–64.
40. Romani KL, Agahi F, Nanda R, Zernik JH. Evaluation of horizontal and vertical differences in facial profiles by orthodontists and lay people. *Angle Orthod* 1993;63:175–82.
41. Scott JA, Aziz K, Yasuda T, Gewirtz H. Integration of clinical and imaging data to predict the presence of coronary artery disease with the use of neural networks. *Coron Artery Dis* 2004;15:427–34.

J Dent Sci 2009;4(3):130–135

ORIGINAL ARTICLE

Platelet-rich fibrin modulates cell proliferation of human periodontally related cells *in vitro*

*Chung-Hung Tsai,[1] Shih-Ya Shen,[2] Jiing-Huei Zhao,[3] Yu-Chao Chang[2,3]**

[1]Department of Oral Pathology, Chung Shan Medical University Hospital, Taichung, Taiwan
[2]Department of Periodontics, Chung Shan Medical University Hospital, Taichung, Taiwan
[3]Graduate School of Dentistry, Chung Shan Medical University, Taichung, Taiwan

Received: Apr 28, 2009
Accepted: Aug 3, 2009

KEY WORDS:
periodontal regeneration;
platelet-rich fibrin

Background/purpose: Platelet-rich fibrin (PRF) is a second-generation platelet concentrate which allows one to obtain fibrin membranes enriched with platelets and growth factors, after an anticoagulant-free blood harvest. However, limited information is currently available concerning the biologic effects of PRF on periodontally related cells. To provide clear evidence for the clinical use of PRF, we investigated the biologic effects of PRF on human gingival fibroblasts (GFs), periodontal ligament (PDL) cells, oral epithelial cells, and osteoblasts.
Materials and methods: Blood collection was carried out on 10 healthy volunteers. PRF was obtained by centrifugation at 3000 rpm for 12 minutes with a PC-02 table centrifuge. Primary cultured human GFs and PDL cells, the GNM oral epithelial cell line, and the U2OS osteoblast cell line were used to evaluate cell viability and proliferation resulting from PRF according to trypan blue and tetrazolium bromide reduction assays.
Results: PRF did not interfere with cell viability of periodontally related cells ($P>0.05$). PRF stimulated cell proliferation of osteoblasts (135% of the control), PDL cells (130% of the control), and GFs (120% of the control) during a 3-day culture period (all $P<0.05$). However, PRF suppressed oral epithelial cell growth to as low as 80% of the control ($P<0.05$). In addition, GFs, PDL cells, and osteoblasts were observed to attach at the margins of PRF by phase-contrast microscopy.
Conclusion: Our results suggest that PRF modulates cell proliferation in a cell type-specific manner. These cell type-specific actions may be beneficial for periodontal regeneration.

Introduction

Periodontal wound healing after surgery requires a series of cell–cell interactions between epithelial cells, gingival fibroblasts (GFs), periodontal ligament (PDL) cells, and osteoblasts, whereas disruption of the vasculature leads to fibrin formation, platelet aggregation, and release of several growth factors into tissues from platelets.[1] These processes involve molecular signals which are primarily mediated by cytokines and growth factors. Platelets contain various growth factors and cytokines that play key

*Corresponding author. Graduate School of Dentistry, Chung Shan Medical University, 110, Chien-Kuo North Road, Section 1, Taichung 40201, Taiwan.
E-mail: cyc@csmu.edu.tw

roles in inflammation and wound repair.[2] Platelets also secrete fibrin, fibronectin, and vitronectin, which act as a matrix for connective tissue and as adhesion molecules for more efficient cell migration.[3] This has led to the idea of using platelets as therapeutic tools to improve tissue repair particularly in periodontal wound healing.

Platelet-rich fibrin (PRF) described by Choukroun et al.[4] is a second-generation platelet concentrate which allows one to obtain fibrin membranes enriched with platelets and growth factors, after starting from an anticoagulant-free blood harvest.[5,6] PRF looks like a fibrin network and leads to more efficient cell migration and proliferation and thus cicatrization. PRF was initially used in implant surgery to improve bone healing.[4] Despite a lack of scientifically proven clinical benefits, the homogeneous fibrin network that is obtained is considered by the promoters of this technique to be a healing biomaterial and is commonly used in implant and plastic periodontal surgery procedures to enhance bone regeneration and soft-tissue wound healing.[7,8] Compared with other autologous platelet concentrates, there are few references in the literature about the biologic properties of PRF.

PRF contains platelets, growth factors and cytokines that may enhance the healing potential of both bone and soft tissues.[1,2] However, the literature mostly contains studies of the experimental use of PRF in animals and humans, and only a few *in vitro* studies on the effects of PRF on cell proliferation and functions have been carried out. The aim of this study was to assess the effects of the PRF on periodontally related cells. We investigated the biologic effects of PRF on the proliferation of the GMN human oral epithelial cell line, the U2OS human osteoblast cell line, primary human GFs, and PDL cells.

Materials and methods

PRF preparation

After receiving approval of the institutional review board at Chung Shan Medical University Hospital, blood collection was carried out on 10 healthy nonsmoking volunteers. Blood samples were treated according to the PRF protocol with a PC-02 table centrifuge and collection kits provided by Process (Nice, France).[3–5] Briefly, samples were taken without an anticoagulant in 10-mL glass-coated plastic tubes (Becton Dickinson Vacutainer, Becton, Dickinson & Co., Franklin Lakes, NJ, USA) and immediately centrifuged at 3000 rpm for 12 minutes. A fibrin clot formed in the middle part of the tube (Fig. 1A), while the upper part contained acellular plasma, and the bottom part contained red corpuscles (Fig. 1A). The fibrin clot was easily separated from the lower part of the centrifuged blood. The PRF clot was gently pressed into a membrane with sterile dry gauze (Fig. 1B). PRF membranes were minced at 0.5×0.5 cm for the following experiments.

Cell cultures

Human PDL cells[9,10] and GFs[11,12] were cultured using an explant technique as described previously. Human PDL cells were cultured from the roots of extracted

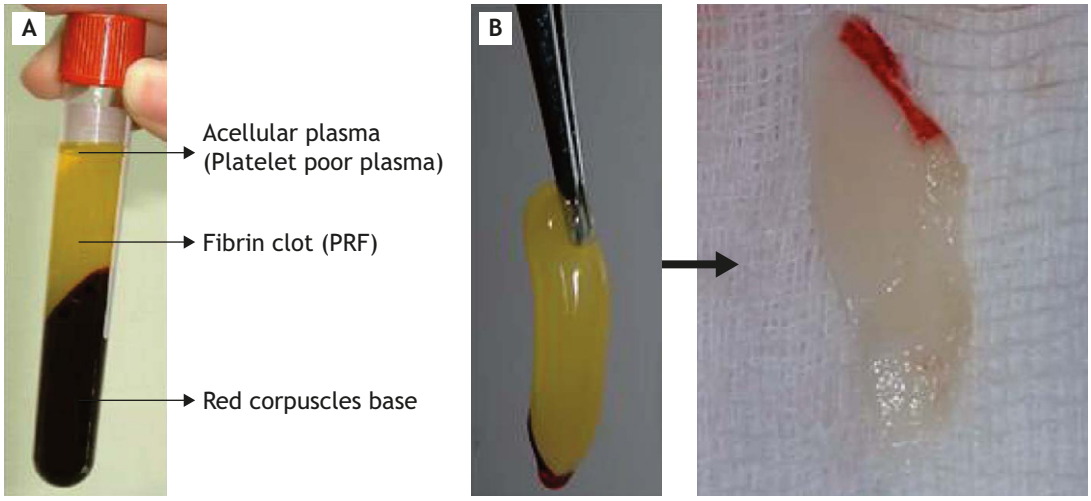

Fig. 1 (A) Platelet-rich fibrin (PRF) formed in the middle part of the tube. The upper part contained acellular plasma, and the bottom part contained red corpuscles. (B) The fibrin clot was easily separated from the lower part of the centrifuged blood. The platelet-rich fibrin clot was gently pressed between two layers of sterile dry gauze to form a membrane.

third molars. After extraction, teeth were rinsed with Hanks' buffered saline solution and then placed in 60-mm Petri dishes containing Dulbecco's modified Eagle's medium (DMEM) and 100 units of penicillin and 100 μg of streptomycin per millimeter. To avoid contamination from the gingiva, the PDL was carefully removed from the middle third of the root with a scalpel. Clinically healthy gingival connective tissues from a third molar extraction were used to culture GFs. The fragments from the PDL and gingiva were grown in DMEM supplemented with 10% fetal calf serum (FCS) and antibiotics. Cultures were maintained at 37°C in a humidified atmosphere of 5% CO_2 and 95% air. Cell cultures between the third and eighth passages were used.

U2OS cells (American Tissue Type Collection HTB 96), derived from a human osteogenic sarcoma, were cultured in DMEM supplemented with 10% FCS, streptomycin at 100 μg/mL, and penicillin at 100 mg/mL.[13] The GNM oral epithelial cell line, derived from a patient with T2N2aM0 gingival carcinoma and metastasis to the cervical lymph node,[14] was grown in RPMI 1640 medium (Gibco Laboratories, Grand Island, NY, USA) supplemented with 10% FCS and antibiotics. Confluent cells were detached with 0.25% trypsin and 0.05% EDTA for 5 minutes, and aliquots of separated cells were subcultured. Cells were subcultured at a 1:4 split ratio every third day.

Cell viability

Each PRF membrane was covered with a 5-mL suspension of cells at a concentration of 5×10^4 cells/mL in 35-mm culture dishes. After a 3-day culture period, the medium was removed, and 0.5 mL of 0.25% trypsin in phosphate-buffered saline (PBS) was added to each culture dish to detach the cells. One milliliter of medium was added to 0.5 mL of this cell suspension. Then 0.5 mL of calcium- and magnesium-free PBS containing 0.25% trypan blue (wt/vol) was added to 0.5 mL of the cell suspension to stain nonviable cells. Fifteen microliters of the cell suspension was dropped into a hemocytometer chamber (Cambridge Instruments, Buffalo, NY, USA), and cell numbers were counted under a phase-contrast microscope.[15] Cell viability is represented as number of viable cells as a percentage of total cells.

Cell proliferation assay

A 3-(4,5-dimethylthiazol-2-yl)-2,5-diphenyltetrazolium bromide (MTT) colorimetric assay was developed to monitor cell proliferation *in vitro*.[16] To elucidate PRF's role in cell proliferation, cells were seeded in 96-well plates at an initial density of 2×10^4 cells per well in DMEM containing PRF for 3 days. In the final 4 hours, 50 μL of the MTT solution was added to each well. Only the mitochondria of viable cells can reduce MTT to formazan. The produced insoluble formazan was dissolved with 150 μL of DMSO to each well. Reduced MTT was then measured spectrophotometrically in a dual-beam microtiter plate reader at 570 nm with 650 nm as a reference. Optical density values of the experimental groups were divided by the control value and are expressed as a percentage of the control.

Statistical analysis

Triplicate experiments were performed throughout this study. All assays were repeated three times to ensure reproducibility. The significance of the results obtained from the control and treated groups were statistically analyzed by Student's *t* test.

Results

The results of cell viability by trypan blue dye are shown in Fig. 2. PRF exhibited no cytotoxic effects to the four types of periodontally related cells ($P>0.05$). Each type of cell maintained its original morphology. Cells from gingiva (Fig. 3A) and the PDL (Fig. 3B) on the flat surface of the culture dishes exhibited a spindle-shaped morphology. Cells of the GMN oral epithelial cell line (Fig. 3C) and U2OS osteoblast cell line (Fig. 3D) have a cuboid/flat appearance. Moreover, GFs, PDL cells, and osteoblasts were also found to attach at the margin of PRF under observation by phase-contrast microscopy.

Figure 4 shows the effects of PRF on periodontally related cells. The cell density and number

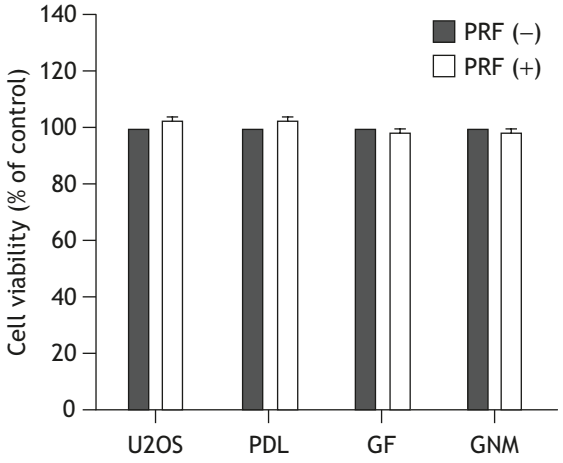

Fig. 2 No differences in cell viability between controls and platelet-rich fibrin (PRF) groups with periodontally related cells ($P>0.05$). PDL=periodontal ligament cells; GF=gingival fibroblasts.

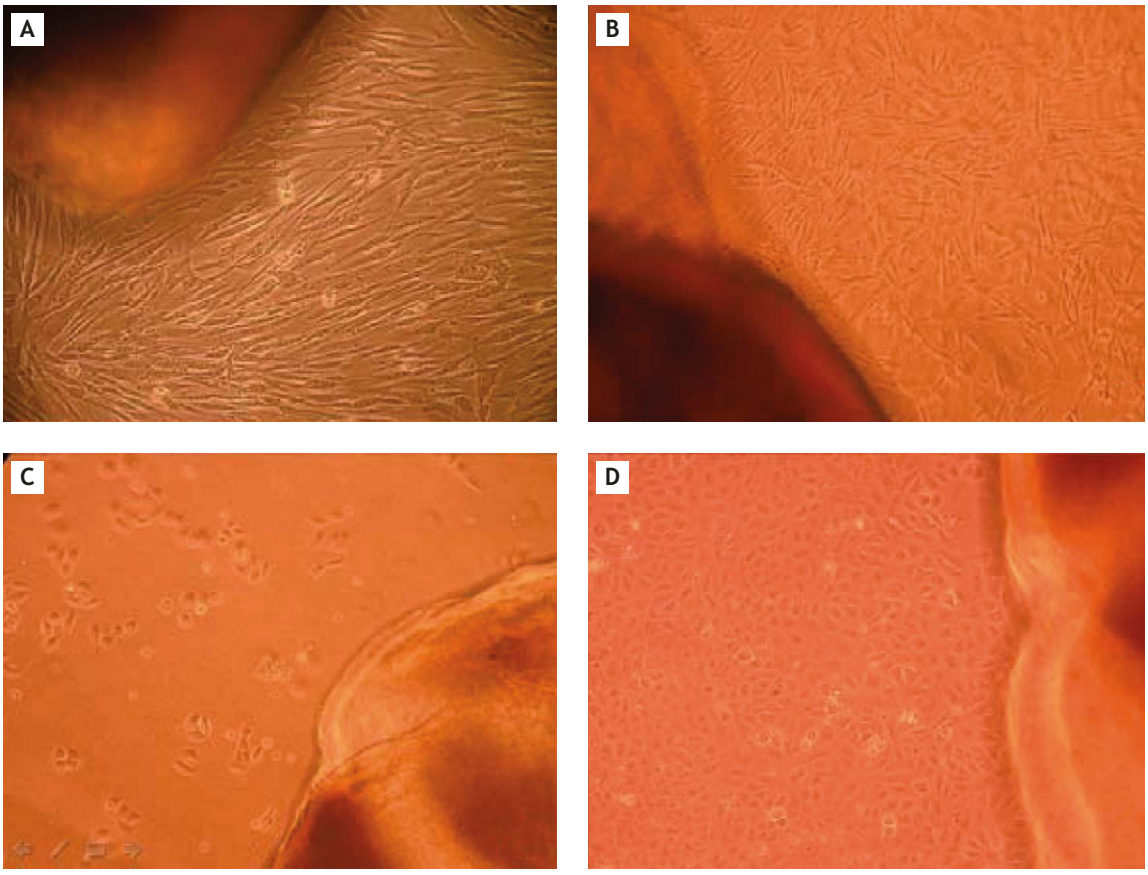

Fig. 3 Periodontally related cells maintained their original morphology when cultured with platelet-rich fibrin membranes. (A) Gingival fibroblasts; (B) periodontal ligament cells; (C) epithelial cells; and (D) osteoblasts.

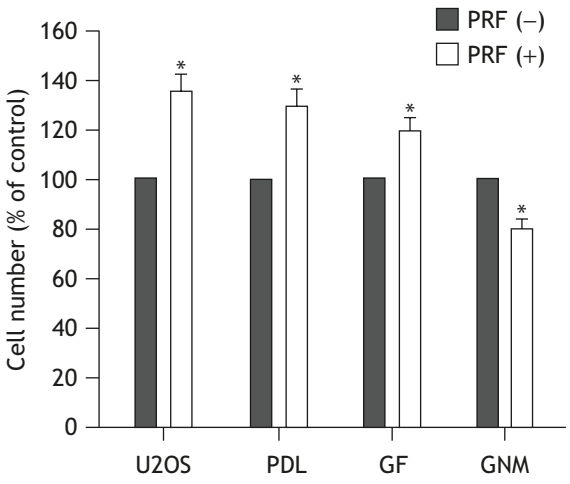

Fig. 4 Effects of platelet-rich fibrin (PRF) on periodontally related cells. Cells were exposed to PRF for 3 days. Viable cell numbers were measured with an MTT assay. The percentage of absorbance of each cell with PRF compared with that of the control was calculated. Each point and bar represent the mean±standard deviation. *Significant difference from the control value at $P<0.05$. PDL=periodontal ligament cells; GF=gingival fibroblasts.

gradually increased during the 3-day incubation period. PRF was found to increase PDL, GF and osteoblast proliferation, and cell numbers increased about 1.2-, 1.3- and 1.35-fold, respectively ($P<0.05$). However, PRF was found to reduce the epithelial cell number by about 20% compared with the untreated control ($P<0.05$).

Discussion

The simple and open-access technique of PRF was first developed in France by Choukroun et al.,[4] and PRF is produced in a totally natural manner, without using an anticoagulant during blood harvesting or bovine thrombin or calcium chloride for platelet activation and fibrin polymerization. The protocol is very simple and cheap. Venous blood is collected in dry 10-mL glass tubes, and centrifuged at about 400*g* for 12 minutes.[3–6] After centrifugation, three layers are formed in the tube: a base of red blood cells at the bottom, acellular plasma on the top (supernatant), and a clot of PRF between them.

PRF presents a complex tridimensional architecture which truly makes it a platelet- and leukocyte-rich fibrin biomaterial.[5,6] When delicately pressed between two layers of gauze, the PRF clot becomes a strong membrane with high potential, both for clinical applications[7,8,17,18] and tissue engineering.[19]

In this study, PRF exhibited no cytotoxicity to periodontally related cells. Our results are in agreement with Dohan et al.,[20] who reported that PRF exhibited no cytotoxicity toward preadipocytes, keratinocytes, osteoblasts, or GFs. Thus, the biocompatibility of PRF is not cell type-specific. Taken together, PRF acts as a biomaterial to periodontally related cells.

To the best of our knowledge, we first found that PRF stimulated osteoblast, GF, and PDL cell proliferation as a mitogen. The mechanism responsible for the cell proliferation by PRF might be explained as follows. Many growth factors such as platelet-derived growth factor (PDGF) and transforming growth factor (TGF)-β, are released from PRF.[5,6,21] Recently, Dohan et al.[21] demonstrated that the PRF membrane has a very significant slow sustained release of key growth factors for at least 1 week, which means that the membrane stimulates its environment for a significant time during remodeling. The properties of this natural fibrin biomaterial thus offer great potential during wound healing.

Interestingly, PRF was found to inhibit epithelial cell proliferation. These biologic actions seem very similar to those of previous reports. PDGF and TGF-β stimulate mitogenic activity in osteoblasts,[22,23] GFs,[24] and PDL cells,[23,24] but TGF-β acts as a growth inhibitor for epithelial cells.[25,26] Taken together, with our data on growth factor levels, these findings suggest that PRF possibly modulates cell proliferation by PDGF- and TGF-β-related mechanisms.

In this study, PRF exhibited no cytotoxicity to epithelial cells according to a trypan blue assay. The MTT assay is also a kind of cytotoxicity assay. However, epithelial cells seemed to be negatively influenced by PRF according to the MTT assay. The reasons are not conflicting and may be explained as follows. The trypan blue assay exhibits the percentage of cell viability. The MTT assay is a colorimetric method for quantifying viable cell numbers. The methyl-tetrazolium ring is cleared by mitochondrial dehydrogenases in viable cells to formazan, which has a blue color and can be measured with a spectrophotometer.[27] Dead cells are unable to produce the colored formazan product; this assay can distinguish live from dead cells. In addition, epithelial cells presented a typical cuboid/flat appearance under observations by phase-contrast microscopy in the present study. Taken together, PRF did not interfere with epithelial cell viability, but it retarded the proliferation of epithelial cells.

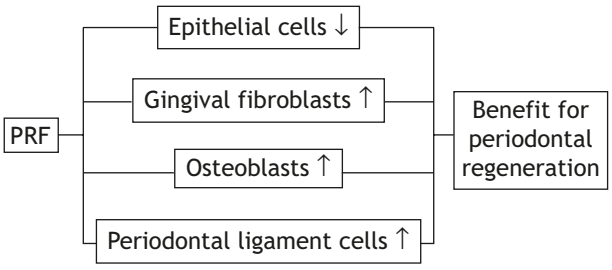

Fig. 5 Platelet-rich fibrin (PRF) modulates cell proliferation in a cell type-specific manner and may be beneficial to periodontal regeneration.

As far as we know, this is the first attempt to evaluate the role of PRF in human periodontally related cells *in vitro*. We demonstrated that PRF exhibits non-cytotoxic effects toward periodontally related cells. PRF can stimulate osteoblast, GF and PDL cell growth and retard epithelial cell proliferation. PRF may modulate cell proliferation in a cell type-specific manner (Fig. 5). The ability of PRF to suppress epithelial cell proliferation seems beneficial for periodontal regeneration. The retardation of the down-growth of junctional epithelium to the root surfaces in the regeneration procedure might avoid interference by the epithelium with the formation of new attachment on root surfaces.

It is our opinion that *in vitro* experiments are very helpful for assaying the biologic effects of PRF on periodontally related cells, but they may be limited in their ability to simulate clinical conditions. It may be unrealistic to translate *in vitro* findings to *in vitro* situations. These *in vitro* observations are very likely to be extrapolated to animal studies such as periodontitis models or critical-sized bony defect models to clarify the potential benefits of using PRF in periodontal regeneration.

Acknowledgments

This study was supported by a research grant (CSMU-96RD-05) from Chung Shan Medical University, Taiwan.

References

1. Deodhar AK, Rana RE. Surgical physiology of wound healing: a review. *J Postgrad Med* 1997;43:52–6.
2. Giannobile WV. Periodontal tissue engineering by growth factors. *Bone* 1996;19(1 Suppl):23S–37S.
3. Dohan DM, Choukroun J, Diss A, et al. Platelet-rich fibrin (PRF): a second-generation platelet concentrate, part I: technological concept and evolution. *Oral Surg Oral Med Oral Path Oral Radiol Endod* 2006;101:E37–44.
4. Choukroun J, Adda F, Schoeffer C, Vervelle A. PRF: an opportunity in perio-implantology. *Implantodontie* 2000;42:55–62. [In French]

5. Dohan DM, Choukroun J, Diss A, et al. Platelet-rich fibrin (PRF): a second-generation platelet concentrate, part II: platelet-related biologic features. *Oral Surg Oral Med Oral Pathol Oral Radiol Endod* 2006;101:E45–50.
6. Dohan DM, Choukroun J, Diss A, et al. Platelet-rich fibrin (PRF): a second-generation platelet concentrate, part III: leucocyte activation: a new feature for platelet concentrates? *Oral Surg Oral Med Oral Pathol Oral Radiol Endod* 2006;101:E51–5.
7. Choukroun J, Diss A, Simonpieri A, et al. Platelet-rich fibrin (PRF): a second-generation platelet concentrate, part IV: clinical effects on tissue healing. *Oral Surg Oral Med Oral Pathol Oral Radiol Endod* 2006;101:E56–60.
8. Choukroun J, Diss A, Simonpieri A, et al. Platelet-rich fibrin (PRF): a second-generation platelet concentrate, part V: histologic evaluations of PRF effects on bone allograft maturation in sinus lift. *Oral Surg Oral Med Oral Pathol Oral Radiol Endod* 2006;101:299–303.
9. Chang YC, Yang SF, Lai CC, Liu JY, Hsieh YS. Regulation of matrix metalloproteinases production by cytokines, pharmacological agents, and periodontal pathogens in human periodontal ligament fibroblast cultures. *J Periodont Res* 2002;37:196–203.
10. Chang YC, Hsieh YS, Lii CK, Huang FM, Tai KW, Chou MY. Induction of c-*fos* expression by nicotine in human periodontal ligament fibroblasts is related to cellular thiol levels. *J Periodontal Res* 2003;38:44–50.
11. Chen CC, Huang FM, Chen SL, Yang SH, Chang YC. Cytopathologic effects of safrole on human gingival fibroblasts in vitro. *J Dent Sci* 2006;1:126–31.
12. Lin HJ, Tsai CH, Huang FM, Chang YC. The upregulation of type I plasminogen activator inhibitor in human gingival fibroblasts stimulated with cyclosporin A. *J Periodontal Res* 2007;42:39–44.
13. Huang FM, Lee SS, Yang SF, Chang YC. Up-regulation of receptor activator nuclear factor-κB ligand expression by root canal sealers in human osteoblastic cells. *J Endod* 2009;35:363–6.
14. Lee SS, Tsai CH, Ho YC, Chang YC. The upregulation of heat shock protein 70 expression in areca quid chewing-associated oral squamous cell carcinomas. *Oral Oncol* 2008;44:884–90.
15. Tai KW, Chang YC. Cytotoxicity evaluation of perforation repair materials on human periodontal ligament cells in vitro. *J Endod* 2000;26:395–7.
16. Huang FM, Tai KW, Chou MY, Chang YC. Resinous perforation repair materials inhibit the growth, attachment, and proliferation of human gingival fibroblasts. *J Endod* 2002;28:291–4.
17. Diss A, Dohan DM, Mouhyi J, Mahler P. Osteotome sinus floor elevation using Choukroun's platelet-rich fibrin as grafting material: a 1-year prospective pilot study with microthreaded implants. *Oral Surg Oral Med Oral Pathol Oral Radiol Endod* 2008;105:572–9.
18. Aroca S, Keglevich T, Barbieri B, Gera I, Etienne D. Clinical evaluation of a modified coronally advanced flap alone or in combination with a platelet-rich fibrin membrane for the treatment of adjacent multiple gingival recessions: a 6-month study. *J Periodontol* 2009;80:244–52.
19. Choukroun JI, Braccini F, Diss A, Giordano G, Doglioli P, Dohan DM. Influence of platelet rich fibrin (PRF) on proliferation of human preadipocytes and tympanic keratinocytes: A new opportunity in facial lipostructure (Coleman's technique) and tympanoplasty? *Rev Laryngol Otol Rhinol (Bord)* 2007;128:27–32. [In French, English abstract]
20. Dohan DM, Del Corso M, Charrier JB. Cytotoxicity analyses of Choukroun's platelet rich fibrin (PRF) on a wide range of human cells: the answer to a commercial controversy. *Oral Surg Oral Med Oral Pathol Oral Radiol Endod* 2007;103:587–93.
21. Dohan DM, de Peppo GM, Doglioli P, Sammartino G. Slow release of growth factors and thrombospondin-1 in Choukroun's platelet-rich fibrin (PRF): a gold standard to achieve for all surgical platelet concentrates technologies. *Growth Factors* 2009;27:63–9.
22. Hughes FJ, Aubin JE, Heersche JNM. Differential chemotactic responses of different populations of fetal rat calvaria cells to platelet-derived growth factor and transforming growth factor β. *Bone Miner* 1992;19:63–74.
23. Piche JE, Graves DT. Study of the growth factor requirements of human bone-derived cells: a comparison with human fibroblasts. *Bone* 1989;10:131–8.
24. Dennison DK, Vallone DR, Pinero GJ, Rittman B, Caffesse RG. Differential effect of TGF-β1 and PDGF on proliferation of periodontal ligament cells and gingival fibroblasts. *J Periodontol* 1994;65:641–8.
25. Tucker RF, Shipley GD, Moses HL, Holley RW. Growth inhibitor from BSC-1 cells closely related to platelet type β transforming growth factor. *Science* 1984;226:705–7.
26. Kawase T, Okuda K, Yoshie H, Burns DM. Anti-TGF-β antibody blocks enamel matrix derived-induced upregulation of $p21^{WAF1/cip1}$ and prevents its inhibition of human oral epithelial cell proliferation. *J Periodontal Res* 2002;37:255–62.
27. Mosmann T. Rapid colorimetric assay for cellular growth and survival: application to proliferation and cytotoxicity assays. *J Immunol Methods* 1983;65:55–63.

J Dent Sci 2009;4(3):136–148

ORIGINAL ARTICLE

Reactions of connective tissue to self-etching/priming dentin bonding systems: oxidative stress, tumor necrosis factor α expression, and tissue reactions

Yahya Orçun Zorba,[1] Mehmet Yildiz,[2] Abdulkadir Yildirim,[3] Nesrin Gursan,[4] Ertugrul Ercan[5]*

[1]Department of Endodontics, Dentistry Faculty, Kirikkale University, Kirikkale, Turkey
[2]Department of Restorative Dentistry, Dentistry Faculty, Ataturk University, Erzurum, Turkey
[3]Department of Biochemistry, School of Medicine, Ataturk University, Erzurum, Turkey
[4]Department of Histopathology, School of Medicine, Ataturk University, Erzurum, Turkey
[5]Department of Restorative Dentistry, Dentistry Faculty, Kirikkale University, Kirikkale, Turkey

Received: May 8, 2009
Accepted: Jul 30, 2009

KEY WORDS:
biocompatibility;
cytokines;
dentin bonding agents;
immune response;
soft tissue

Background/purpose: Few data have been published concerning tissue and systemic responses to resinous dental materials. The aim of this study was to compare and evaluate the biocompatibility of four kinds of dental self-etching/priming adhesives by measuring tissue responses, local and systemic tumor necrosis factor (TNF) α expression, and oxidative stress parameters.
Materials and methods: Eighty rats were equally divided into 10 groups. Four dental adhesives (Clearfil SE Bond, iBond, Clearfil Protect Bond, and Adper Prompt L-Pop) were applied to connective tissue of the rats. In the control group, rats were operated on with no material being applied. Biocompatibilities of the bonding agents were evaluated according to tissue responses, histopathologic and biochemical TNF-α expressions, and levels of malondialdehyde, glutathione, superoxide dismutase and glutathione peroxidase activities 1 week and 1 month after initiation of treatment.
Results: All neutrophil levels and edema formation between the iBond group and the other groups were statistically significant after 1 week. Fibroblast levels in the Clearfil SE Bond group were higher than all other groups. Vascularization levels statistically differed between the Clearfil SE Bond and iBond groups, and between the Adper Prompt L-Pop and control groups. Tissue TNF-α levels statistically differed in all groups other than the control group. At the end of 1 month, the neutrophil level in the iBond group was higher than that in the control group. The differences in fibroblast levels after 1 month were statistically significant between the Clearfil SE Bond and Clearfil Protect Bond groups, and between the control and iBond groups. Tissue TNF-α levels were higher in the iBond, Clearfil Protect Bond, and Adper Prompt L-Pop groups than in the Clearfil SE Bond and control groups.
Conclusion: There were no statistical differences in levels of serum TNF-α and oxidative stress parameters in any groups during the course of the study. The four different adhesive systems exhibited different degrees of local toxicity to the subsurface of the skin of rats, but no systemic toxicity was detected.

*Corresponding author. Department of Endodontics, Faculty of Dentistry, Kırıkkale University, Kırıkkale 71100, Turkey.
E-mail: orcunzorba@kku.edu.tr

Introduction

The increasing use of esthetic restorations has led to extensive use of dental adhesives. Today, many commercial brands of bonding agents are available for clinical use. The latest generation of dentin-bonding agents seems to be simpler to use and more efficient than earlier generations.[1] However, the use of new materials with new chemical properties has raised questions concerning the biologic effects of the materials and techniques. Additionally, the reported biologic effects of dentin-bonding agents range from none to severe, depending on several factors.[2]

To evaluate the biocompatibility of dental materials, a sequence of tests must be performed, including *in vitro* assays for mutagenesis and cytotoxicity (initial tests), local toxicity reactions by intraosseous or subcutaneous implantation of the material in small laboratory animals (secondary tests), and finally usage tests.[3]

The immune system triggers inflammatory reactions to limit tissue damage against invading or foreign molecules.[4] The inflammatory response occurs in vascularized connective tissue, including plasma, circulating cells, blood vessels, and cellular and extracellular constituents of connective tissue, such as mast cells, fibroblasts and lymphocytes.[5]

Cytokines are proteins produced by many types of cells that modulate the function of other cell types. Long known to be involved in cellular immune responses, these products have additional effects that play important roles in both acute and chronic inflammation.[5] The major cytokines that mediate inflammation are interleukin 1 and tumor necrosis factor (TNF). There are two types of TNF: TNF-α and TNF-β.[6]

In the biologic evaluation of adhesive systems, one interesting possibility would be to detect the production of intracellular reactive oxidative species (ROS) induced by leachable monomers.[7] Oxidative stress (OS) is a general term used to describe the steady-state level of oxidative damage in a cell, tissue or organ caused by ROS. This damage can affect a specific molecule or the entire organism. ROS, such as free radicals and peroxides, represent a class of molecules derived from the metabolism of oxygen and inherently exist in all aerobic organisms.[8,9] Oxygen-centered free radicals are known as oxygen free radicals (OFRs).[10] Examples of OFRs are the superoxide anion ($O_2^{\bullet -}$), hydroxyl ($OH^{\bullet -}$), peroxyl ($RO_2^{\bullet -}$), alkoxyl ($RO^{\bullet -}$), and hydroperoxyl ($HO_2^{\bullet -}$) radicals.[11] These play different roles *in vivo*. However, OFRs may be very damaging, because they can oxidize lipids in cell membranes, enzymes, proteins in tissues, carbohydrates, and DNA.[9,10]

To prevent damage caused by OFRs, multiple defense systems, collectively called antioxidants, are present in serum, erythrocytes, and other organs and tissues. The antioxidant system consists of antioxidant molecules such as glutathione (GSH), vitamins A, E and C, ceruloplasmin, transferrin, albumin, and various antioxidant enzymes. Erythrocytes are excellently equipped to handle intracellular OS through the combined activity of glutathione peroxidase (GPX), and superoxide dismutase (SOD). SOD is believed to play a major role in the first line of antioxidant defense.[12]

Lipid peroxidation is the oxidative conversion of polyunsaturated fatty acid products such as malondialdehyde (MDA), which is usually measured as total thiobarbituric acid-reactive substances (TBARSs), or lipid peroxides. This is the most studied and biologically relevant free radical reaction.[13,14]

It was reported that hypertonic acidic agents applied to dentin following cavity preparation remove the smear layer and smear plugs as well as decalcify the peritubular dentin.[15] The outward dentin fluid movement then interferes with the penetration and setting of the bonding agent, from which uncured residual components that diffuse through the dentin are released during the light-curing procedure. Therefore, it is important to employ biocompatible dental materials near pulp tissues. However, few data have been published concerning tissue responses to self-etching/priming dental adhesives.[16]

Several *in vivo* studies have reported that both dental materials and their components as well as microleakage play influential roles in the inflammatory tissue response.[17,18] The aim of this study was to investigate tissue reactions of dentin bonding agents without the effect of microleakage or bacterial contamination.

The null hypotheses to be tested were: (1) there is no difference in the tissue reaction ability and local/systemic TNF-α production among the four commercially available self-etching/priming dentin-bonding agents; and (2) that all bonding agents will cause OS in rats.

Materials and methods

The study was conducted at the Ataturk University Experimental Animal and Research Center. The Ataturk University Ethics and Research Committee on the Care, Welfare and Use of Laboratory Animals approved the experimental protocol. Eighty male Sprague-Dawley rats, 80–100 days old and weighing 140–268 g, were used.

The rats were divided into 10 groups with eight rats in each, placed in cages ($60 \times 60 \times 45$ cm), and

with permitted *ad libitum* consumption of a conventional diet formulated to meet nutrient requirements assessed by the National Research Council.[19] Fresh water was also available *ad libitum* during the experiment. Rat adaptation was observed for 1 week before the experiment began.

The bonding agents used were Clearfil SE Bond (Kuraray America, Inc., New York, NY, USA), iBond (Heraeus Kulzer GmbH, Hanau, Germany), Clearfil Protect Bond (Kuraray America, Inc.), and Adper Prompt L-Pop (3M Dental Products, St. Paul, MN, USA). Applications of these agents to the rats in the groups, the durations of treatment courses, and manufacturers are shown in Tables 1 and 2. Groups CI and CII were assigned for control purposes. Group CI represented a control group of 1-week findings and Group CII of 1-month findings. Rats in the control groups were operated on, but no material was applied.

An induction mixture of ketamine hydrochloride (Ketalar, Eczacıbaşı, Lüleburgaz, Turkey) at 50 mg/kg and xylazine hydrochloride (Rompun, Bayer, Istanbul, Turkey) at 5 mg/kg was administered intramuscularly, followed by maintaining inhalation anesthesia using 1.5–4% sevoflurane (Sevorane; Abbott Laboratories, Istanbul, Turkey) volatilized with oxygen and delivered by means of a snout mask.

Table 1. Applied materials, experimental times, and groups

Group	Applied materials	Time	Weight (g)
Group SEI	Clearfil SE Bond	1 wk	190–226
Group iBI	iBond	1 wk	210–240
Group PBI	Clearfil Protect Bond	1 wk	176–242
Group PLPI	Adper Prompt L-Pop	1 wk	190–206
Group CI	Control	1 wk	166–268
Group SEII	Clearfil SE Bond	1 mo	144–190
Group iBII	iBond	1 mo	206–246
Group PBII	Clearfil Protect Bond	1 mo	174–234
Group PLPII	Adper Prompt L-Pop	1 mo	168–220
Group CII	Control	1 mo	140–208

Table 2. Components and manufacturers of the bonding agents

Classification	Product	Manufacturer	Components	Batch no.	pH
One-step self-etching	Adper Prompt L-Pop	3M Dental Products, St. Paul, MN, USA	Liquid A or compartment: methacrylated phosphoric acid esters, photoinitiator, stabilizers Liquid B or compartment: water, HEMA, polyalkenoic acid, stabilizers	187444	<1
One-step self-etching (no mixing required)	iBond	Heraeus Kulzer GmbH, Hanau, Germany	UDMA, 4-META, acetone, water, glutaraldehyde, camphorquinone	010067	2.0–2.2
Two-step self-etching	Clearfil SE Bond	Kuraray America, Inc., New York, NY, USA	Primer: MDP, HEMA, dimethacrylates, water, photoinitiator Bond: MDP, Bis-GMA, HEMA, photoinitiator, colloidal silica	389	1.9
Two-step self-etching (with an antibacterial feature)	Clearfil Protect Bond	Kuraray America, Inc., New York, NY, USA	Primer: MDP, MDPB, HEMA, water Bond: MDP, Bis-GMA, HEMA, camphorquinone, colloidal silica, NaF	Primer 5B Adeziv 10B	1.9

HEMA=hydroxyethyl methacrylate; UDMA=urethane dimethacrylate; 4-META=4-methacryloxyethyltrimellitic acid anhydride; MDP=10-methacryloyloxydecyl dihydrogen phosphate; Bis-GMA=bisphenol A diglycidyl methacrylate.

Under general anesthesia, the dorsal side was shaved and the material applied using a 10% povidone iodine antiseptic solution (Poviiodeks; Kim-Pa Co., Istanbul, Turkey), and a sterile drape was placed over the side with the animal in the lateral recumbent position. An incision was made using a 1-cm scalpel (no. 11) inserted unilaterally under the skin. A gap was prepared by inserting a retractor into the incision region to provide an application zone for the bonding agents away from the incision side. The implantation area for the applied material was then separated from the area of wound inflammation. Dental bonding systems (DBSs) were applied in accordance with the manufacturers' instructions onto subcutaneous connective tissue (Table 3). The wound was then closed and the skin sutured using 4.0 sterile sutures (Maxon 4.0, lot R77386G; Cyanamid of Great Britain, Gosport, Hampshire, UK). In the control groups, the same operation was performed but no material was applied. The animals were free to move about.

At the end of the procedure, blood from all of the rats was drawn into vacutainer tubes from the heart under the same anesthetic procedure as described above, allowed to clot, and then centrifuged at 3500*g* (5 minutes, 4ºC). The serum was immediately frozen in 1-mL aliquots and stored at −80ºC until the biochemical analyses were performed. One subject from the PLPI group died at the time of anesthesia. Specimens were thawed immediately before the assay, and hemolyzed specimens were excluded. Serum TNF-α was measured using a commercial enzyme-linked immunosorbent assay kit according to the manufacturer's instructions (series no. 11828014; Bender MedSystems, Vienna, Austria).

The subjects were sacrificed using the surgical exsanguination technique. The operative zone was extracted together with the connective tissue and fixed with 10% neutralized buffered formalin. Specimens were then embedded in paraffin, and serial sections 5 μm thick were cut on a microtome and stained with hematoxylin and eosin. All sections were blindly evaluated by two examiners for five histologic features: neutrophils, fibroblasts, lymphocytes, vascularization, and edema formation. The state of the various types of inflammatory cells, their occurrence, and tissue responses were graded from 0 to 3 as described in Table 4.

Local production of TNF-α was evaluated immunohistochemically using an anti-TNF-α kit (series no. 10026.05; DakoCytomation, Glostrup, Denmark) according to the manufacturer's protocol. Briefly, tissue samples on polylysine-coated slides were deparaffinized and rehydrated. Microwave antigen retrieval was then performed, and samples were incubated in a 3% H_2O_2 solution to inhibit endogenous peroxidase. To block nonspecific background staining, sections were incubated with a blocking solution. Sections were then incubated with a primary anti-TNF-α antibody, followed by incubation with a biotinylated goat anti-mouse antibody. After

Table 3. Application techniques of the dental bonding systems

Product	Application procedure
Adper Prompt L-Pop	1. Press compartment 1. 2. Fold the red chamber onto the yellow chamber. 3a. Press on the chambers. 3b. Spin or churn applicator to mix adhesive. 4. Apply 0.1 mL of adhesive to the connective tissue. 5. Wait 15 s. 6. Gently but thoroughly air-dry to remove the aqueous solvent. 7. Light-cure for 10 s.
iBond	1. Shake vigorously. 2. Apply 0.1 mL of adhesive to the connective tissue. 3. Wait 20 s. 4. Gently but thoroughly air-dry to remove the aqueous solvent. 5. Light-cure for 10 s.
Clearfil SE Bond	1. Apply 0.05 mL of primer to the connective tissue and let sit for 20 s. 2. Dry with mild air flow. 3. Apply 0.05 mL (total 0.1 mL) of bonding agent and distribute with gentle air flow. 4. Light-cure for 10 s.
Clearfil Protect Bond	1. Apply 0.05 mL of primer to the connective tissue and let sit for 20 s. 2. Dry gently with mild air flow. 3. Apply 0.05 mL (total 0.1 mL) of bonding agent and distribute with gentle air flow. 4. Light-cure for 10 s.

Table 4. Inflammatory tissue response

	Score 0	Score 1	Score 2	Score 3
Neutrophils	None or a few scattered neutrophils present in the operative area	Some neutrophils present in the operative area	A moderate number of neutrophils present in the operative area	Many neutrophils present in the operative area
Fibroblasts	None or a few scattered fibroblasts present in the operative area	Some fibroblasts present in the operative area	A moderate number of fibroblasts present in the operative area	Many fibroblasts present in the operative area
Lymphocytes	None or a few scattered lymphocytes present in the operative area	Some lymphocytes present in the operative area	A moderate number of lymphocytes present in the operative area	Many lymphocytes present in the operative area
Vascularization	None or slight scattered vascularization present in the operative area	Some vascularization present in the operative area	Moderate vascularization present in the operative area	Much vascularization present in the operative area
Edema	None or slight scattered edema formation present in the operative area	Some edema formation present in the operative area	Moderate edema formation present in the operative area	Severe edema formation present in the operative area

incubation with the chromogenic substrate (DAB), sections were counterstained with hematoxylin and eosin.

The intensities of local TNF-α levels and tissue reactions were evaluated using a light microscope (100× and 200× magnification; Olympus BX51; Olympus Europa Holding, Hamburg, Germany). All analyses were performed by two pathologists who were blinded to the group assignments. The evaluation of staining of cytoplasmic TNF-α in the tissue was scored as a percentage of results, and the tissue reactions were classified as mild, moderate or severe.

To measure OS, 1 mL of blood was taken from the heart using a 24-gauge angiocatheter (Hayat Medical Instruments Co., Istanbul, Turkey) 1 week and 1 month after implantation. Erythrocyte sediments were prepared for the analyses. Erythrocytes were then hemolyzed by diluting with deionized water (50-fold), and the analyses were carried out in these hemolyzed supernatant fractions. Hemoglobin (Hb) values of samples were measured using a Gen-S counter hematology analyzer (Beckman Coulter, Inc., Fullerton, CA, USA). Hemolysate samples were kept at −80ºC until biochemical determination.

The MDA measurement, an important indicator of OS, was based on the spectrophotometric absorbance of the pink-colored product of the thiobarbituric acid-reactive substance (TBARS) complex.[20] Total TBARSs were expressed as MDA. Results are expressed as nanomole per gram of Hb. SOD activity was measured by nitroblue tetrazolium reduction by $O_2^{\bullet -}$ generated by the xanthine/xanthine oxidase system.[21] SOD activity was measured at 560 nm by detecting the inhibition of this reaction, and was expressed as unit per milligram of Hb. GPX activity was detected according to the method described by Paglia and Valentine.[22] By measuring the absorbance change in NADPH at 340 nm per minute and using the molar extinction coefficient of NADPH, GPX activity was calculated as unit per gram of Hb. The total GSH level was measured spectrophotometrically at 412 nm using a glutathione disulfide reductase recycling method, as described by Tietze.[23] In this method, the rate of yellow-colored 5-thio-2-nitrobenzoic acid production is directly proportional to the concentration of GSH in the sample. Results were expressed as micromole per gram of Hb.

Statistical analyses were carried out using analysis of variance among MDA, GSH, SOD, and GPX levels, and serum and tissue TNF-α levels. Differences between groups were evaluated using Duncan's multiple comparison test at a significance level of $P<0.05$.

For the statistical analysis of the tissue reaction, Mann-Whitney *U* and Kruskal-Wallis tests were performed to determine whether there was a statistically significant difference ($P<0.05$) among ranked groups and times.

Results

Gross findings

In the 1-week findings, Groups CI and SEI, with the exception of two subjects (for which exudate was observed after scab removal), showed healing in the wound. However, there was no evidence of healing in the operative zone, and a thick scab,

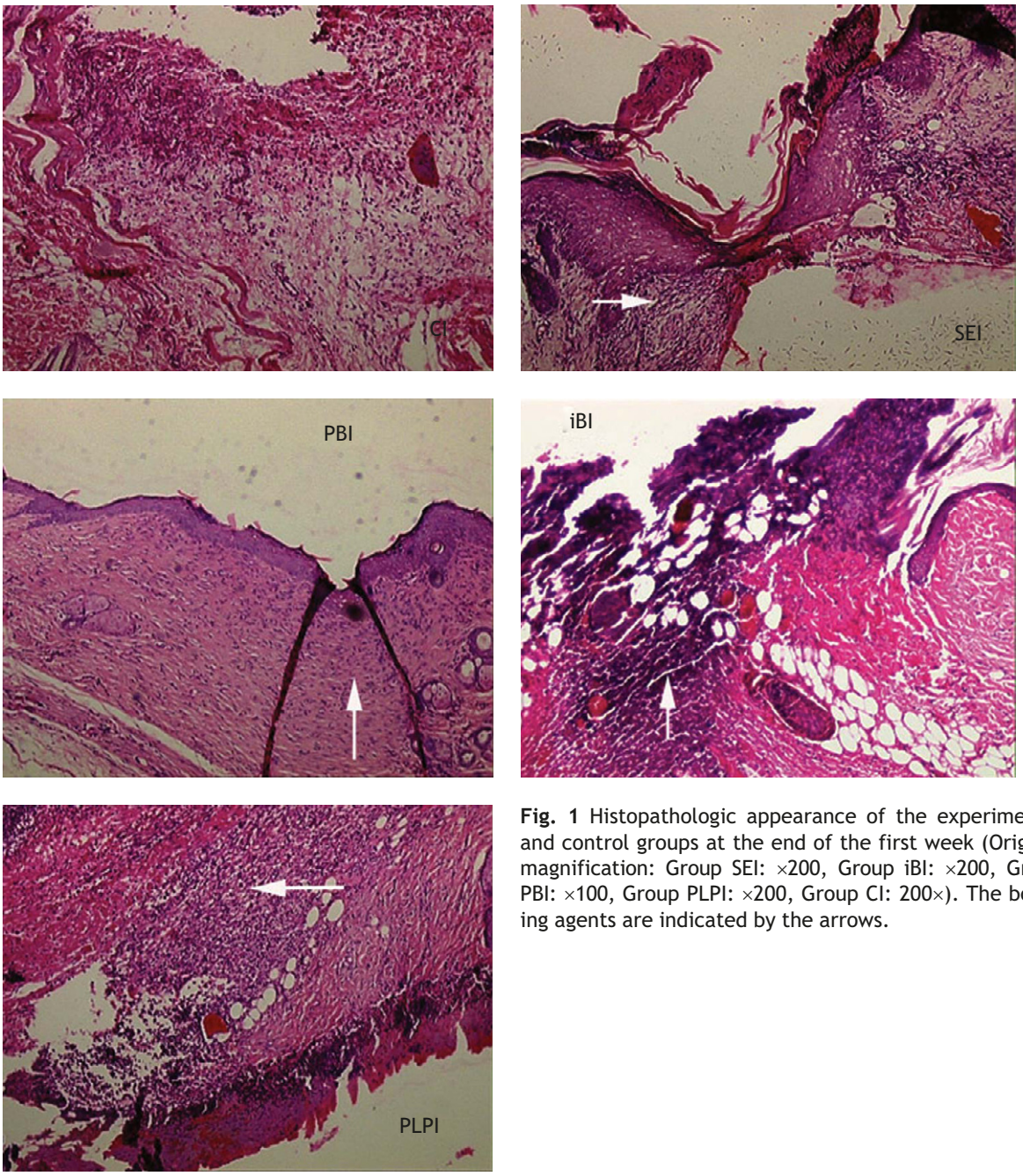

Fig. 1 Histopathologic appearance of the experimental and control groups at the end of the first week (Original magnification: Group SEI: ×200, Group iBI: ×200, Group PBI: ×100, Group PLPI: ×200, Group CI: 200×). The bonding agents are indicated by the arrows.

inflammation and exudate were present in all subjects in the groups.

In the 1-month findings, the SEII, PBII and CII groups exhibited healed wounds, and no scabs were seen. However, no healing was observed in two subjects in the iBII group and one in the PLPII group.

Histopathologic findings at 1 week

Fibroblast levels in Group SEI were higher than in the other groups ($P<0.01$). Although neutrophil and vascularization levels were similar to those in the control group, edema formation and lymphocyte counts were slightly higher than in Group CI (control group, 1-week findings), although the difference was not statistically significant (Fig. 1).

Neutrophil, vascularization and edema levels were significantly higher in Group iBI compared with the other groups ($P<0.01$), and fibroblast levels were lower than those in the other groups ($P<0.01$), except for the controls (Fig. 1).

Vascularization and edema formation were higher in the PBI group than in the SEI and CI groups. Neutrophil levels were higher in the PBI group than in all other groups ($P<0.01$) except for Group iBI at 1 week (Fig. 1).

Neutrophil levels were higher in Group PLPI than in Groups SEI and CI ($P<0.01$) but were lower

than in Group iBI. Lymphocyte and fibroblast levels were higher than in the other groups, except for Group SEI. However, these findings were not statistically significant. In addition, the vascularization level was lower in Group PLPI than in Groups iBI and PBI and higher than in the controls and in Group SEI ($P<0.01$) (Fig. 1).

Levels of lymphocyte and neutrophil infiltration were low in density in Group CI (control). Edema and fibroblast levels were determined to be small, except in two subjects. The neutrophil level in the control group differed from that in Groups iBI and PBI ($P<0.01$). Fibroblast and vascularization levels differed from those in Group iBI ($P<0.01$) (Fig. 1).

Histopathologic findings at 1 month

Fibroblast and lymphocyte counts were higher in Group SEII than in Group CII (1-month findings in the control group; $P<0.001$ for fibroblasts and $P<0.01$ for lymphocytes), but the other data were similar to the controls. When compared with the 1-week findings, neutrophil and vascularization levels had decreased ($P<0.05$) but the fibroblast level had increased ($P<0.05$; Fig. 2).

Although neutrophil and lymphocyte levels were higher in Group iBII than in the other groups ($P<0.05$), the fibroblast level was lower ($P<0.001$). Compared with the 1-week findings, the fibroblast

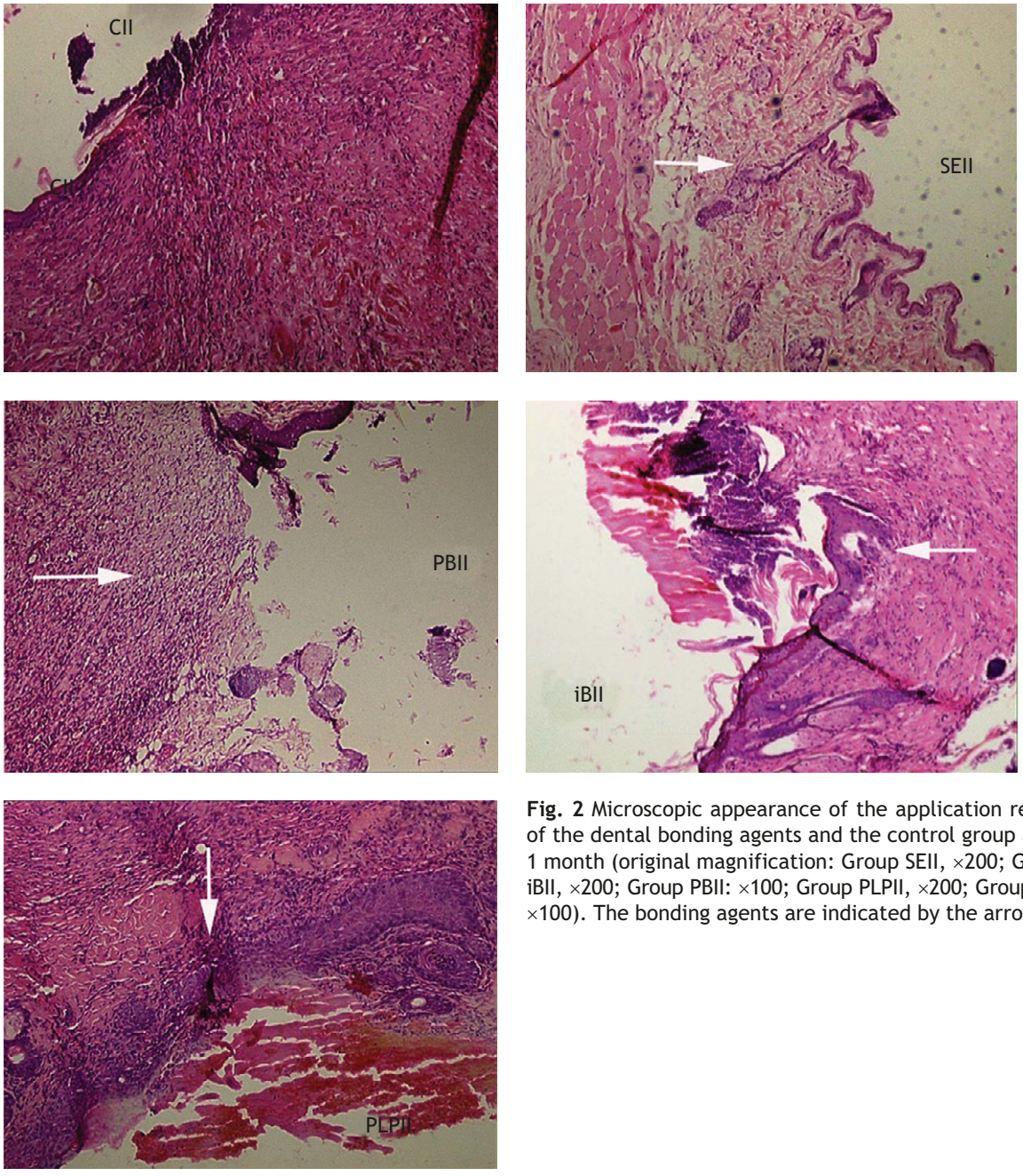

Fig. 2 Microscopic appearance of the application region of the dental bonding agents and the control group after 1 month (original magnification: Group SEII, ×200; Group iBII, ×200; Group PBII: ×100; Group PLPII, ×200; Group CII, ×100). The bonding agents are indicated by the arrows.

level had increased ($P<0.05$) but edema, neutrophil ($P<0.05$), and vascularization ($P<0.01$) levels had decreased (Fig. 2).

All findings in Group PBII were higher than those in Group CII. When compared with the 1-week data, fibroblastic activity had risen ($P<0.05$) but neutrophil ($P<0.05$) and vascularization levels ($P<0.01$) had decreased (Fig. 2).

All findings in Group PLPII were higher than in the controls. Lymphocyte activity differed from those in groups SEII and PBII. Compared with 1-week data, fibroblastic activity had risen ($P<0.05$) but the other findings had decreased ($P<0.05$) (Fig. 2).

All inflammation values in Group CII (control) were lower than those in the other 1-month groups. The values were lower in degree, and all findings were statistically significant ($P<0.05$), except for the vascularization level compared with group SEII (Fig. 2). The statistical analyses showed that the 1-week and 1-month findings differed with respect to neutrophil ($P<0.05$), fibroblast ($P<0.05$) and vascularization levels ($P<0.01$).

Tissue TNF-α

During the first week, the result for local TNF-α secretion in Group CI (control) was statistically lower than in the other groups. In Groups SEI and PBI, TNF-α levels were higher than in the controls but lower than in Groups iBI and PLPI. The TNF-α receptor-binding level was concentrated in Groups iBI and PLPI. Differences between Groups SEI and PBI and between Groups iBI and PLPI were not significant, but those between the first-week groups and Group CI were significant ($P<0.001$) (Fig. 3).

At the end of the first month, no differences were determined between Groups SEII and CII (control) in terms of TNF-α levels, but Groups iBII, PBII and PLPII statistically differed from Groups CII and SEII. Differences in Groups iBII, PBII and PLPII were statistically significant ($P<0.001$; Fig. 4).

In addition, the TNF-α level in the control group decreased compared with the first-week level. In Groups iBII and PBII, TNF-α values were lower compared with those in the first week, but were still higher than those in Groups SEII and PLPII ($P<0.001$; Table 5).

Biochemical findings

There were no differences between the control and the other groups in terms of serum TNF-α and OFR production (MDA, GSH, SOD, and GPX) levels at either 1 week or 1 month. Results of the study are summarized in Tables 5–7.

Discussion

No studies have so far investigated the biocompatibility of the systemic toxicity of DBSs via ROS production. We determined no differences between the control and experimental groups in terms of MDA, GSH, SOD, and GPX values, important indicators of OS.

The biocompatibility of dentin-bonding agents is imperative, since they are placed on etched dentin near the pulp, where tubular density and diameter are the greatest.[24]

With all materials used in restorative dentistry, there is some risk of biologic reactions because of incomplete polymerization. DBSs are usually polymerized by photoactivation, and free monomers may be released from resinous materials before and after polymerization. Theoretically, a 100% conversion of monomers to polymers is possible, but as much as 25–50% of the methacrylate monomer double-bonds actually remain unreacted in the polymer.[25] The unpolymerized monomer may be responsible for biologic reactions if it passes through the dentinal tubules and reaches the pulp tissue.[26]

The immune system triggers inflammatory reactions to limit tissue damage from invading or foreign molecules.[4] In considering compatibility and its relationship to other *in vivo* elements following implantation tests, appreciation of wound healing is essential.[27] The first phase of healing is the acute inflammatory response, which includes exudation of fluid and plasma proteins (edema) and the emigration of leukocytes, predominantly neutrophils. Following the acute inflammatory response, chronic inflammation and normal wound healing occur, with the presence of lymphocytes and macrophages, the proliferation of blood vessels, and fibroblasts.[5] We used edema, and neutrophil and lymphocyte levels to assess the acute inflammatory tissue response and fibroblast and vascularization levels to assess wound healing levels. We found that when adhesive systems were applied to connective tissue, they caused an inflammatory tissue response and delayed the wound healing time compared with the control groups, at both 1 week and 1 month.

Some researchers recently determined that no adverse effect occurs when adhesive systems are applied as pulp capping materials, in spite of the manufacturers' instructions to the contrary.[28] Consequently, the biocompatibility and cytotoxicity of dental composites and their components have been analyzed, because these materials were initially recommended for application to dentin or, more recently, for direct pulp capping.[29] Jontell et al.[30] emphasized that resin components may evoke an immune reaction by spleen cells. In our study, all DBSs exhibited inflammatory reactions to differing

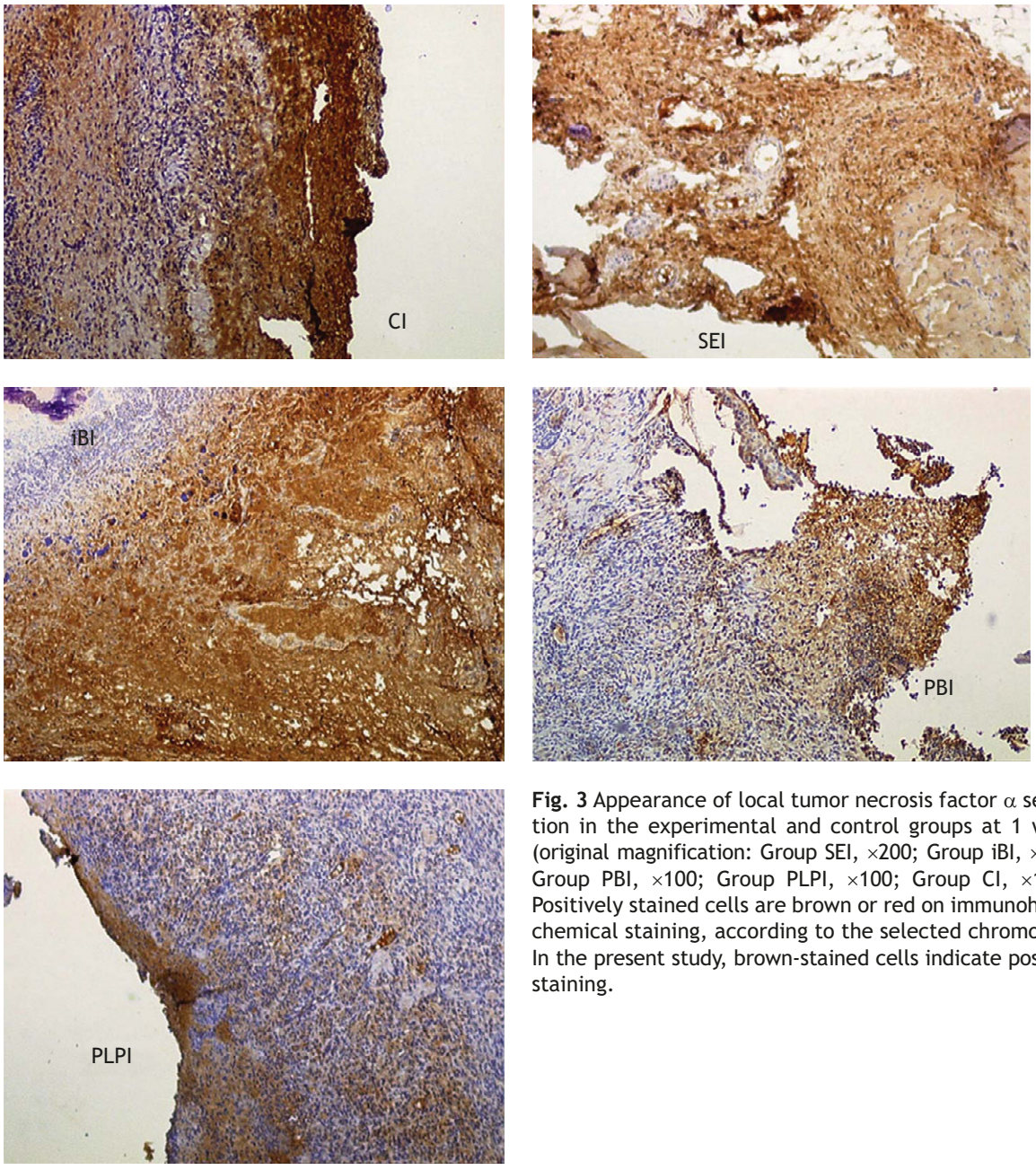

Fig. 3 Appearance of local tumor necrosis factor α secretion in the experimental and control groups at 1 week (original magnification: Group SEI, ×200; Group iBI, ×100; Group PBI, ×100; Group PLPI, ×100; Group CI, ×100). Positively stained cells are brown or red on immunohistochemical staining, according to the selected chromogen. In the present study, brown-stained cells indicate positive staining.

degrees. Wound healing was delayed in all subjects compared with control groups at both 1 week and 1 month. Reactions induced by DBSs can also enhance their acidity.[31] We used four different self-etching/priming DBSs with different acidities. Some researchers suggested that applying self-etching/priming adhesive systems to contacted pulp of healthy dog teeth does not lead to acceptable repair of the dentine-pulp complex.[32] Additionally, de Souza Costa et al.[33] determined that calcium hydroxide remains the pulp capping agent of choice for mechanically exposed human pulp. Self-etching adhesive systems do not allow complete connective tissue repair adjacent to the pulp exposure site. These findings are in agreement with those of the present study.

TNF-α is an inflammatory cytokine produced by macrophages/monocytes during acute inflammation, is responsible for a diverse range of signaling events within cells, and leads to necrosis or apoptosis. Proteins are also important for resistance to infection.[6]

We used local TNF-α levels to compare the biologic reactions of the DBSs. The eight working groups exhibited differing degrees of tissue reactions. Inflammation was maintained at different levels at 1 week and 1 month. In addition, wound healing was slow in all groups compared with the

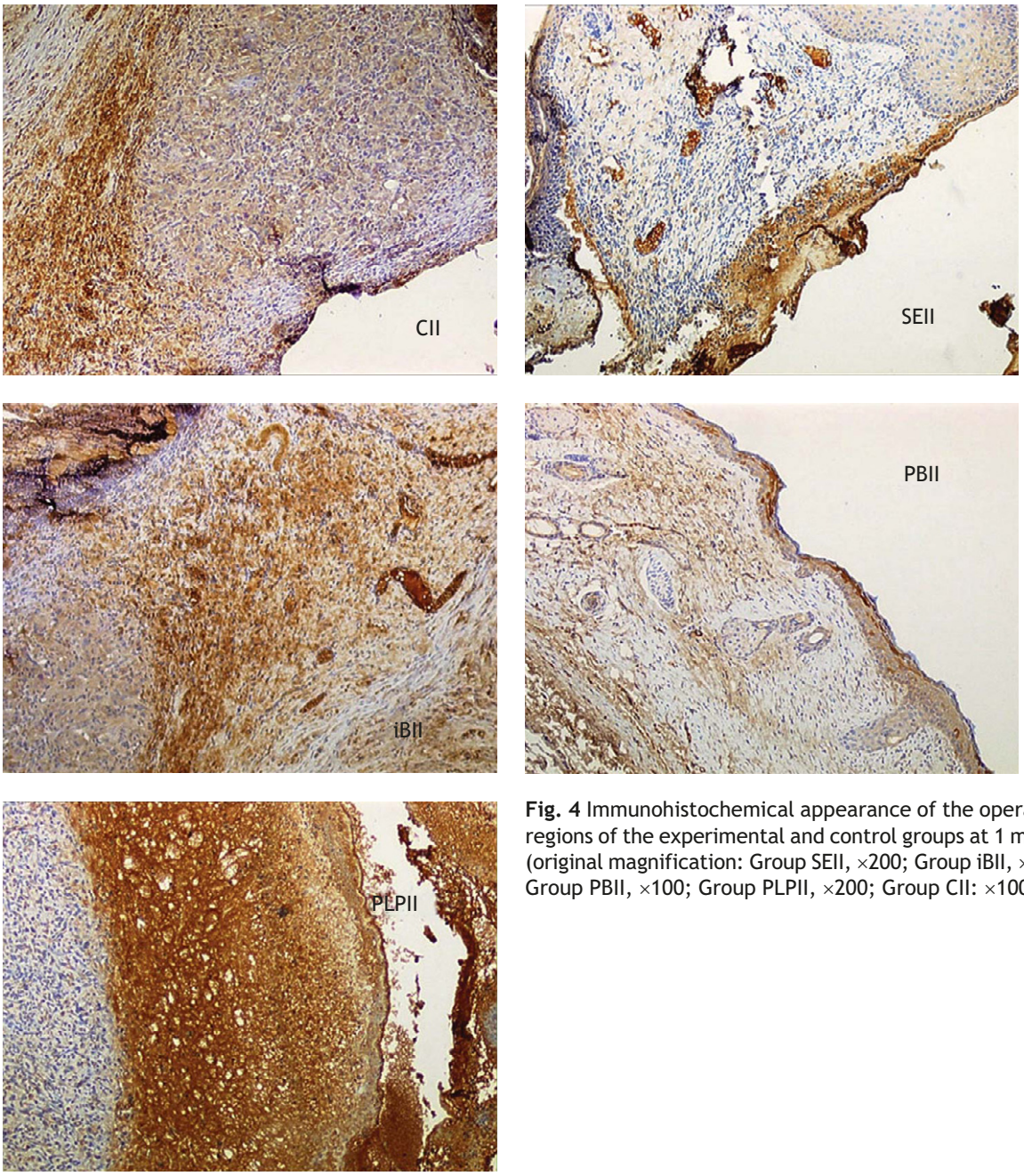

Fig. 4 Immunohistochemical appearance of the operative regions of the experimental and control groups at 1 month (original magnification: Group SEII, ×200; Group iBII, ×100; Group PBII, ×100; Group PLPII, ×200; Group CII: ×100).

Table 5. Tissue tumor necrosis factor (TNF) α level*

	Control	Clearfil SE Bond	iBond	Clearfil Protect Bond	Adper Prompt L-Pop
TNF-α, mean (SD) (%)					
1 wk	23.125[†] (9.6130)	38.75[‡] (19.5941)	78.7500[§] (11.2599)	47.50[‡] (7.5592)	76.42[§] (14.6385)
1 mo	13.750[‖] (4.4320)	15.00[‖] (7.0710)	70.62[¶] (10.5008)	25.00[#] (10.3509)	16.87[‖#] (5.9386)

*Means with different symbols in a given row statistically differ ($P<0.05$). SD=standard deviation.

Table 6. Neutrophil, fibroblast, vascularization, and edema scores at 1 week and 1 month

	Control	Clearfil SE Bond	iBond	Clearfil Protect Bond	Adper Prompt L-Pop
Neutrophil score (%)					
1 wk					
1	87.5	62.5	–	12.5	42.9
2	12.5	25.0	37.5	62.5	42.9
3	–	12.5	62.5	25.0	14.2
1 mo					
1	87.5	75.0	25.0	75.0	50.0
2	12.5	25.0	50.0	25.0	50.0
3	–	–	25.0	–	–
Fibroblast score (%)					
1 wk					
1	87.5	12.5	75.0	50.0	42.9
2	12.5	25.0	25.0	50.0	42.9
3	–	62.5	–	–	14.2
1 mo					
1	87.5	–	50.0	37.5	87.5
2	12.5	37.5	50.0	62.5	12.5
3	–	62.5	–	–	–
Lymphocyte score (%)					
1 wk					
1	100	37.5	62.5	50.0	42.9
2	–	50.0	37.5	50.0	42.9
3	–	12.5	–	–	14.2
1 mo					
1	75.0	12.5	–	50.0	62.5
2	25.0	62.5	75.0	50.0	37.5
3	–	25.0	25.0	–	–
Vascularization score (%)					
1 wk					
1	62.5	50.0	–	25.0	57.2
2	37.5	50.0	37.5	62.5	28.6
3	–	–	62.5	12.5	14.2
1 mo					
1	87.5	87.5	75.0	62.5	50.0
2	12.5	12.5	25.0	37.5	50.0
3	–	–	–	–	–
Edema score (%)					
1 wk					
1	87.5	37.5	–	37.5	28.6
2	12.5	50.0	37.5	50.0	42.9
3	–	12.5	62.5	12.5	28.6
1 mo					
1	75.0	75.0	25.0	37.5	62.5
2	25.0	25.0	50.0	50.0	37.5
3	–	–	25.0	12.5	–

control groups in terms of histopathologic and biochemical findings. Our results are in agreement with those of Cortes et al.[34] who determined localized abscess formation and no dentinal bridge formation after applying different adhesives to rat molar tooth pulp. Rakich et al.[35] also demonstrated that the application of dentin bonding agents to cell culture medium causes secretion of TNF-α from macrophages. However, other researchers reported that resin-based materials allow pulp healing and tertiary dentine deposition.[28]

In this study, tissue levels of TNF-α were compared to evaluate systemic biologic reactions to the various dentin bonding agents. No systemic toxicity derived from the dentin bonding agents was determined. The findings of this study are compatible

Table 7. Serum tumor necrosis factor (TNF) α, malondialdehyde (MDA), and glutathione (GSH) levels and superoxide dismutase (SOD) and glutathione peroxidase (GPX) activities*

	Control	Clearfil SE Bond	iBond	Clearfil Protect Bond	Adper Prompt L-Pop
MDA (nmol/g Hb)					
1 wk	5.52 (1.09)	4.66 (2.15)	5.98 (1.98)	4.92 (2.06)	4.05 (1.78)
1 mo	4.67 (0.19)	6.58 (2.42)	3.8 (1.69)	5.12 (0.84)	5.94 (2.54)
SOD (U/mg Hb)					
1 wk	226.23 (132.31)	240.4 (146.5)	249.79 (154.49)	176.85 (141.85)	248.38 (190.63)
1 mo	294.44 (46.46)	273.59 (177.99)	327.15 (175.84)	374.04 (173.94)	248.47 (81.29)
GSH (μmol/g Hb)					
1 wk	53.64 (17.27)	75.96 (44.69)	113.96 (48.64)	72.06 (40.82)	88.07 (45.09)
1 mo	81.41 (19.33)	76.55 (45.09)	50.73 (27.12)	98.22 (48.54)	83.54 (23.6)
GPX (U/g Hb)					
1 wk	9.66 (4.89)	8.11 (3.23)	7.95 (3.22)	8.06 (4.57)	9.86 (5.194)
1 mo	8.54 (4.79)	8.42 (2.49)	9.2 (2.3)	11.79 (6.17)	9.6 (4.4)
TNF-α (pg/mL)					
1 wk	$437.25^{\dagger}$ (73.43)	$630.63^{\dagger\ddagger}$ (103.39)	$774.38^{\ddagger}$ (94.97)	$484.38^{\dagger\ddagger}$ (94.21)	$702.86^{\dagger\ddagger}$ (147.59)
1 mo	$366.875^{\S}$ (35.41)	$615.63^{\|}$ (54.11)	$362.5^{\S}$ (89.36)	$438.13^{\S\|}$ (88.21)	$554.38^{\S\|}$ (94.02)

*Values are expressed as mean (standard deviation), and means with different symbols in a given row significantly differ ($P<0.05$). Hb=hemoglobin.

with previous results that dentin bonding agents cause no systemic toxicity, because resin-based materials release components in relatively small amounts.[36] Therefore, systemic toxicity is of less value for assessing the biocompatibility of resin-based dental materials.

OFRs may directly induce cell damage, or act as an intracellular messenger during cell death induced by various other kinds of stimuli.[37] Recently, OFR production was described as an early expression of cellular stress in dental monomer cytotoxicity. Some components of resin-based dental materials, such as monomers and photoinitiators, were described as increasing OFR production.[38–40] Furthermore, assaying enzymatic and non-enzymatic antioxidants provides an indirect assessment of OFR generation in OS.[41] When the balance between OFR production and antioxidative defense mechanisms is impaired, OFR levels may rise. When the OFRs are not removed by natural scavengers, damage occurs through peroxidation within the phospholipid structure of membranes.[42]

In conclusion, the null hypotheses were rejected. Histopathologic findings in this study demonstrated that DBSs caused local toxicity and delayed wound healing to different degrees when applied to connective tissue of rats. However, the findings also showed that DBSs did not induce oxidative stress or an increase in serum TNF-α. Further studies are needed to evaluate the biocompatibility of components of such adhesives and to determine the possible causes of these tissue reactions.

Acknowledgments

This study was supported by a grant-in-aid (2003-166) from the Ataturk University Scientific Project Research Foundation, Turkey. The iBond and Clearfil Protect Bond used in this study was generously supplied by Heraeus Kulzer GmbH and the Dental Department of Kuraray America, Inc. We thank Dr Yunus Emre Ozkanlar for critically reviewing the manuscript.

References

1. Imazato S, Imai T, Ebisu S. Antibacterial activity of proprietary self-etching primers. *Am J Dent* 1998;11:106–8.
2. al-Dawood A, Wennberg A. Biocompatibility of dentin bonding agents. *Endod Dent Traumatol* 1993;9:1–7.
3. Craig RG. *Restorative Dental Materials*, 10th ed. St Louis, MO: Mosby, 1997:146–56.
4. Jontell M, Okiji T, Dahlgren U, Bergenholtz G. Immune defense mechanisms of the dental pulp. *Crit Rev Oral Biol Med* 1998;9:179–200.
5. Cotran RS, Kumar V, Robbins SL. *Robbins Pathologic Basis of Disease*, 5th ed. Philadelphia: WB Saunders, 1994.
6. Idriss HT, Naismith JH. TNF alpha and the TNF receptor superfamily: structure-function relationship(s). *Microsc Res Tech* 2000;50:184–95.
7. Spagnuolo G, Annunziata M, Rengo S. Cytotoxicity and oxidative stress caused by dental adhesive systems cured with halogen and LED lights. *Clin Oral Investig* 2004;8:81–5.
8. Davies KJ. Oxidative stress: the paradox of aerobic life. *Biochem Soc Symp* 1995;61:1–31.
9. Halliwell B. Antioxidants and human disease: a general introduction. *Nutr Rev* 1997;55:S44–9; discussion S49–52.
10. Mantovani G, Maccio A, Madeddu C, et al. Quantitative evaluation of oxidative stress, chronic inflammatory indices

and leptin in cancer patients: correlation with stage and performance status. *Int J Cancer* 2002;98:84–91.
11. Fang YZ, Yang S, Wu G. Free radicals, antioxidants, and nutrition. *Nutrition* 2002;18:872–9.
12. Hristozov D, Gadjeva V, Vlaykova T, Dimitrov G. Evaluation of oxidative stress in patients with cancer. *Arch Physiol Biochem* 2001;109:331–6.
13. Polat MF, Taysi S, Gul M, et al. Oxidant/antioxidant status in blood of patients with malignant breast tumour and benign breast disease. *Cell Biochem Funct* 2002;20:327–31.
14. Taysi S, Uslu C, Akcay F, Sutbeyaz MY. Malondialdehyde and nitric oxide levels in the plasma of patients with advanced laryngeal cancer. *Surg Today* 2003;33:651–4.
15. Costa CAS, Nascimento ABL, Teixeira HM. Response of human pulps following acid conditioning and application of a bonding agent in deep cavities. *Dent Mater* 2002;18:543–51.
16. de Souza Costa CA, Teixeira HM, Lopes do Nascimento AB, Hebling J. Biocompatibility of resin-based dental materials applied as liners in deep cavities prepared in human teeth. *J Biomed Mater Res B Appl Biomater* 2007;81:175–84.
17. Cox CF, Keall CL, Keall HJ, Ostro E, Bergenholtz G. Biocompatibility of surface-sealed dental materials against exposed pulps. *J Prosth Dent* 1987;57:1–8.
18. Akimoto N, Momoi Y, Kohno A, et al. Biocompatibility of Clearfil Liner Bond 2 and Clearfil AP-X system on nonexposed and exposed primate teeth. *Quintessence Int* 1998;29: 177–88.
19. National Research Council. *Nutritional Requirements of Laboratory Animals*, 4th rev ed. Washington, DC: National Academy Press, 1995:1–173.
20. Jain SK, McVie R, Duett J, Herbst JJ. Erythrocyte membrane lipid peroxidation and glycosylated hemoglobin in diabetes. *Diabetes* 1989;38:1539–43.
21. Sun Y, Oberley LW, Li Y. A simple method for clinical assay of superoxide dismutase. *Clin Chem* 1988;34:497–500.
22. Paglia DE, Valentine WN. Studies on the quantitative and qualitative characterization of erythrocyte glutathione peroxidase. *J Lab Clin Med* 1967;70:158–69.
23. Tietze F. Enzymic method for quantitative determination of nanogram amounts of total and oxidized glutathione: applications to mammalian blood and other tissues. *Anal Biochem* 1969;27:502–22.
24. Bouillaguet S. Biological risks of resin-based materials to the dentin-pulp complex. *Crit Rev Oral Biol Med* 2004;15: 47–60.
25. Imazato S, McCabe JF, Tarumi H, Ehara A, Ebisu S. Degree of conversion of composites measured by DTA and FTIR. *Dent Mater* 2001;17:178–83.
26. Hume WR, Gerzina TM. Bioavailability of components of resin-based materials which are applied to teeth. *Crit Rev Oral Biol Med* 1996;7:172–9.
27. Hill RB, LaVia MF. *Principles of Pathobiology*. New York: Oxford University Press, 1980.
28. Costa CA, Oliveira MF, Giro EM, Hebling J. Biocompatibility of resin-based materials used as pulp-capping agents. *Int Endod J* 2003;36:831–9.
29. Costa CA, Hebling J, Hanks CT. Current status of pulp capping with dentin adhesive systems: a review. *Dent Mater* 2000;16:188–97.
30. Jontell M, Hanks CT, Bratel J, Bergenholtz G. Effects of unpolymerized resin components on the function of accessory cells derived from the rat incisor pulp. *J Dent Res* 1995; 74:1162–7.
31. Murray PE, Windsor LJ, Smyth TW, Hafez AA, Cox CF. Analysis of pulpal reactions to restorative procedures, materials, pulp capping, and future therapies. *Crit Rev Oral Biol Med* 2002;13:509–20.
32. Koliniotou-Koumpia E, Tziafas D. Pulpal responses following direct pulp capping of healthy dog teeth with dentine adhesive systems. *J Dent* 2005;33:639–47.
33. de Souza Costa CA, Lopes do Nascimento AB, Teixeira HM, Fontana UF. Response of human pulps capped with a self-etching adhesive system. *Dent Mater* 2001;17:230–40.
34. Cortes O, Garcia C, Bernabe A. Pulpal evaluation of two adhesive systems in rat teeth. *J Clin Pediatr Dent* 2000; 25:73–7.
35. Rakich DR, Wataha JC, Lefebvre CA, Weller RN. Effect of dentin bonding agents on the secretion of inflammatory mediators from macrophages. *J Endod* 1999;25:114–7.
36. Geurtsen W. Biocompatibility of resin-modified filling materials. *Crit Rev Oral Biol Med* 2000;11:333–55.
37. Mates JM, Sanchez-Jimenez FM. Role of reactive oxygen species in apoptosis: implications for cancer therapy. *Int J Biochem Cell Biol* 2000;32:157–70.
38. Baumgardner KR, Sulfaro MA. The anti-inflammatory effects of human recombinant copper-zinc superoxide dismutase on pulp inflammation. *J Endod* 2001;27:190–5.
39. Atsumi T, Murata J, Kamiyanagi I, Fujisawa S, Ueha T. Cytotoxicity of photosensitizers camphorquinone and 9-fluorenone with visible light irradiation on a human submandibular-duct cell line in vitro. *Arch Oral Biol* 1998; 43:73–81.
40. Engelmann J, Leyhausen G, Leibfritz D, Geurtsen W. Effect of TEGDMA on the intracellular glutathione concentration of human gingival fibroblasts. *J Biomed Mater Res* 2002;63: 746–51.
41. Yildiz M, Taysi S, Yildiz A, Bakan N, Akcay F, Kuskay S. Effect of composite resin filling material implantation into connective tissue of rabbits on oxidative stress in erythrocytes. *Pain Clin* 2004;16:323–8.
42. Prayag S. Role of oxygen free radicals in septic shock. *J Assoc Physicians India* 2000;48:953–5.

J Dent Sci 2009;4(3):149–158

CASE REPORT

Long-term stability of an adult Class III open-bite malocclusion treated with multiloop edgewise archwire

*Chien-Chun Kuo,[1] Yi-Jane Chen,[2,3] Eddie Hsiang-Hua Lai,[2,3] Chung-Chen Jane Yao,[2,3] Jenny Zwei-Chieng Chang[2,3]**

[1]Department of Dentistry, Mackey Memorial Hospital, Taipei, Taiwan
[2]Department of Orthodontics, National Taiwan University Hospital, Taipei, Taiwan
[3]School of Dentistry, College of Medicine, National Taiwan University, Taipei, Taiwan

Received: Jun 11, 2009
Accepted: Aug 25, 2009

KEY WORDS:
Class III malocclusion;
multiloop edgewise archwire;
open-bite

This case report describes the treatment of a 17-year-old girl with an anterior open-bite and Class III malocclusion, who had a history of thumb-sucking habit in childhood. The multiloop edgewise archwire technique was used on the mandibular arch to facilitate uprighting of the mandibular posterior teeth, change the cant of occlusal plane, close the anterior open-bite, and correct the Class III malocclusion. At the end of treatment, Class I occlusion and correction of the anterior open-bite had been achieved. An examination 8 years 8 months after treatment revealed long-term stability of the treatment results.

Introduction

Open-bite, defined as the open vertical dimension between the incisal edges of the maxillary and mandibular anterior teeth,[1] is often considered challenging to treat orthodontically because of its high tendency to relapse.[2,3] Various etiologic factors, including thumb and finger sucking,[4] lip and tongue habits,[5,6] airway obstruction,[7] excessive dentoalveolar development with the eruption of posterior teeth[8] and skeletal growth abnormalities,[9] have all been reported. A skeletal anterior open-bite is often characterized cephalometrically by a steep mandibular plane, an obtuse gonial angle, a long lower facial height, an upwardly and forward-rotated palatal plane,[10] divergent upper and lower occlusal planes, a mesial inclination of the posterior dentition, and the lack of a normal curve of Spee in the lower arch.[11]

The treatment approach for correcting an anterior open-bite ranges from observation and monitoring, myofunctional therapy, and conventional orthodontic treatment to complex surgical procedures.[12] Orthodontic appliances such as tongue cribs and lingual prongs are used to treat open-bites by redirecting an anteriorly positioned tongue posture.[13,14] On the other hand, in order to impede posterior dental eruption, reduce or redirect vertical skeletal growth and control vertical development, various appliances such as bite-blocks,[15,16] high-pull headgear[17] and chin caps[12] are used. Vertical elastics are used for incisor extrusion.[18] Severe skeletal

*Corresponding author. School of Dentistry, College of Medicine, National Taiwan University, 1, Changde Street, Taipei 10048, Taiwan.
E-mail: jennyzc@ms3.hinet.net

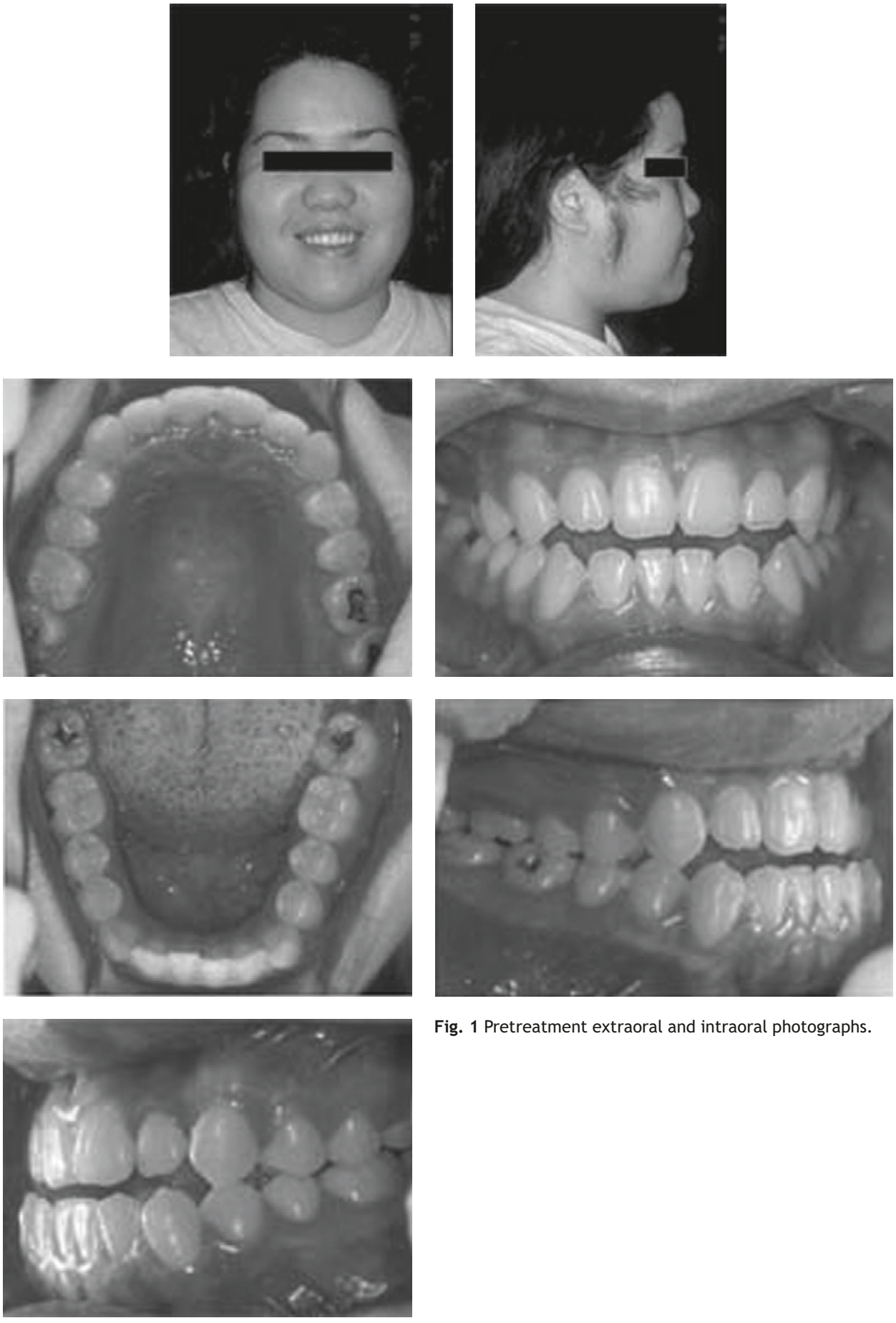

Fig. 1 Pretreatment extraoral and intraoral photographs.

open-bites in adults are often treated by means of a combined orthodontic-surgical approach.[19] Multiloop edgewise archwire (MEAW) therapy was also introduced to improve anterior open-bites by cant correction of individual occlusal planes and uprighting of the posterior teeth.[20] More recently, temporary anchorage devices (TADs) implanted in the posterior dentoalveolar area have been used for intrusion of the posterior teeth to allow counterclockwise rotation of the mandible, followed by closure of an anterior open-bite.[21] Each approach has its own pros and cons. In this article, we present a case of anterior open-bite with an Angle Class III malocclusion treated with the MEAW technique. Optimal treatment results and long-term stability were observed even after 8 years 8 months of follow-up.

Case presentation

The patient was a 17-year-old female with the chief complaint of anterior open-bite. Her medical health history was noncontributory. She reported a thumb-sucking habit in childhood. She had a mildly concave profile with an excessive lower facial height and mild chin projection (Fig. 1). Approximately 1–2 mm of gum display with a full smile was noted. No facial asymmetry was observed. The maxillary and mandibular dental midlines on observation coincided with the facial midline. The maxillary dentition was well-aligned, and the mandibular dentition exhibited a mild space deficiency in the anterior region (Fig. 1). The buccal segments had a bilateral Class III molar relationship, whereas the incisors

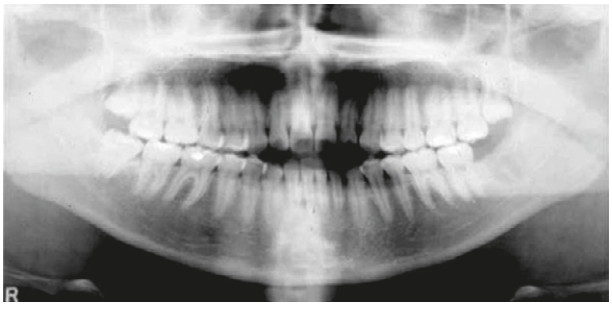

Fig. 2 Pretreatment panoramic radiograph.

Table 1. Pretreatment cephalometric analysis results

Angular and linear measurements	Pretreatment	Norm
Skeletal		
SNA (°)	81.0	81.5±3.5
SNB (°)	82.5	77.7±3.2
ANB (°)	−1.5	4.0±1.8
A-Nv (mm)	2.5	0±2.0
Pog-Nv (mm)	5.0	−5.0±8.0
SN-MP (°)	37.0	33.0±1.8
UFH/LFH (%/%)	42/58	45/55
Dental		
U1-SN (°)	108.0	108.2±5.4
L1-MP (°)	87.5.0	93.7±6.3
U1-L1 (°)	129.0	119.9±8.5

S=sella; N=nasion; A=point A (subspinale point); B=point B (supramentale point); Nv=nasion perpendicular; Pog=pogonion; MP=mandibular plane; UFH=upper anterior facial height; LFH=lower facial height; U1=long axis of upper incisor; L1=long axis of lower incisor.

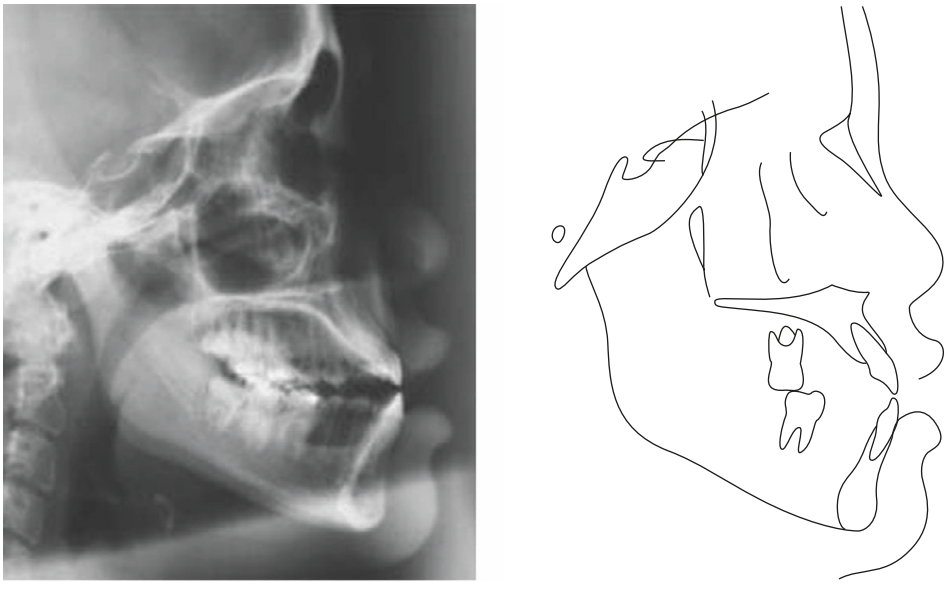

Fig. 3 Pretreatment cephalogram and tracing.

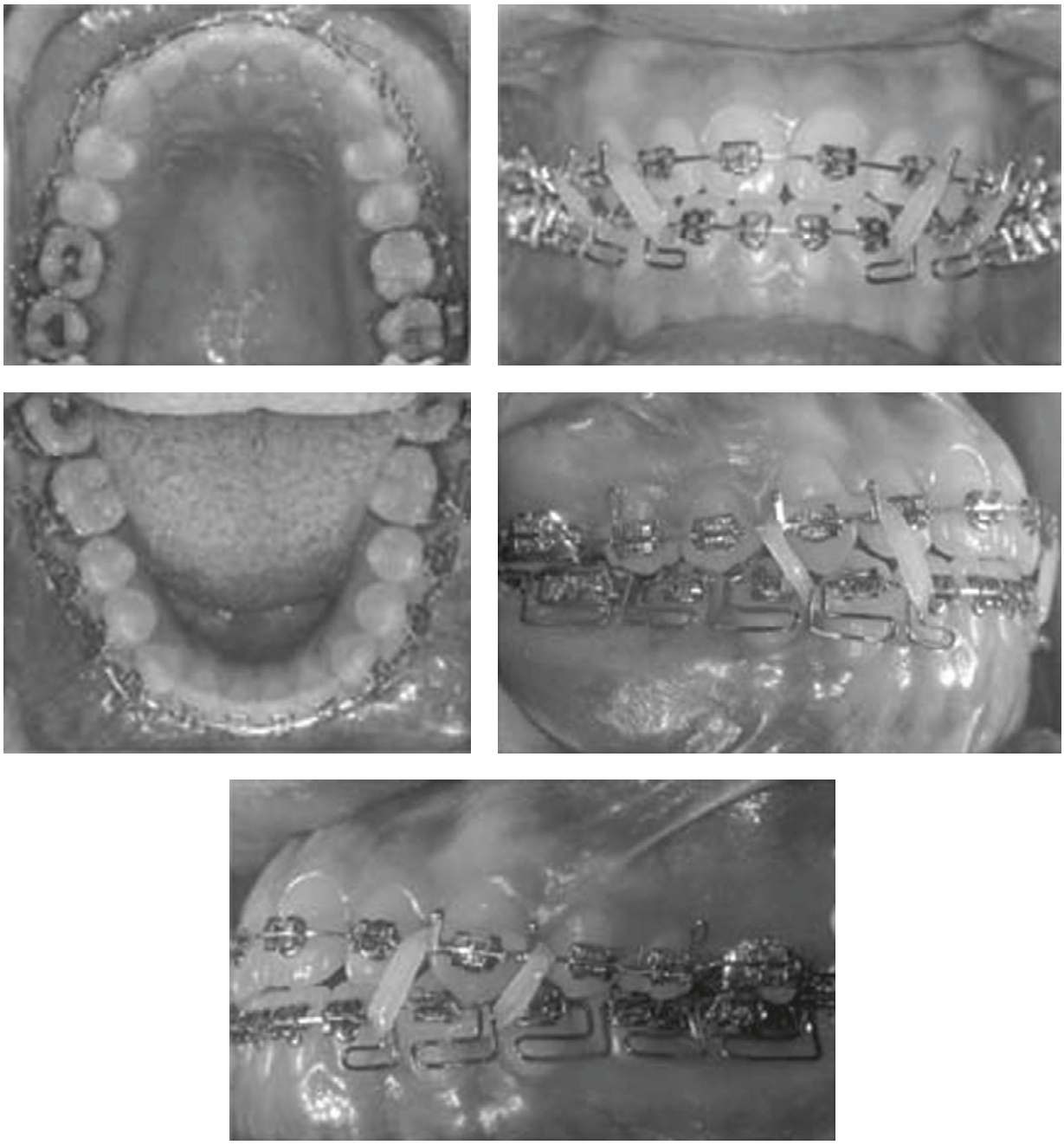

Fig. 4 Fixed appliance therapy with multiloop edgewise archwire on the lower arch augmented by short Class III elastics.

had an edge-to-edge relationship, and 2.0 mm of anterior open-bite was observed.

A panoramic radiograph showed that all teeth were present except for the mandibular left third molar which had been extracted not too long ago before she came to our clinic (Fig. 2).

Compared with Taiwanese norms, the cephalometric analysis showed a skeletal Class III relationship with mandibular prognathism (Fig. 3, Table 1). Facial hyperdivergency was observed in this patient with a component of an increased mandibular plane angle. A relatively long lower facial height and divergent upper and lower occlusal planes were also noted.

The concluding diagnoses of this patient, hence, were as follows: an Angle Class III malocclusion, a skeletal Class III jaw base relationship, and an anterior open-bite. The treatment objectives were to: (1) correct the anterior open-bite; (2) obtain a Class I canine and molar relationship; (3) establish an ideal overjet and overbite; and (4) improve the occlusal function without compromising the facial esthetics.

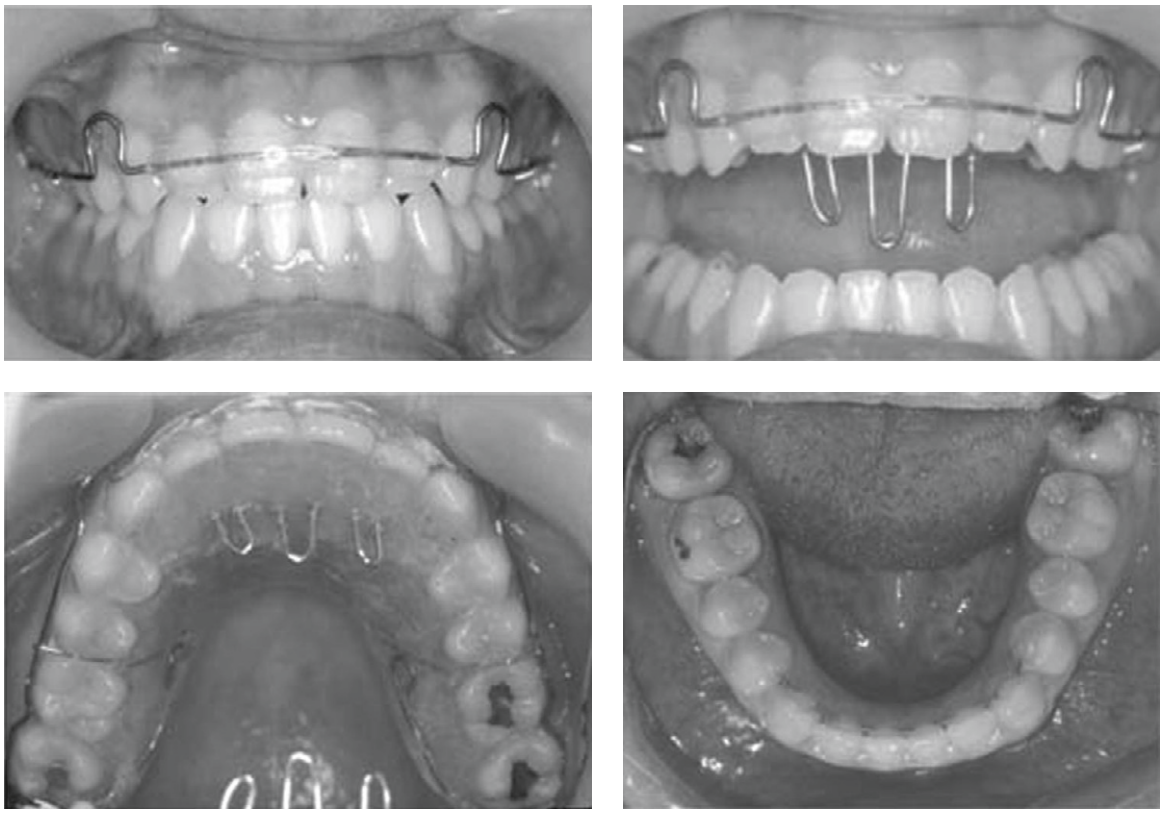

Fig. 5 Wrap-around retainer with a tongue crib on the upper arch and a lingually fixed retainer on the lower arch.

The ideal treatment approach for mandibular prognathism with a vertical skeletal discrepancy is a combination of conventional orthodontic treatment with orthognathic surgery. However, the patient refused to have surgery because of the high cost and its invasive nature. TADs such as miniscrews or miniplates were originally proposed to intrude the posterior dentition followed by closure of the anterior open-bite. However, it would have resulted in counterclockwise rotation of the mandible, which might have produced a pronounced chin projection and negatively impacted her facial profile. Since the patient did not display excessive gum with a full smile, we decided to use MEAW therapy to allow some extrusion of the incisors, have the mesially tilted mandibular molars uprighted, correct the Class III malocclusion, and close the anterior open-bite.

Initially, we suggested extracting the three remaining third molars, but the patient only agreed to extract the mandibular right third molar.

During the initial stage of leveling, edgewise appliances (0.018×0.025 inch slot) were placed in both arches. Thereafter, a MEAW was placed in the lower arch and a 0.016×0.022 inch stainless steel archwire in the upper arch, which was augmented by short Class III elastics (Fig. 4). After 7 months of treatment, the anterior open-bite had successfully been closed, and a Class I molar relationship had been established. A subsequent detailed adjustment of the occlusion of the upper and lower arches was carefully incorporated.

The duration of treatment was 13 months, and optimal occlusion was obtained. At the end of treatment, a lingual fixed retainer was bonded to the lower anterior teeth. In addition to the upper and lower Hawley-type retainers, a removable retainer with a circumferential labial bow and tongue crib was fabricated for the upper dentition (Fig. 5). The patient was instructed to wear the special-type upper Hawley retainer with the tongue crib as much as possible on a full-time basis. An alternative regular-type upper Hawley retainer was provided for use during her daily social activities.

Posttreatment photographs showed few change in her facial appearance (Fig. 6). The mildly concave profile and facial proportions had been maintained. Class I occlusion with a normal overjet and overbite was achieved (Fig. 6). A posttreatment panoramic radiograph showed root parallelism (Fig. 7). A cephalometric superimposition revealed clockwise rotation of the mandible (Fig. 8, Table 2); accordingly, the mandibular plane angle had increased from 37º to 37.5º. Both the posterior and anterior facial heights had increased by 1 mm. The upper occlusal plane had moved downward anteriorly, and the lower

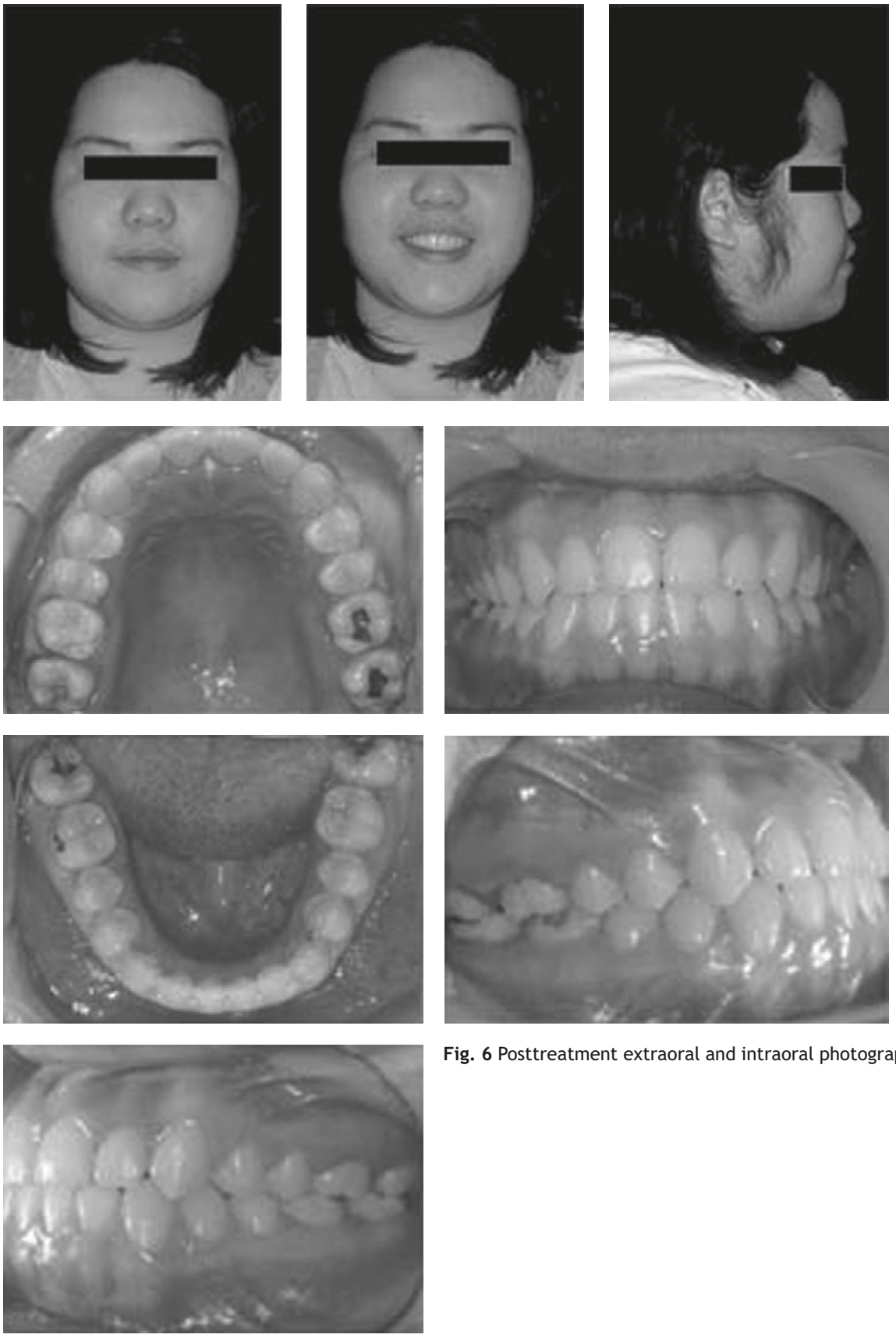

Fig. 6 Posttreatment extraoral and intraoral photographs.

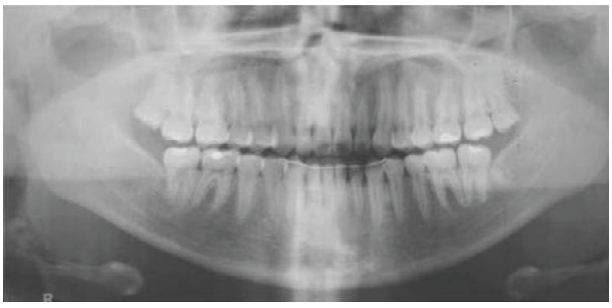

Fig. 7 Posttreatment panoramic radiograph.

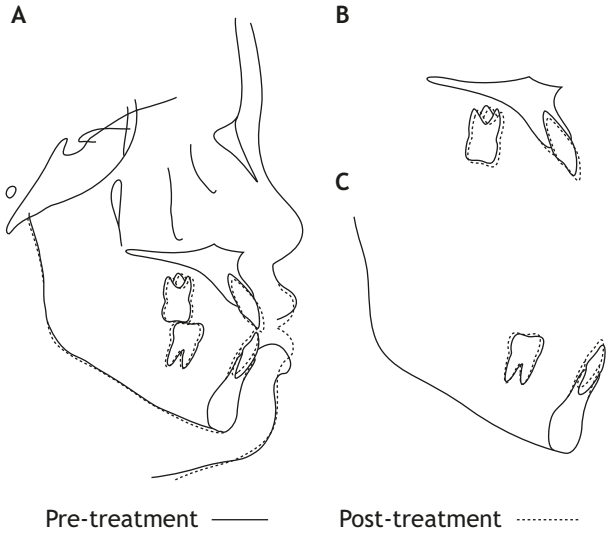

Fig. 8 Superimposition tracings from pretreatment to posttreatment. (A) Craniofacial tracings were superimposed along the outlines of the cranial base and registered at the sella. (B) Maxillary tracings were superimposed on the key ridge, pterygomaxillary fissure, and floor of the nose. (C) Mandibular tracings were superimposed on the mandibular border and symphysis.

occlusal plane had moved upward anteriorly. The maxillary incisors and molars were protracted as well as extruded. The mandibular molars had been uprighted 8° relative to the bisected occlusal plane, and the mandibular incisors had been retracted and extruded. Long-term stability was noted at the recall appointment check 7 years 11 months after treatment. The patient had stopped wearing the removable retainers for more than 1 year. Bilateral Class I molar relationships and a normal overjet and overbite had been maintained (Fig. 9). The overbite had slightly decreased over the left maxillary lateral incisor area. Cephalometric superimposition between the immediate posttreatment and 8 years 8 months after treatment (21 months out of retention) showed continuing vertical facial growth with slight retroclination of the upper and lower anterior teeth and maintenance of a positive overbite (Fig. 10).

Discussion

Several approaches for treating an anterior open-bite have been reported in the literature.[2–7,12,15–23] This patient presented with a skeletal anterior open-bite, excessive lower facial height, and skeletal Class III malocclusion. Treatment with a combination of orthodontics and orthognathic surgery would have provided a more stable occlusion and significant improvement in facial esthetics. However, the patient was satisfied with her facial profile and refused orthognathic surgical intervention because of the higher cost and its invasive nature. Therefore, a nonsurgical treatment option to camouflage the skeletal discrepancies was selected. Although TADs implanted in the posterior dentoalveolar area to intrude posterior teeth would have been effective in closing the anterior open-bite,[20,23] the counterclockwise rotation of the mandible would have tended to increase the chin prominence and further compromise her facial profile. Thus, MEAW therapy was chosen to correct her anterior crossbite and open-bite by changing the cant of the upper and lower occlusal planes, having the mandibular molars uprighted, and extruding the anterior teeth.

The MEAW technique was designed to incorporate many loops in an "L" shape to provide second-order control of the posterior teeth, reduce the load deflection rate, permit individual tooth movement, and transmit the force generated by the intermaxillary elastics throughout the entire arch.[24] It was recommended that the MEAW be applied to the lower arch and a rigid plain archwire to the upper arch in Class III cases.[20] The treatment outcome of our patient was in agreement with findings in previous reports.[25,26] The upper and lower occlusal planes moved toward each other during treatment, followed by closure of the anterior open-bite. The dentoalveolar changes included an increase of 4 mm in the overbite and 2 mm in the overjet. The upper incisors were protracted and extruded, and the lower incisors were retracted as well as extruded. The interincisal angle changed from 129° to 126.5° (Table 2). The maxillary molars were slightly extruded and protracted, and the mandibular molars were uprighted. The skeletal variables did not exhibit any changes, except that the mandibular plane angle increased by 0.5°, which was caused by extrusion of the maxillary molars and uprighting of the mandibular molars. Consequently, the posterior and anterior facial heights increased. A posttreatment cephalometric analysis revealed that her skeletal discrepancies had successfully been dentoalveolarly camouflaged.

In view of the patient's history of the thumb-sucking habit combined with an unfavorable tongue

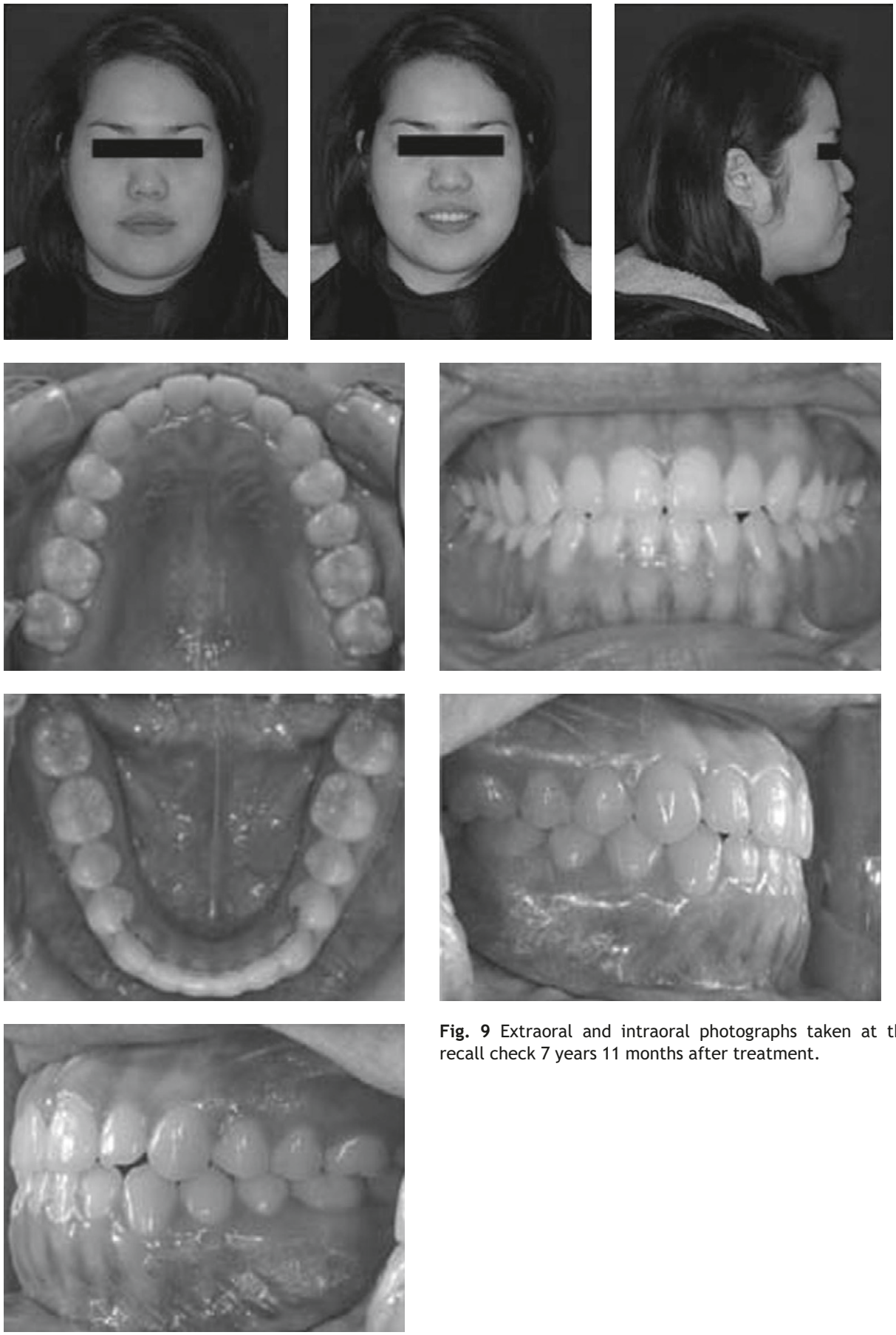

Fig. 9 Extraoral and intraoral photographs taken at the recall check 7 years 11 months after treatment.

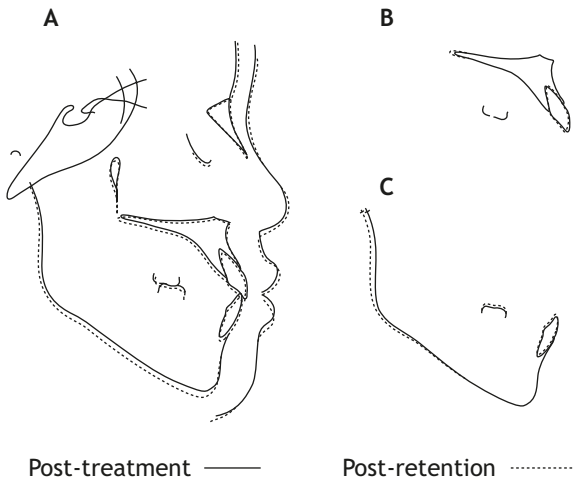

Fig. 10 Cephalometric superimposition between the immediate posttreatment and at 8 years 8 months after treatment (21 months out of retention).

Table 2. Cephalometric changes during treatment

Angular and linear measurements	T1	T2	T2−T1
Skeletal			
SNA (°)	81.0	81.0	0
SNB (°)	82.5	82.5	0
ANB (°)	−1.5	−1.5	0
A-Nv (mm)	2.5	2.5	0
Pog-Nv (mm)	5.0	5.0	0
SN-MP (°)	37.0	37.5	0
UFH/LFH (%/%)	42/58	41.5/58.5	−0.5/+0.5
Anterior LFH (mm)	81.0	82.0	+1
Anterior FH (mm)	139.0	140.0	+1
Posterior FH (mm)	85.0	86.0	+1
Gonial angle (°)	129.0	129.0	0
Dental			
U1-SN (°)	108.0	109.0	+1
L1-MP (°)	87.5	88.5	+1
U1-L1 (°)	129.0	126.5	−2.5
Overjet (mm)	0	2.0	+2
Overbite (mm)	−2.0	2.0	+4
FH-UOP (°)	3.0	5.0	+2
FH-BOP (°)	4.0	3.0	−1
FH-LOP (°)	5.0	1.0	−4
U6-PP (°)	92.5	95.5	+3
L6-MP (°)	95.5	103.5	+8
U1-PP (mm)	34.0	36.0	+2
U6-PP (mm)	31.0	31.5	+0.5
L1-MP (mm)	43.5	45.0	+1.5
L6-MP (mm)	34.0	34.5	+0.5

T1=pretreatment; T2=posttreatment; S=sella; N=nasion; A=point A (subspinale point); B=point B (supramentale point); Nv=nasion perpendicular; Pog=pogonion; MP=mandibular plane; UFH=upper anterior facial height; LFH=lower facial height; FH=Frankfort horizontal plane; U1=long axis of upper incisor; L1=long axis of lower incisor; UOP=upper occlusal plane; BOP=bisecting occlusal plane; LOP=lower occlusal plane; U6=upper first molar; PP=palatal plane; L6=lower first molar.

posture which are all contributory factors for relapse of open-bite malocclusion cases,[6,13,27–29] we incorporated the upper retainer with components of a full circumferential labial bow and tongue crib to prevent relapse. A bonded lingually fixed retainer was used in the lower arch to prevent relapse of anterior crowding. This patient was very compliant in wearing the removable retainer, and the treatment results were stable during the retention phase. An examination 8 years 8 months after treatment, which was 21 months after discontinuing retention, revealed a persisting characteristic of a vertical facial growth pattern during these years. Despite the unfavorably increased vertical relationship of the face, a normal occlusal relationship had been maintained. The posterior teeth had remained upright, and the anterior teeth had become more retroclined with time. It was suggested that etiologic factors of an open-bite malocclusion should be determined at the time of the initial diagnosis and should be controlled during treatment and retention to prevent relapse.[30] Although we could not delineate the roles of soft tissue and muscle dysfunction in the development of the open-bite malocclusion in our present study, the MEAW technique and retainer with a tongue crib seemed to have encouraged natural dentoalveolar compensation on a long-term basis.

References

1. Subtelny JD, Sakuda M. Open-bite: diagnosis and treatment. *Am J Orthod* 1964;50:337–58.
2. Remmers D, Van't Hullenaar RW, Bronkhorst EM, Bergé SJ, Katsaros C. Treatment results and long-term stability of anterior open bite malocclusion. *Orthod Craniofac Res* 2008;11:32–42.
3. Bondemark L, Holm AK, Hansen K, et al. Long-term stability of orthodontic treatment and patient satisfaction: a systematic review. *Angle Orthod* 2007;77:181–91.
4. Yokota R, Mishiro M, Abe T, et al. Pressure on anterior region of palate during thumb-sucking. *Bull Tokyo Dent Coll* 2007; 48:57–66.
5. Peng CL, Jost-Brinkmann PG, Yoshida N, Chou HH, Lin CT. Comparison of tongue functions between mature and tongue-thrust swallowing—an ultrasound investigation. *Am J Orthod Dentofacial Orthop* 2004;125:562–70.
6. Fraser C. Tongue thrust and its influence in orthodontics. *Int J Orthod Milwaukee* 2006;17:9–18.
7. Padwa BL, Hayward PG, Ferraro NF, Mulliken JB. Cervicofacial lymphatic malformation: clinical course, surgical intervention, and pathogenesis of skeletal hypertrophy. *Plast Reconstr Surg* 1995;95:951–60.
8. Nielsen IL. Vertical malocclusions: etiology, development, diagnosis and some aspects of treatment. *Angle Orthod* 1991;61:247–60.
9. Ngan P, Fields HW. Open bite: a review of etiology and management. *Pediatr Dent* 1997;19:91–8.
10. Tsang WM, Cheung LK, Samman N. Cephalometric characteristics of anterior open bite in a southern Chinese population. *Am J Orthod Dentofacial Orthop* 1998;113:165–72.

11. Kim YH, Han UK, Lim DD, Serraon ML. Stability of anterior openbite correction with multiloop edgewise archwire therapy: a cephalometric follow-up study. *Am J Orthod Dentofacial Orthop* 2000;118:43–54.
12. Ng CS, Wong WK, Hagg U. Orthodontic treatment of anterior open bite. *Int J Paediatr Dent* 2008;18:78–83.
13. Meyer-Marcotty P, Hartmann J, Stellzig-Eisenhauer A. Dentoalveolar open bite treatment with spur appliances. *J Orofac Orthop* 2007;68:510–21. [In English and German]
14. Ovsenik M, Farcnik FM, Korpar M, Verdenik I. Follow-up study of functional and morphological malocclusion trait changes from 3 to 12 years of age. *Eur J Orthod* 2007;29:523–9.
15. Darendeliler MA, Darendeliler A, Mandurino M. Clinical application of magnets in orthodontics and biological implications: a review. *Eur J Orthod* 1997;19:431–42.
16. Arat ZM, Sezer FE, Arslan AD. A new approach in the treatment of skeletal open bite: vertically activated bite block. *World J Orthod* 2006;7:345–56.
17. Saito I, Yamaki M, Hanada K. Nonsurgical treatment of adult open bite using edgewise appliance combined with high-pull headgear and class III elastics. *Angle Orthod* 2005;75:277–83.
18. Miyajima K, Iizuka T. Treatment mechanics in Class III open bite malocclusion with Tip Edge technique. *Am J Orthod Dentofacial Orthop* 1996;110:1–7.
19. Iannetti G, Fadda MT, Marianetti TM, Terenzi V, Cassoni A. Long-term skeletal stability after surgical correction in Class III open-bite patients: a retrospective study on 40 patients treated with mono- or bimaxillary surgery. *J Craniofac Surg* 2007;18:350–4.
20. Kim YH. Anterior openbite and its treatment with multiloop edgewise archwire. *Angle Orthod* 1987;57:290–321.
21. Kuroda S, Sakai Y, Tamamura N, Deguchi T, Takano-Yamamoto T. Treatment of severe anterior open bite with skeletal anchorage in adults: comparison with orthognathic surgery outcomes. *Am J Orthod Dentofacial Orthop* 2007; 132:599–605.
22. Swinnen K, Politis C, Willems G, et al. Skeletal and dentoalveolar stability after surgical-orthodontic treatment of anterior open bite: a retrospective study. *Eur J Orthod* 2001;23:547–57.
23. Xun C, Zeng X, Wang X. Microscrew anchorage in skeletal anterior open-bite treatment. *Angle Orthod* 2007;77: 47–56.
24. Yang WS, Kim BH, Kim YH. A study of the regional load deflection rate of multiloop edgewise arch wire. *Angle Orthod* 2001;71:103–9.
25. Baek SH, Shin SJ, Ahn SJ, Chang YI. Initial effect of multiloop edgewise archwire on the mandibular dentition in Class III malocclusion subjects. A three-dimensional finite element study. *Eur J Orthod* 2008;30:10–5.
26. Endo T, Kojima K, Kobayashi Y, Shimooka S. Cephalometric evaluation of anterior open-bite nonextraction treatment, using multiloop edgewise archwire therapy. *Odontology* 2006;94:51–8.
27. Hotokezaka H, Matsuo T, Nakagawa M, Mizuno A, Kobayashi K. Severe dental open bite malocclusion with tongue reduction after orthodontic treatment. *Angle Orthod* 2001;71: 228–36.
28. Park HS, Kwon OW, Sung JH. Nonextraction treatment of an open bite with microscrew implant anchorage. *Am J Orthod Dentofacial Orthop* 2006;130:391–402.
29. Pedrazzi ME. Treating the open bite. *J Gen Orthod* 1997;8: 5–16.
30. Chang YI, Moon SC. Cephalometric evaluation of the anterior open bite treatment. *Am J Orthod Dentofacial Orthop* 1999; 115:29–38.

J Dent Sci 2009;4(3):159–164

CASE REPORT

Delayed formation of multiple supernumerary teeth

*Yai-Tin Lin,[1] Sung-Wen Chang,[2] Yng-Tzer J. Lin[1]**

[1]Pediatric Dentistry, Chang Gung Memorial Hospital-Kaohsiung Medical Center, Chang Gung University College of Medicine, Kaohsiung, Taiwan
[2]Department of Oral Surgery, Chang Gung Memorial Hospital-Kaohsiung Medical Center, Chang Gung University College of Medicine, Kaohsiung, Taiwan

Received: Jun 18, 2009
Accepted: Aug 29, 2009

KEY WORDS:
impacted incisor;
multiple supernumerary teeth;
orthodontic traction

Multiple supernumerary teeth in either the maxillary anterior or premolar region can cause uneruption or impaction of the succedaneous permanent teeth. Supernumerary premolars are special in terms of their late development and recurrence. This case report details the use of multiple phases of orthodontic traction in order to obtain ideal clinical results. An 8-year 4-month-old healthy boy had an impacted left upper central incisor and multiple supernumerary teeth among the incisors and premolars. The impacted incisor was successfully moved to its proper position by orthodontic traction and a closed eruption technique. One year later, surgical extraction of three supernumerary premolars was performed. The same traction procedure with the closed eruption technique was successfully used to pull the mandibular left first premolar into its occlusion. A normal appearance of the anterior teeth and posterior occlusion were achieved after two phases of orthodontic traction. The exposed incisor and premolar presented a proper gingival contour and acceptable attached gingiva. Multiple supernumerary teeth can cause multiple sites of unerupted permanent teeth that make the treatment procedures variable and complicated. The impacted teeth can be moved to their proper position by multiple phases of orthodontic traction and a closed eruption technique.

Introduction

Supernumerary teeth can occur in any site in the oral cavity. The incidence of supernumerary teeth among the general population is approximately 1 in 110 children in which maxillary midline supernumeraries (mesiodentes) are the most commonly found.[1,2] There may be multiple supernumerary teeth which can remain impacted for many years, creating complicated clinical situations. Among supernumeraries, supernumerary premolars are more common than formerly estimated and are special in terms of their late development and recurrence, which make treatment procedures variable and complicated.[3]

The etiology and mechanisms that can give rise to supernumerary teeth in the maxillary midline or premolars are fairly similar. Gardiner[4]

*Corresponding author. Department of Pediatric Dentistry, Chang Gung Memorial Hospital-Kaohsiung Medical Center, 123, Ta-Pei Road, Niaosung, Kaohsiung County 83301, Taiwan.
E-mail: joe0430@ms13.hinet.net

suggested three possible mechanisms, including an abnormal proliferation of the dental lamina, an additional follicle, and an extension of the dental lamina after the deciduous as well as permanent follicles (post-permanent type). The mechanism of post-permanent supernumerary teeth is possible owing to the fact that supernumerary premolar root development is considerably delayed for 7–10 years.

It is always a great concern for parents to discover unpleasant anterior dentition when unerupted maxillary permanent incisors occur because of obstruction of the supernumerary teeth during a child's mixed dentition. Recent reports showed that impacted canines and incisors can be properly positioned with the aid of direct orthodontic traction instead of surgical extraction.[5–7] Although many approaches, such as surgical extraction with replacement of prostheses, adjacent incisors for substitution and orthodontic traction, have been recommended, orthodontic traction of the unerupted or impacted tooth to complete the normal dentition is still the first treatment choice if the tooth is not ankylosed.[5–7]

This report describes a case with multiple supernumerary incisors and premolars causing uneruption of the left maxillary central incisors and mandibular first premolar. The impacted maxillary incisor and mandibular premolar were successfully moved to their proper positions through the use of orthodontic traction and a closed eruption technique.

Case presentation

An 8-year 4-month-old boy was referred to the children's clinic of Chang Gung Memorial Hospital with the complaint of an unerupted upper left central incisor. The patient was physically healthy and had no apparent medical abnormalities. The patient had a Class I malocclusion and a balanced facial pattern. A cephalometric analysis revealed normal cephalometric values except for a slightly deep bite.

An intraoral examination revealed a late mixed dentition and a Class I molar relationship. A clinical examination showed an unerupted maxillary left central incisor and no apparent arch length discrepancy in either the maxillary or mandibular arch (Fig. 1). The midline deviated to the left owing to drifting of the adjacent teeth into the unoccupied space. Radiographic examinations demonstrated an impacted maxillary left central incisor with two mesiodentes among the permanent maxillary incisors and a supernumerary tooth in the region of the mandibular left premolars (Fig. 2).

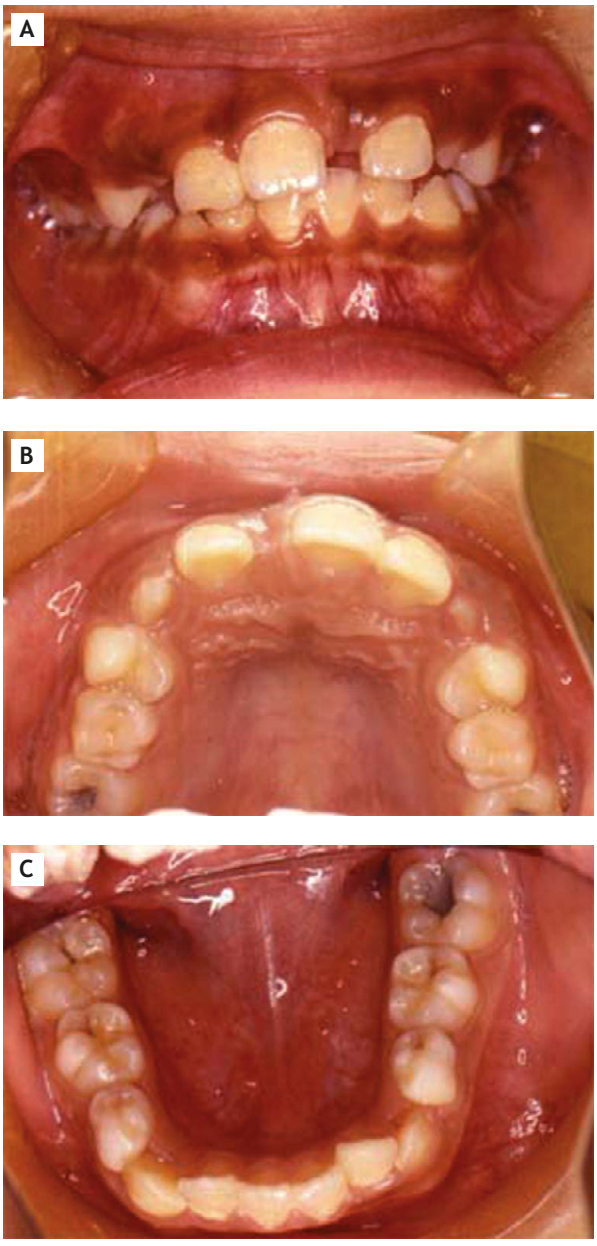

Fig. 1 Pretreatment intraoral photographs showing an unerupted maxillary left central incisor.

Diagnosis

The diagnosis consisted of multiple supernumerary teeth and impaction of the maxillary left central incisor due to two mesiodentes among permanent incisors, while a genetic disturbance associated with the supernumerary teeth was excluded.

Treatment objectives

The treatment objectives included removing the two supernumerary teeth in the upper anterior region, redistributing the space and restoring the normal appearance of the maxillary anterior region, and

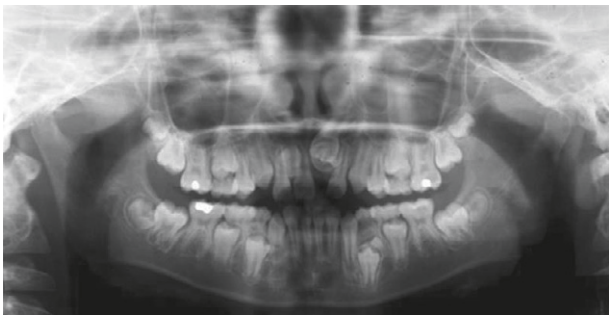

Fig. 2 Pretreatment panoramic radiograph showing an impacted maxillary left central incisor with two mesiodentes among the permanent maxillary incisors and a supernumerary tooth in the region of the mandibular left premolars.

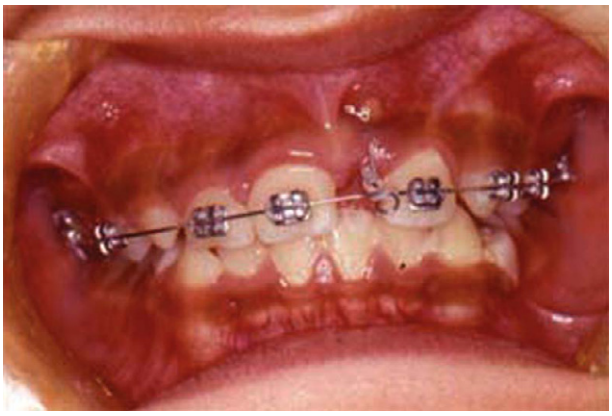

Fig. 3 Closed eruption technique and light force used to pull the impacted incisor.

monitoring and delaying treatment of the supernumerary tooth in the mandibular arch.

Treatment alternatives

Treatment alternatives included the following: (1) extraction of the impacted central incisor and restoration with temporary or semi-permanent prostheses in case the central incisor was ankylosed; (2) extraction of the impacted central incisor and closure of the space, substituting the lateral incisor for central incisor with subsequent prosthetic restoration; and (3) surgical exposure, followed by orthodontic traction to bring the impacted central incisor into the proper position.

Treatment progress

After understanding the possible treatment options, the parents decided to proceed with surgical removal of the two supernumerary teeth to allow the impacted central incisor to be brought into its proper position. The removal of the two mesiodentes and crown exposure of the impacted central incisor were simultaneously performed under general anesthesia. However, delayed removal of the supernumerary tooth in the mandible premolar area was recommended, because it was not clearly visible on the radiograph. A lingual button was bonded onto the labial surface of the maxillary left central incisor, and 0.010-inch ligature wire was tied to the button, leaving the end protruding out of the oral cavity. The flap was sutured back in place (closed eruption technique) in such a way that the bracketed crown was not exposed to the oral cavity.

The patient came back 1 week later for suture removal. Orthodontic treatment was then begun the following week with banding of the maxillary first molars and bonding brackets onto all of the maxillary teeth. The initial leveling was performed with 0.014-inch nickel-titanium wire, followed by 0.016-inch stainless steel wire with an open coil spring in the position of the unerupted incisor. Once adequate space was achieved, orthodontic traction of the impacted tooth was begun. A light force of approximately 60–90 g was applied using an elastomeric chain between the helix of the 0.016×0.016-inch main archwire and the protruding ligature wire (Fig. 3). As the impacted tooth moved downward, the ligature wire was shortened to maintain the effective elastomeric chain. The attached button was changed to a standard incisor bracket when the impacted incisor became exposed to the oral environment. The final alignment was completed with a 0.016×0.022-inch archwire. The first phase was completed within 8 months (Fig. 4). The bands and bracket were removed and replaced with a maxillary Hawley retainer.

On the recall visit 3 months later, two additional supernumerary teeth in the mandibular right premolar region were accidentally found on the panoramic radiograph (Fig. 5). One year later, surgical extraction of the three supernumerary teeth was performed in the operating room with the closed eruption technique described above that bonded a lingual button onto the impacted mandibular left first premolar (Fig. 6). The same traction procedures as previously described were successfully used to pull the mandibular left first premolar into its proper position. Acceptable anterior esthetics and posterior occlusion were obtained after completion of phase II orthodontic treatment within 7 months (Fig. 7). The bands and brackets were removed and replaced with a mandibular Hawley retainer. On the subsequent 6-month follow-up, the panoramic radiograph showed four additional supernumerary teeth, three of which were in between the maxillary canines and premolars and the other one which was in the region of the mandibular left premolars. These supernumerary

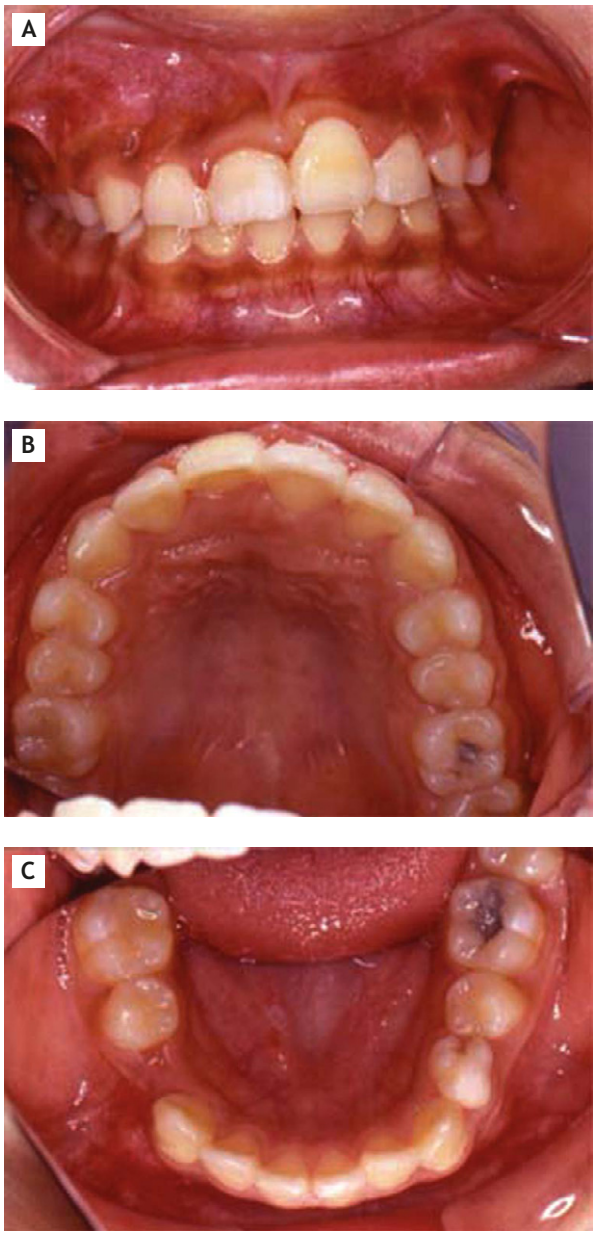

Fig. 4 The impacted incisor successfully pulled into its proper position after completion of phase I treatment.

teeth needed to be removed when crown formation of each supernumerary tooth had been noted (Fig. 8).

Discussion

Multiple supernumerary teeth are frequently associated with cleidocranial dysplasia and Gardner syndrome, and are recognized as a part of their characteristics.[8,9] However, it is rare to find multiple supernumeraries in individuals with no other associated disease or syndrome. The most frequent supernumerary teeth identified are mesiodentes, followed by premolars and fourth molars or distal

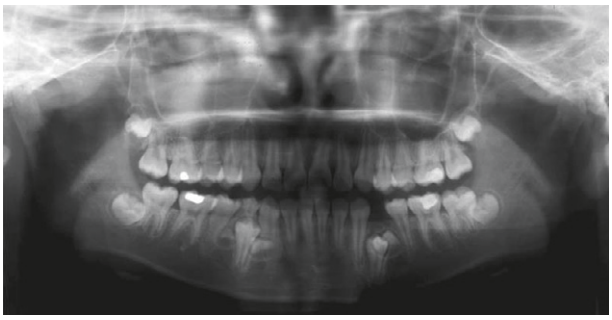

Fig. 5 Two supernumerary premolars found in the right mandibular premolar region 3 months later.

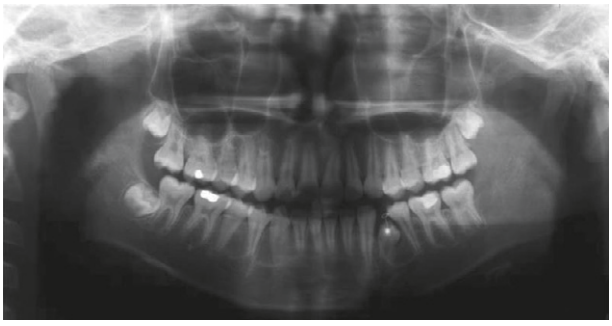

Fig. 6 A lingual button bonded onto the impacted left mandibular first premolar for orthodontic traction.

molars.[10,11] Yusof[12] reviewed most of the literature and found that a predominance of non-syndrome multiple supernumerary teeth occurred in the mandibular premolar area. Solares and Romero,[3] in their comprehensive review of supernumerary premolars, found a male to female ratio of 3 to 1, a mean age of 16.4 years, and an extremely high occurrence rate of 74% for mandibular premolars. The present case had no history of combined diseases or syndromes and was consistent with previous findings that seven supernumerary teeth were in the premolar area, including three in the maxilla and four in the mandible.

Supernumerary teeth, especially in the upper anterior region, can cause various pathologic conditions such as delayed or non-eruption of permanent teeth and displacement of permanent teeth. Root resorption, rotation, root malformation of the adjacent teeth, and dentigerous cyst formation are also cited in the literature. However, dentigerous cyst formation and root resorption of adjacent teeth were found to be rare in long-term observations.[13,14] A special phenomenon of supernumerary premolars reported in the literature is their recurrence and new development of supernumerary teeth.[15–17] The dental lamina is not completely resorbed and is reactivated at the time of crown completion of the normal permanent teeth, which can create multiple supernumerary teeth especially in the premolar region.[18]

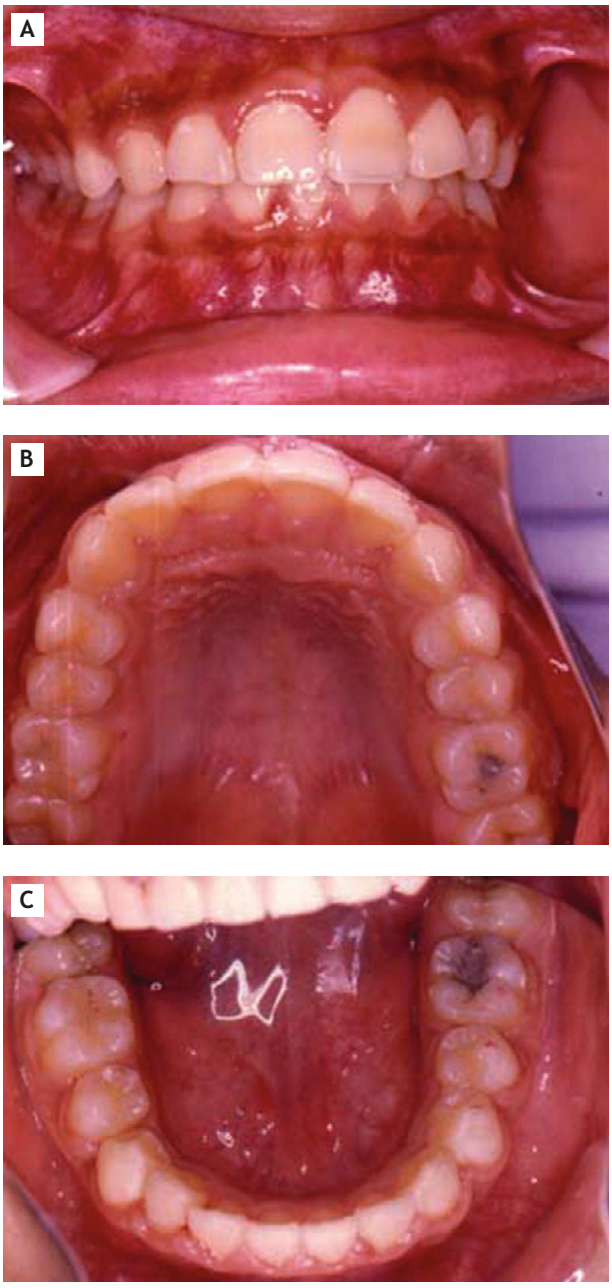

Fig. 7 Acceptable anterior esthetics and posterior occlusion obtained after completion of phase II orthodontic treatment.

Early surgical intervention of mesiodentes as in this case is recommended because of esthetic concerns. However, the timing for surgical removal of supernumerary premolars is still controversial. Most authors recommend that supernumerary premolars left *in situ* until further development allows for uncomplicated surgery with less damage to roots and adjacent structures.[19–21] It seems that late one-session treatment of the overall condition is preferred because of the late development or recurrence of supernumerary premolars. As this case presented, delayed treatment of supernumerary

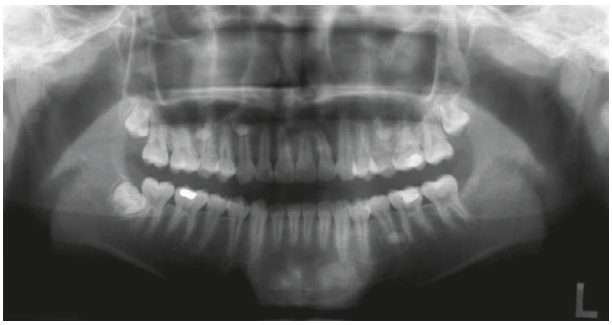

Fig. 8 An additional four supernumerary premolars found in a follow-up panoramic radiograph.

premolars seems reasonable to prevent multiple phases of orthodontic treatment. Hanratty[21] suggested removal of more developed supernumerary premolars be accomplished soon after diagnosis, but less developed premolars be left *in situ* and removed later in order to avoid damage to adjacent structures and allow for bone regeneration.

Surgical removal of a supernumerary tooth followed by crown exposure and orthodontic traction of the unerupted or impacted tooth is considered the first choice of treatment if the tooth is not ankylosed. In terms of the uncovering flap design, it was shown that the closed eruption technique has more advantages than the open eruption technique, such as rapid wound healing, less discomfort, good postoperative hemostasis, and greater bonding reliability.[22–24] Vermette et al.[25] compared these two surgical techniques and found that the apically positioned flap technique (open eruption technique) had more negative esthetic effects such as increased crown length and gingival scars than did the closed eruption technique. The closed eruption technique which returns the flap to its original location induces natural eruption of the impacted tooth. We also placed a lingual button attachment rather than a bracket on the crown end of the impacted teeth as soon as possible in order to prevent more bone destruction. Studies found that the greater amount of bone that is removed during surgical exposure, the greater the bone loss is after orthodontic treatment and the chance of a long exposed crown length.[26,27] The periodontal status of the exposed incisor and premolar of this case after orthodontic traction revealed an acceptable gingival contour and attached gingiva (Fig. 7).

Patients with a previous history of supernumerary teeth in the anterior region had a 24% possibility of developing supernumerary premolars at a later stage in the review by Solares and Romero.[3] It is, therefore, important to have panoramic radiographs taken periodically as well as long-term follow-up. A relatively high percentage of cases with supernumerary teeth are accidentally found during

radiographic examinations. As this case presented, overall nine supernumerary teeth were found in the following 2 years. It is sometimes difficult for clinicians to make a proper treatment plan for cases with multiple supernumerary teeth because of their recurrence or newly developed supernumerary teeth, especially in the premolar region. Multiple phases of treatment may be necessary in order to achieve an ideal clinical result.

A fixed retainer for maintaining teeth after orthodontic traction in a stable occlusion is better and more effective than a removable retainer. Compliance with wearing a removable retainer in teenagers is always a problem. However, careful cleaning of the fixed retainer is another problem for youngsters. This patient exhibited compliance of wearing the removable retainer, and the occlusion was fortunately quite stable.

References

1. Stafne EC. Supernumerary teeth. *Dent Cosmos* 1932;74: 653–9.
2. Schulze EC. Incidence of supernumerary teeth. *Dent Abstr* 1961;6:23.
3. Solares R, Romero MI. Supernumerary premolars: a literature review. *Pediatr Dent* 2004;26:450–8.
4. Gardiner JH. Supernumerary teeth. *Dent Pract* 1961;12: 63–73.
5. Bishara SE. Impacted maxillary canines: a review. *Am J Orthod Dentofacial Orthop* 1992;101:159–71.
6. Crawford LB. Impacted maxillary central incisor in mixed dentition treatment. *Am J Orthod Dentofacial Orthop* 1997; 112:1–7.
7. Lin YT. Treatment of an impacted dilacerated maxillary central incisor. *Am J Orthod Dentofacial Orthop* 1999;115: 406–9.
8. Ida M, Nakamura T, Utsunomiya J. Osteomatous changes and tooth abnormalities found in the jaw of patients with adenomatosis coli. *Oral Surg* 1981;52:2–11.
9. Jansen BL, Kreiborg S. Development of the dentition in cleidocranial dysplasia. *J Oral Pathol Med* 1990;19:89–93.
10. Fernandez Montenegro P, Valmaseda Castellon E, Berini Aytes L, Gay Escoda C. Retrospective study of 145 supernumerary teeth. *Med Oral Patol Oral Cir Bucal* 2006;11:E339–44.
11. Umweni AA, Osunbor GE. Non-syndrome multiple supernumerary teeth in Nigerians. *Odontostomatol Trop* 2002; 25:43–8.
12. Yusof WZ. Non-syndrome multiple supernumerary teeth: literature review. *J Can Dent Assoc* 1990;56:147–9.
13. Lustmann J, Bodner L. Dentigerous cysts associated with supernumerary teeth. *Int J Oral Pathol Med* 1990;19: 89–93.
14. Sian JS. Root resorption of first permanent molar by a supernumerary premolar. *Dent Update* 1999;26:210–1.
15. Poyton GH, Morgan GA, Crouch SA. Recurring supernumerary mandibular premolars: report of a case of postmature development. *Oral Surg Oral Med Oral Pathol* 1960;13: 964–6.
16. Stevenson W, McKechnie AD. Recurring supernumerary teeth: report of a case. *Oral Surg Oral Med Oral Pathol* 1975;40:76–80.
17. Shapira Y, Haskell BS. Late developing supernumerary premolar. *J Clin Orthod* 1981;15:571.
18. Saito T. A genetic study on the degenerative anomalies of deciduous teeth. *Jpn J Hum Genet* 1959;4:27–30.
19. Cochrane SM, Clark JR, Hunt NP. Late developing supernumerary teeth in the mandible. *Br J Orthod* 1997;24: 293–6.
20. Marre JM. Supernumerary teeth. *J Am Dent Assoc* 1940;27: 212–4.
21. Hanratty WJ. Odontectomy of seven impacted supernumerary bicuspids. *J Am Dent Assoc* 1960;61:80–2.
22. Burden DJ, Mullally BH, Robinson SN. Palatally ectopic canines: closed eruption versus open eruption. *Am J Orthod Dentofacial Orthop* 1999;115:640–4.
23. Becker A, Brin I, Ben-Bassat Y, Zilberman Y, Chaushu S. Closed-eruption surgical technique for impacted maxillary incisors: a postorthodontic periodontal evaluation. *Am J Orthod Dentofacial* Orthop 2002;122:9–14.
24. Chaushu S, Becker A, Zeltser R, Branski S, Vasker N, Chaushu G. Patients' perception of recovery after exposure of impacted teeth: a comparison of closed- versus open-eruption techniques. *J Oral Maxillofac Surg* 2005;63: 323–9.
25. Vermette ME, Kokich VG, Kennedy DB. Uncovering labially impacted teeth: apically positioned flap and closed-eruption techniques. *Angle Orthod* 1995;65:23–32.
26. McDonald F, Yap WL. The surgical exposure and application of direct traction of unerupted teeth. *Am J Orthod* 1982;89: 331–40.
27. Kohavi D, Becker A, Zilberman Y. Surgical exposure, orthodontic movement, and final tooth position as factors in periodontal breakdown of treated palatally impacted canines. *Am J Orthod* 1984;85:72–7.

Standard World Leader

This is the First

TSIII SA

OSSTEM IMPLANT

OSSTEM IMPLANT RESEARCH & EDUCATION CENTER
OSSTEM AIC

آزاد تجارت پارس
AZAD TEJARAT PARS.LTD

Tel: +98 21 88 98 80 63 - 6

Web: Azadmed.com